

การเร่งปฏิกิริยาเชิงไฟฟ้าสำหรับออกซิเดชันของเมทานอลโดยอนุภาคนาโนของโลหะ
ที่เคลือบบนขั้วไฟฟ้าฟิล์มบางของเพชรที่โดปด้วยโบรอน



นายวรยุทธ ทยาวิวัฒน์

สถาบันวิทยบริการ

จุฬาลงกรณ์มหาวิทยาลัย

วิทยานิพนธ์นี้เป็นส่วนหนึ่งของการศึกษาตามหลักสูตรปริญญาวิทยาศาสตรมหาบัณฑิต

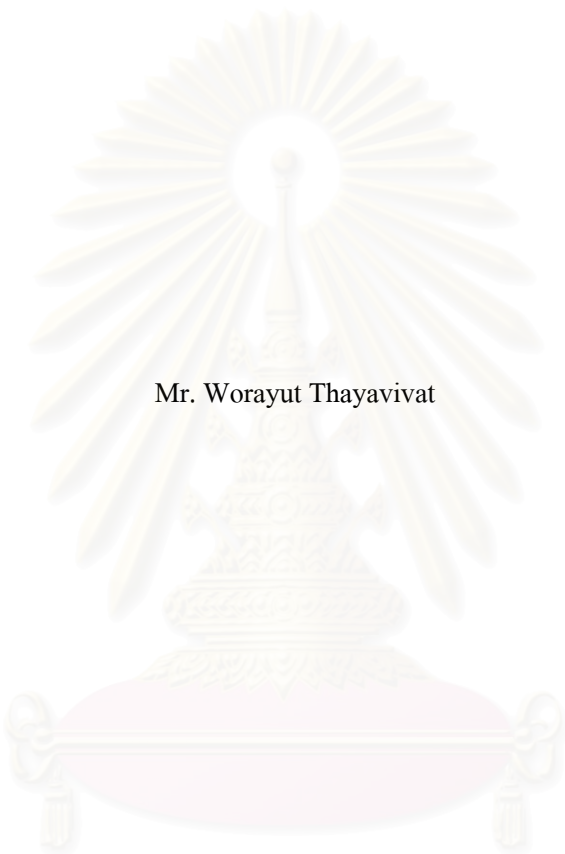
สาขาวิชาปิโตรเคมีและวิทยาศาสตร์พอลิเมอร์

คณะวิทยาศาสตร์ จุฬาลงกรณ์มหาวิทยาลัย

ปีการศึกษา 2550

ลิขสิทธิ์ของจุฬาลงกรณ์มหาวิทยาลัย

ELECTROCATALYSIS FOR METHANOL OXIDATION BY METAL NANOPARTICLES
DEPOSITED ON BORON-DOPED DIAMOND THIN FILM ELECTRODE



Mr. Worayut Thayavivat

สถาบันวิทยบริการ
จุฬาลงกรณ์มหาวิทยาลัย

A Thesis Submitted in Partial Fulfillment of the Requirements
for the Degree of Master of Science Program in Petrochemistry and Polymer Science

Faculty of Science

Chulalongkorn University

Academic Year 2007

Copyright of Chulalongkorn University

Thesis Title ELECTROCATALYSIS FOR METHANOL OXIDATION BY METAL NANOPARTICLES DEPOSITED ON BORON-DOPED DIAMOND THIN FILM ELECTRODE


By Mr. Worayut Thayavivat

Field of Study Petrochemistry and Polymer Science

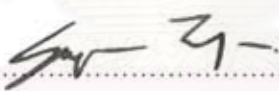
Thesis Advisor Associate Professor Orawon Chailapakul, Ph.D.


Thesis Co-advisor Parichatr Vanalabhpataana, Ph.D.


Accepted by the Faculty of Science, Chulalongkorn University in Partial Fulfillment of the Requirements for the Master's Degree



..... Dean of the Faculty of Science
(Professor Supot Hannongbua, Ph.D.)

THESIS COMMITTEE


..... Chairman
(Associate Professor Supawan Tantayanon, Ph.D.)


..... Thesis Advisor
(Associate Professor Orawon Chailapakul, Ph.D.)


..... Thesis Co-advisor
(Parichatr Vanalabhpataana, Ph.D.)


..... Member
(Assistant Professor Voravee Hoven, Ph.D.)


..... Member
(Assistant Professor Warinthorn Chavasiri, Ph.D.)

วรยุทธ ทหาวิวัฒน์: การเร่งปฏิกิริยาเชิงไฟฟ้าสำหรับออกซิเดชันของเมทานอลโดยอนุภาคนาโนของโลหะที่เคลือบบนขั้วไฟฟ้าฟิล์มบางของเพชรที่โคปด้วยโบรอน.

(ELECTROCATALYSIS FOR METHANOL OXIDATION BY METAL NANOPARTICLES DEPOSITED ON BORON-DOPED DIAMOND THIN FILM ELECTRODE) อ. ที่ปรึกษา : รศ.ดร. อรรพรรณ ชัยลภากุล, อ.ที่ปรึกษาร่วม : อาจารย์ ดร. ปาริฉัตร วนลาภพัฒนา, 81 หน้า.

งานวิจัยนี้ ศึกษาวิธีการเตรียมและการประยุกต์ใช้ขั้วไฟฟ้าฟิล์มบางของเพชรที่โคปด้วยโบรอน โดยการเคลือบด้วยตัวเร่งปฏิกิริยาโลหะ 1, 2, และ 3 ชนิดสำหรับปฏิกิริยาออกซิเดชันของเมทานอล ตัวเร่งปฏิกิริยาซึ่งมีแพลทินัม เป็นหลักและโลหะอื่น ได้แก่ รูทีเนียม โรเดียม และทองถูกเคลือบลงบนขั้วไฟฟ้าฟิล์มบางของเพชรที่โคปด้วยโบรอนด้วยวิธีการทางเคมีไฟฟ้า แบบให้ศักย์ไฟฟ้าคงที่ จากการนำเอาขั้วไฟฟ้าที่เตรียมได้ไปตรวจสอบการเร่งปฏิกิริยาออกซิเดชันของเมทานอลด้วยวิธีไซคลิกโวลแทมเมตรีพบว่า ขั้วไฟฟ้าฟิล์มบางของเพชรที่โคปด้วยโบรอนที่มีการเคลือบโลหะแพลทินัม-รูทีเนียม-โรเดียม มีประสิทธิภาพสูงสุดในการเร่งปฏิกิริยาออกซิเดชันของเมทานอลโดยให้กระแสแอโนดิก 17.58 มิลลิแอมแปร์ต่อตารางเซนติเมตร สำหรับสารละลาย 1.00 โมลาร์เมทานอลใน 0.50 โมลาร์ กรดซัลฟิวริก และจากการพิสูจน์เอกลักษณ์ด้วยเทคนิคสแกนนิ่งอิเล็กตรอนไมโครสโคป/เอเนอร์จิสเปกโทรสโกปีพบว่า ขนาดอนุภาคของโลหะที่เคลือบอยู่บนขั้วไฟฟ้ามีขนาดอยู่ในช่วงนาโนเมตร

สถาบันวิทยบริการ จุฬาลงกรณ์มหาวิทยาลัย

สาขาวิชา...ปิโตรเคมีและวิทยาศาสตร์พอลิเมอร์.....ลายมือชื่อนิสิต.....

ปีการศึกษา...2550.....ลายมือชื่ออาจารย์ที่ปรึกษา.....

ลายมือชื่ออาจารย์ที่ปรึกษาร่วม.....

4872449923 : MAJOR PETROCHEMISTRY AND POLYMER SCIENCE

KEY WORD: METHANOL OXIDATION / BORON-DOPED DIAMOND ELECTRODE

WORAYUT THAYAVIVAT : ELECTROCATALYSIS FOR METHANOL OXIDATION BY METAL NANOPARTICLES DEPOSITED ON BORON-DOPED DIAMOND THIN FILM ELECTRODE. THESIS ADVISOR : ASSOC. PROF. ORAWON CHAILAPAKUL, Ph.D., THESIS COADVISOR : PARICHATR VANALABHPATANA, Ph.D., 81 pp.

In this research, the preparation of mono-, di-, and trimetallic catalysts deposited on boron-doped diamond (BDD) thin film electrodes and their applications towards methanol oxidation have been studied. In combination with other metals including ruthenium, rhodium, and gold, the platinum based catalysts were electrochemically deposited on the BDD electrode under potentiostatic conditions. Cyclic voltammetry was used to examine the electrocatalytic activity of the modified BDDs for the oxidation of methanol. Among the prepared electrodes, the platinum–ruthenium–rhodium/BDD showed the best catalytic performance with the anodic current of 17.58 mAcm^{-2} for 1.00 M methanol in 0.50 M sulfuric acid. Characterized by means of scanning electron microscope/energy dispersive spectrometry (SEM/EDS), the metal particles deposited on the BDD surface were distributed in the range of nanometers.

สถาบันวิทยบริการ
จุฬาลงกรณ์มหาวิทยาลัย

Field of study...Petrochemistry and polymer science.....Student's signature.....*Worayut Thayavivat*
Academic year2007.....Advisor's signature.....*Orawon Chailapakul*
Co-advisor's signature.....*Parichatr Vanalabhpattana*

ACKNOWLEDGEMENTS

Firstly, I would like to thank my advisor, Assoc. Prof. Dr. Orawan Chailapakul and my co-advisor, Dr. Parichatr Vanalabhpatana for their help, guidance, and encouragement during the whole three years in the program. I also would like to thank my thesis examination committee members: Assoc. Prof. Dr. Supawan Tantayanon, Assist. Prof. Dr. Vorawee Hoven, and Assist. Prof. Dr. Warinthorn Chavasiri, for their valuable comments.

In addition, I would like to thank all members of the Electrochemical Research Group for their great friendship, help, and support during my study.

I am grateful to the financial supports which are the research assistant from Materials Chemistry and Catalysis Research Unit, the graduate grant from Graduate School, Chulalongkorn University, and the scholarship from Energy Research Institute (ERI), Chulalongkorn University.

Ultimately, I would like to express my inmost gratitude to my family and my best friends for their love, understanding, encouragement, and moral support throughout my entire education.



สถาบันวิทยบริการ
จุฬาลงกรณ์มหาวิทยาลัย

LIST OF CONTENTS

	PAGE
ABSTRACT IN THAI	iv
ABSTRACT IN ENGLISH	v
ACKNOWLEDGEMENTS	vi
LIST OF CONTENTS	vii
LIST OF TABLES	xi
LIST OF FIGURES	xiii
ABBREVIATIONS	xx
CHAPTER I INTRODUCTION	1
1.1 Introduction.....	1
1.2 Literature Review: Development of DMFC Anode.....	6
1.3 Objective and Scopes of This Thesis.....	13
CHAPTER II THEORY	14
2.1 Electrochemical Techniques.....	14
2.1.1 Cyclic Voltammetry.....	14
2.1.2 Chronoamperometry.....	16
2.2 Scanning Electron Microscopy.....	16
2.3 Energy Dispersive X-ray Spectroscopy.....	17
CHAPTER III EXPERIMENTAL	19
3.1 Instruments and Apparatus.....	19
3.1.1 Electrochemical Instruments.....	19
3.1.2 Electron Microscope Instruments.....	20
3.2 Chemicals.....	20
3.3 Preparation of Reagents.....	21
3.3.1 Electrolyte solutions.....	21
3.3.1.1 Sulfuric Acid Solution (0.10 M).....	21
3.3.1.2 Sulfuric Acid Solution (0.50 M).....	21
3.3.2 Stock Solutions.....	21

	PAGE
3.3.2.1 Platinum (IV) Solution (2.00 mM).....	21
3.3.2.2 Ruthenium (III) Solution (2.00 mM).....	21
3.3.2.3 Gold (III) Solution (2.00 mM).....	21
3.3.2.4 Rhodium (III) Solution (2.00 mM).....	22
3.3.2.5 Chromium (III) Solution (2.00 mM).....	22
3.3.2.6 Iron (II) Solution (2.00 mM).....	22
3.3.2.7 Palladium (II) Solution (2.00 mM).....	22
3.3.2.8 Cobalt (II) Solution (2.00 mM).....	22
3.3.2.9 Silver (I) Solution (2.00 mM).....	22
3.3.3 Metal Composite Solutions.....	23
3.3.3.1 Platinum–Ruthenium Solutions.....	23
3.3.3.2 Platinum–Gold Solutions.....	23
3.3.3.3 Platinum–Rhodium Solutions.....	24
3.3.3.4 Platinum–Ruthenium–Gold Solutions.....	24
3.4 Experimental Procedures.....	25
3.4.1 Electrode Modification.....	25
3.4.1.1 Platinum Electrode.....	25
3.4.1.2 Boron-Doped Diamond Electrode.....	26
3.4.2 Effects of Deposition Conditions.....	27
3.4.2.1 Deposition Methodology.....	27
3.4.2.2 Effect of Deposition Time.....	27
3.4.2.3 Effect of Potentiostatic Step.....	27
3.4.3 Characterization of The Modified Electrodes.....	28
3.4.3.1 Background Current.....	28
3.4.3.2 Morphology of The Modified Electrodes.....	28
3.4.4 Catalytic Activity of The Modified Electrodes.....	28
3.4.5 Stability of The Modified Electrodes.....	28
CHAPTER IV RESULTS AND DISCUSSION.....	29
4.1 Platinum Electrode.....	29

	PAGE
4.1.1 Background Current.....	29
4.1.2 Methanol Oxidation by Platinum Electrode.....	29
4.1.3 Effect of Oxygen.....	31
4.2 Modification of Platinum Electrode with Co-metal Catalysts.....	32
4.2.1 Electrochemical Reactions of Metal Solutions and Metal Deposition on Platinum Electrode.....	32
4.2.2 Electrochemical Characterization of Metal Modified Platinum Electrodes.....	34
4.2.3 Catalytic Activity of Metal Modified Electrodes.....	36
4.3 Boron-Doped Diamond Electrode.....	37
4.3.1 Background Current.....	37
4.3.2 Methanol Oxidation by Boron-Doped Diamond Electrode.....	38
4.4 Modification of Boron-Doped Diamond Electrode with Platinum.....	38
4.4.1 Effect of Potentiostatic Step.....	43
4.4.2 Effect of Total Deposition Time.....	43
4.5 Modification of Boron-Doped Diamond Electrode with Bi-metallic Catalysts....	45
4.5.1 Platinum–Ruthenium Modified Boron-Doped Diamond Electrode.....	46
4.5.1.1 Effect of Deposition Methodology.....	46
4.5.1.2 Effect of Total Deposition Time	50
4.5.1.3 Effect of Potentiostatic Step	52
4.5.2 Platinum–Gold Modified Boron-Doped Diamond Electrode.....	54
4.5.2.1 Effect of Deposition Methodology.....	54
4.5.3 Platinum–Rhodium Modified Boron-Doped Diamond Electrode.....	58
4.5.3.1 Effect of Deposition Methodology.....	58
4.6 Modification of Boron-Doped Diamond Electrode with Tri-metallic Catalysts...	62
4.6.1 Platinum–Ruthenium–Gold Modified Boron-Doped Diamond Electrode..	62
4.6.2 Platinum–Ruthenium–Rhodium Modified Boron-Doped Diamond Electrode.....	64
4.7 Characterization of The Modified Electrodes.....	67
4.7.1 Platinum/Boron-Doped Diamond Electrode.....	67

	PAGE
4.7.2 Platinum–Ruthenium/Boron-Doped Diamond Electrode.....	68
4.7.3 Platinum–Ruthenium–Rhodium/Boron-Doped Diamond Electrode.....	69
4.8 Stability Studies of The Modified Electrodes.....	70
CHAPTER V CONCLUSIONS.....	72
REFERENCES.....	73
APPENDIXES.....	77
VITA.....	81



สถาบันวิทยบริการ
จุฬาลงกรณ์มหาวิทยาลัย

LIST OF TABLES

TABLE		PAGE
3.1	Electrochemical instruments.....	19
3.2	Electron microscope instruments.....	20
3.3	Chemicals.....	20
3.4	Pt–Ru composite solutions.....	23
3.5	Pt–Au composite solutions.....	23
3.6	Pt–Rh composite solutions.....	24
3.7	Pt–Ru–Au composite solutions.....	24
4.1	Anodic peak potentials and currents for the oxidation of 1.00 M methanol in 0.50 M sulfuric acid using Pt electrode at the scan rate of 50 mVs ⁻¹ (number of repetitive scans = 5).....	31
4.2	Cathodic peak potentials of 2.00 mM metal solutions and their potentiostatic conditions for the deposition at the Pt electrode.....	34
4.3	Potentiostatic conditions for preparing Pt/BDD electrodes (deposition potential = -0.24 V and total deposition time = 450 s).....	43
4.4	Potentiostatic conditions for preparing Pt _{0.95} Ru _{0.05} /BDD electrodes with various potentiostatic step widths (deposition potential = -0.24 V and total deposition time = 810 s).....	52
4.5	Effect of deposition method on the cluster and particle sizes of Pt at BDD surfaces.....	67

TABLE	PAGE
4.6 Effect of potentiostatic step on Pt-Ru cluster and particle sizes at BDD surfaces of Pt _{0.95} Ru _{0.05} /BDD electrodes (preparation: deposition potential = -0.24 V and total deposition time = 810 s).....	69



สถาบันวิทยบริการ
จุฬาลงกรณ์มหาวิทยาลัย

LIST OF FIGURES

FIGURE	PAGE
2.1 Schematic of (a) cyclic voltammetric waveform and (b) cyclic voltammogram....	15
2.2 Potential-time waveform of chronoamperometry.....	16
2.3 Schematic of general SEM.....	17
3.1 Electrochemical cell with Pt working electrode.....	25
3.2 Electrochemical cell with BDD working electrode	26
4.1 Cyclic voltammogram for the electrolyte solution of 0.50 M sulfuric acid recorded with Pt electrode at the scan rate of 50 mVs^{-1}	30
4.2 Cyclic voltammogram for 1.00 M methanol in 0.50 M sulfuric acid solution recorded with the Pt electrode at the scan rate of 50 mVs^{-1}	30
4.3 Cyclic voltammograms recorded with Pt electrode at the scan rate of 50 mVs^{-1} for 0.50 M sulfuric acid (solid lines) and 0.50 M sulfuric acid containing 2.00 mM of (a) Ru (III), (b) Rh (III), (c) Cr (III), (d) Co (II), (e) Fe (II), (f) Pd (II), and (g) Ag (I) solutions (dash lines).....	33
4.4 Cyclic voltammograms for 0.50 M sulfuric acid recorded with the Pt electrode (solid lines) and the modified electrodes: (a) PtRu, (b) PtRh, (c) PtPd, and (d) PtAg (dash lines) at the scan rate of 50 mVs^{-1}	35
4.5 Relationships between current density for methanol oxidation in 0.50 M sulfuric acid and methanol concentration of Pt, PtRu, PtRh, and PtPd electrodes at the scan rate of 50 mVs^{-1}	37

FIGURE	PAGE
4.6 Cyclic voltammograms for 0.50 M sulfuric acid containing 0.00 M (solid line) and 1.00 M (dash line) methanol recorded with BDD electrode at the scan rate of 50 mVs ⁻¹	38
4.7 Cyclic voltammograms for 0.50 M sulfuric acid containing 0.00 mM (solid line) and 2.00 mM (dash line) Pt (IV) solution recorded with BDD electrode at the scan rate of 50 mVs ⁻¹	39
4.8 Current vs. time plot obtained during the deposition of 2.00 mM Pt (IV) solution on BDD electrode with potentiostatic conditions (initial potential = 1.10 V; deposition potential = -0.24 V; potentiostatic step = 90 s; and total deposition time = 450 s).....	40
4.9 Cyclic voltammogram for 0.50 M sulfuric acid recorded with Pt/BDD electrode at the scan rate of 50 mVs ⁻¹	41
4.10 Cyclic voltammogram for 1.00 M methanol in 0.50 M sulfuric acid solution recorded with Pt (solid line) and Pt/BDD (dash line) electrodes at the scan rate of 50 mVs ⁻¹	42
4.11 Current density vs. methanol concentration curves of Pt (solid line) and Pt/BDD (dash line) electrodes obtained in 0.50 M sulfuric acid at the scan rate of 50 mVs ⁻¹	42
4.12 Current density vs. methanol concentration curves of Pt/BDD electrodes prepared with one-step deposition (solid line) and multi-step deposition (dash line) obtained in 0.50 M sulfuric acid at the scan rate of 50 mVs ⁻¹	44

FIGURE	PAGE
4.13 Cyclic voltammograms for 0.50 M sulfuric acid recorded at the scan rate of 50 mVs ⁻¹ by Pt/BDD electrodes prepared with the total deposition times of (a) 270 s, (b) 450 s, and (c) 630 s (electrode preparation: deposition potential = -0.24 V and potentiostatic step = 90 s).....	44
4.14 Current density vs. methanol concentration curves of Pt electrode and Pt/BDD electrodes prepared with the total deposition times of (a) 270 s, (b) 450 s, and (c) 630 s for methanol oxidation in 0.50 M sulfuric acid at the scan rate of 50 mVs ⁻¹	45
4.15 Cyclic voltammograms for 0.50 M sulfuric acid containing 0.00 mM (solid line) and 2.00 mM (dash line) Ru (III) solution recorded with the Pt/BDD electrode at the scan rate of 50 mVs ⁻¹	46
4.16 Cyclic voltammograms for 0.50 M sulfuric acid recorded at the scan rate of 50 mVs ⁻¹ by Pt/BDD electrode (solid line) and PtRu/BDD electrodes using the Ru deposition times of (a) 10 s, (b) 90 s, and (c) 450 s.....	47
4.17 Current density vs. methanol concentration curves of Pt/BDD electrode and PtRu/BDD electrodes using the Ru deposition times of (a) 10 s, (b) 90 s, and (c) 450 s for methanol oxidation in 0.50 M sulfuric acid at the scan rate of 50 mVs ⁻¹	48
4.18 Cyclic voltammograms for 0.50 M sulfuric acid recorded at the scan rate of 50 mVs ⁻¹ by Pt/BDD electrode (solid line) and PtRu/BDD electrodes prepared with Pt:Ru composite precursors of (a) 95:5, (b) 90:10, and (c) 80:20.....	49
4.19 Current density vs. methanol concentration curves of Pt/BDD, (a) Pt _{0.95} Ru _{0.05} /BDD, (b) Pt _{0.90} Ru _{0.10} /BDD, and (c) Pt _{0.80} Ru _{0.20} /BDD electrodes for	

FIGURE	PAGE
methanol oxidation in 0.50 M sulfuric acid at the scan rate of 50 mVs ⁻¹	49
4.20 Cyclic voltammograms for 0.50 M sulfuric acid recorded at the scan rate of 50 mVs ⁻¹ by Pt _{0.95} Ru _{0.05} /BDD electrodes prepared with the total deposition times of (a) 270 s, (b) 450 s, (c) 630 s, (d) 720 s, (e) 810 s, and (f) 900 s.....	51
4.21 Current density vs. methanol concentration curves of Pt _{0.95} Ru _{0.05} /BDD electrodes prepared with the total deposition times of (a) 270 s, (b) 450 s, (c) 630 s, (d) 720 s, (e) 810 s, and (f) 900 s for methanol oxidation in 0.50 M sulfuric acid at the scan rate of 50 mVs ⁻¹	51
4.22 Cyclic voltammograms for 0.50 M sulfuric acid recorded at the scan rate of 50 mVs ⁻¹ by Pt _{0.95} Ru _{0.05} /BDD electrodes prepared with the potentiostatic step widths of (a) 10.0 s, (b) 22.5 s, (c) 45.0 s, (d) 90.0 s, (e) 135.0 s, and (f) 202.5 s..	53
4.23 Current density vs. methanol concentration curves of Pt _{0.95} Ru _{0.05} /BDD electrodes prepared with the potentiostatic step widths of (a) 10.0 s, (b) 22.5 s, (c) 45.0 s, (d) 90.0 s, (e) 135.0 s, and (f) 202.5 s for methanol oxidation in 0.50 M sulfuric acid solution at the scan rate of 50 mVs ⁻¹ (electrode preparation: deposition potential = -0.24 V and total deposition time = 810 s).....	53
4.24 Cyclic voltammograms recorded with Pt/BDD at the scan rate of 50 mVs ⁻¹ for 0.50 M sulfuric acid containing 0.00 mM (dash line) and 2.00 mM (solid line) Au (III) solution.....	54
4.25 Cyclic voltammograms for 0.50 M sulfuric acid recorded at the scan rate of 50 mVs ⁻¹ by Pt/BDD electrode (solid line) and PtAu/BDD electrodes with the Au deposition times of (a) 10 s, (b) 45 s, and (c) 90 s.....	55

FIGURE	PAGE
4.26 Current density vs. methanol concentration curves of Pt/BDD electrode and PtAu/BDD electrodes prepared with the Au deposition times of (a) 10 s, (b) 45 and (c) 90 s for methanol oxidation in 0.50 M sulfuric acid at the scan rate of 50 mVs^{-1}	56
4.27 Cyclic voltammograms for 0.50 M sulfuric acid recorded at the scan rate of 50 mVs^{-1} by Au/BDD electrode (solid line) and PtAu/BDD electrodes with the Pt:Au precursors of (a) 95:5, (b) 90:10, and (c) 80:20.....	57
4.28 Current density vs. methanol concentration curves of Pt/BDD, (a) $\text{Pt}_{0.95}\text{Au}_{0.05}$ /BDD, (b) $\text{Pt}_{0.90}\text{Au}_{0.10}$ /BDD, and (c) $\text{Pt}_{0.80}\text{Au}_{0.20}$ /BDD electrodes for methanol oxidation in 0.50 M sulfuric acid at the scan rate of 50 mVs^{-1}	57
4.29 Cyclic voltammograms of Pt/BDD electrode for 0.50 M sulfuric acid containing 0.00 mM (solid line) and 2.00 mM (dash line) Rh (III) solution at the scan rate of 50 mVs^{-1}	58
4.30 Cyclic voltammograms for 0.50 M sulfuric acid recorded with Pt/BDD electrode (solid line) and PtRh/BDD electrodes prepared with the Rh deposition times of (a) 10 s, (b) 45 s, and (c) 90 s at the scan rate of 50 mVs^{-1}	59
4.31 Current density vs. methanol concentration curves of Pt/BDD electrode and PtRh/BDD electrodes prepared with the Rh deposition times of (a) 10 s, (b) 45 s, and (c) 90 s for methanol oxidation in 0.50 M sulfuric acid at the scan rate of 50 mVs^{-1}	60
4.32 Cyclic voltammograms for 0.50 M sulfuric acid recorded at the scan rate of 50 mVs^{-1} by Pt/BDD, (a) $\text{Pt}_{0.95}\text{Rh}_{0.05}$ /BDD, (b) $\text{Pt}_{0.90}\text{Rh}_{0.10}$ /BDD, and (c) $\text{Pt}_{0.80}\text{Rh}_{0.20}$ /BDD electrodes.....	61

FIGURE	PAGE
<p>4.33 Current density vs. methanol concentration curves of Pt/BDD, (a) Pt_{0.95}Rh_{0.05}/BDD, (b) Pt_{0.90}Rh_{0.10}/BDD, and (c) Pt_{0.80}Rh_{0.20}/BDD electrodes for methanol oxidation in 0.50 M sulfuric acid at the scan rate of 50 mVs⁻¹</p>	61
<p>4.34 Cyclic voltammograms for 0.50 M sulfuric acid recorded with (a) Pt_{0.95}Ru_{0.04}Au_{0.01}/BDD, (b) Pt_{0.95}Ru_{0.03}Au_{0.02}/BDD, (c) Pt_{0.95}Ru_{0.02}Au_{0.03}/BDD, and (d) Pt_{0.95}Ru_{0.01}Au_{0.04}/BDD at the scan rate of 50 mVs⁻¹ ((i) Pt–Ru oxide reduction region and (ii) Au oxide reduction region).....</p>	63
<p>4.35 Current density vs. methanol concentration curves of (a) Pt_{0.95}Ru_{0.05}/BDD, (b) Pt_{0.95}Au_{0.05}/BDD, (c) Pt_{0.95}Ru_{0.04}Au_{0.01}/BDD, (d) Pt_{0.95}Ru_{0.03}Au_{0.02}/BDD, (e) Pt_{0.95}Ru_{0.02}Au_{0.03}/BDD, and (f) Pt_{0.95}Ru_{0.01}Au_{0.04}/BDD electrodes for methanol oxidation in 0.50 M sulfuric acid at the scan rate of 50 mVs⁻¹</p>	64
<p>4.36 Cyclic voltammogram for Rh (III) solution recorded with Pt_{0.95}Ru_{0.05}/BDD electrode at the scan rate of 50 mVs⁻¹</p>	65
<p>4.37 Cyclic voltammograms for 0.50 M sulfuric acid recorded at the scan rate of 50 mVs⁻¹ by Pt_{0.95}Ru_{0.05}/BDD electrode (solid line) and PtRuRh/BDD electrodes with the Rh deposition times of (a) 10 s, (b) 45 s, and (c) 90 s.....</p>	66
<p>4.38 Current density vs. methanol concentration curves of Pt_{0.95}Ru_{0.05}/BDD electrode and PtRuRh/BDD electrodes with the Rh deposition times of (a) 10 s, (b) 45 s, and (c) 90 s for methanol oxidation in 0.50 M sulfuric acid at the scan rate of 50 mVs⁻¹</p>	66
<p>4.39 SEM images of Pt/BDD electrodes prepared by multi-step deposition (5×90 s, a and b) and one-step deposition (450 s, c and d) at the magnification of 10,000 (a and c) and 50,000 (b and d).....</p>	68

FIGURE	PAGE
<p>4.40 SEM images of Pt_{0.95}Ru_{0.05}/BDD electrode prepared by potentiostatic conditions (deposition potential = -0.24 V; total deposition time = 810 s; and potentiostatic step width = 10 s) at the magnification of (a) 10,000 and (b) 50,000.....</p>	69
<p>4.41 SEM images of Pt_{0.95}Ru_{0.05}Rh/BDD electrodes with Rh deposition time of 10 s at the magnification of (a) 10,000 and (b) 50,000.....</p>	70
<p>4.42 Current density measured at the potential of 0.64 V vs. time for the electrooxidation of 1.00 M methanol at (a) Pt/BDD, (b) PtRu/BDD, and (c) PtRuRh/BDD electrodes.....</p>	71

ABBREVIATIONS

A	Ampere
i_{pa}	Anodic Peak Current
E_{pa}	Anodic Peak Potential
AFM	Atomic Force Microscopy
BDD	Boron-Doped Diamond Thin Film Electrode
CO ₂	Carbon Dioxide
CO	Carbon Monoxide
CNFs	Carbon Nanofibers
CNTs	Carbon Nanotubes
i_{pc}	Cathodic Peak Current
E_{pc}	Cathodic Peak Potential
°C	Degree Celsius
°F	Degree Fahrenheit
DEFC	Direct Ethanol Fuel Cell
DMFC	Direct Methanol Fuel Cell
Au	Gold
H ₂	Hydrogen Gas
MCFC	Molten Carbonate Fuel Cell
NO _x	Nitrogen Oxides
O ₂	Oxygen Gas
PAFC	Phosphoric Acid Fuel Cell
Pt	Platinum
PEMFC	Proton Exchange Membrane Fuel Cell
RHE	Reversible Hydrogen Electrode
Rh	Rhodium
Ru	Ruthenium
SEM	Scanning Electron Microscopy
s	Second

Ag/AgCl

Silver/Silver Chloride

V

Volt

XPS

X-ray Photoelectron Spectroscopy



สถาบันวิทยบริการ
จุฬาลงกรณ์มหาวิทยาลัย

CHAPTER I

INTRODUCTION

1.1 Introduction

Global warming due to greenhouse gases has been a worldwide problem since 1970s. Air pollutions such as carbon monoxide (CO), nitrogen oxides (NO_x), benzene, and many other volatile inorganic and organic compounds are emitted into our environment by motor vehicles. Road transportation, an important requirement of modern society, is presently hindered by traffic emission legislations as well as the limited availability of petroleum fuels, and as a consequence, their high prices. For nearly 270 years, we have burned our fossil fuels and have reached the era of exhausting the liquid part of them. In order to decrease the use of non-renewable and environmentally harmful petroleum, advances in electric vehicles that produce negligible amounts of harmful emissions are essential. Fuel cells are considered as environmentally friendly power sources for the vehicles. They are electrochemical energy conversion devices that can convert the chemical energy of a reaction directly into electrical energy. Fuel cells produce electricity by externally supplying fuel on the anode side and oxidant on the cathode side. These reactants react in the presence of an electrolyte. Generally, the reactants flow in and the reaction products flow out whereas the electrolyte remains in the cell. Fuel cells can operate virtually continuously as long as the necessary flows of reactants are maintained.

In 1970s, the main focus about clean energy research was on large-scale power generation and most investment was primarily directed towards molten carbonate fuel cell (MCFC) and phosphoric acid fuel cell (PAFC) technologies. In 1990s, transport, in particular light duty vehicles, gained more attention, leading to greater concentration of effort on the development of proton exchange membrane fuel cell (PEMFC). Due to the fact that there has been increasing interest in small-to-medium scale power generation for portable or mobile products since 2000, one of the most popular devices has become direct methanol fuel cell (DMFC).

Molten Carbonate Fuel Cell (MCFC)

The electrolyte of MCFC is a molten mixture of alkali metal carbonates ($\text{Li}_2\text{CO}_3\text{-K}_2\text{CO}_3$ or $\text{Li}_2\text{CO}_3\text{-Na}_2\text{CO}_3$), which is retained in a ceramic matrix of lithium aluminium oxide (LiAlO_2). At the high operating temperatures ranging from 600 to 700°C, the alkali carbonates form a highly conductive molten salt of which carbonate ions (CO_3^{2-}) provide ionic conduction. As a fuel, carbon dioxide (CO_2) needs to be supplied to the MCFC cathode in accompany with oxygen gas (O_2) for carbonate ion generation. At the same time, CO_2 will be formed at the anode; therefore, the recycling of CO_2 from the anode to cathode is required in MCFC. MCFC is only suitable for high power units such as power plant.

Phosphoric Acid Fuel Cell (PAFC)

PAFC is a fuel cell operating in an acid media. Using liquid phosphoric acid as an electrolyte, PAFC is operated at approximately 180-220°C to maintain reasonable ionic conductivity and prevent cell corrosion from electrolyte decomposition and volatilization. At the operating temperatures, the expelled water can be reused as a steam for water heating. PAFC is the first commercially available fuel cell and has been frequently used in energy storage applications. Typically, PAFCs are utilized as stationary power generating systems, but some PAFCs are for powering large vehicles such as city buses. Unfortunately, their costs are too high compared with other conventional power generating systems.

Proton Exchange Membrane Fuel Cell (PEMFC)

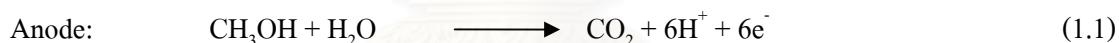
PEMFC is believed to be the best type of fuel cell for transport applications as well as stationary and portable applications. PEMFC uses a solid polymer membrane as an electrolyte. When this polymer is saturated with water, it allows proton to permeate through itself causing ionic, not electronic conduction. As PEMFC fuel, a stream of hydrogen gas (H_2) is delivered to the anode side where the hydrogen molecule is splitted into protons and electrons by appropriate catalyst. Then, the protons permeate across the polymer electrolyte to the cathode whereas the electrons flow through an external circuit to produce electric power. At the same time, a stream

of oxygen gas (O_2), usually in the form of air, is supplied to the cathode side where it can react with the permeated protons and the electrons arriving through the external circuit to produce water.

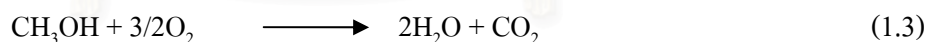
Direct Methanol Fuel Cell (DMFC)

DMFC is a subcategory of PEMFC using methanol as a direct fuel with no need of fuel reforming step. Since methanol is a liquid at temperature from -97.0°C to 64.7°C (-142.6°F to 148.5°F), handling and transportation of methanol are much easier than those of H_2 which have always been big safety issues. Moreover, methanol is a readily available and low-cost liquid fuel that produces energy density in comparable level with gasoline. Therefore, methanol can be deployed in a consumer environment with little concern and portable power systems with methanol are conceivable.

DMFC is operated at relatively low temperatures (<100.0 - 150.0°C) and uses either vaporized or liquid methanol. The overall cell reaction is the combustion of methanol to CO_2 and water via the two reactions at anode and cathode:



Thus, the overall reaction in the DMFC is represented by the equation



Thermodynamically, the reversible potentials for the overall cell reactions at 25°C are 1.214 V for DMFC and 1.23 V for the hydrogen fuel cell. Consequently, this fact has generated the interest in the DMFC as an alternative power source. Nevertheless, the most challenging problem of DMFC is that the anode reaction proceeds much more slowly than the reaction in hydrogen fuel cell because the oxidation of methanol is a much more complex process. If this problem is solved, DMFC could be used in all mobile fuel cell applications, including such high power applications as motor vehicles.

Anode Catalyst for DMFC

In 1988, methanol oxidation was electrochemically investigated by Parsons and Vandernoot [1]. It was found that the oxidation would possibly involve two main processes:

- (i) electrosorption of methanol onto a substrate
- (ii) addition of oxygen to adsorbed carbon-containing intermediates to generate carbon dioxide

There are few electrode materials that are capable of adsorbing methanol in acid solutions; only platinum (Pt) and alloys thereof show practical activities and stability. Adsorption and subsequent reactions of methanol on Pt take place by the following steps [2]:



The extension of the potential may include the formation of platinum hydroxide ($\text{Pt-OH}_{\text{ads}}$) and oxidation of CO to CO_2 , as shown in equations (1.8) to (1.12).



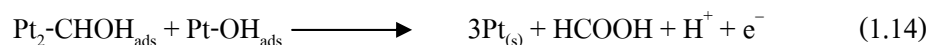
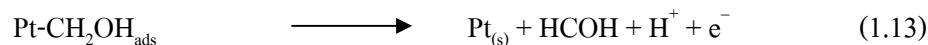
or



or



Additional reactions that have been suggested are:



or





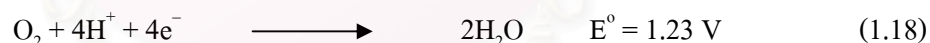
or



Equations (1.4)-(1.7) present electroadsorption process whereas subsequent reactions involve oxygen transfer or oxidation of surface-bonded intermediates. Arising from the equation (1.7), the stable $\text{Pt-CO}_{\text{ads}}$ species might possibly poison the Pt catalyst. $\text{Pt-CO}_{\text{ads}}$ can mostly be removed by the oxygenated species, $\text{Pt-OH}_{\text{ads}}$, as described in equation (1.9). Since the dissociative adsorption of water (equation (1.10)) occurs slowly at the normal operating potentials of DMFC. Therefore, on a pure Pt surface, the dissociative chemisorption of water has become the rate-determining step when the applied potential is below 0.70 V. This result has led to the investigation of any catalyst that can dissociate water at relatively lower potentials than 0.70 V and show high reactivity towards oxidation of CO as well as high stability for DMFC anodic reactions.

Cathode Catalyst for DMFC

In addition, the reduction of O_2 at the cathode is another important factor in the operation of DMFC.



Several classes of materials, including noble metals, their alloys, macrocyclic complexes, transition metal oxides, and transition metal sulfides, show sufficient activity towards oxygen reduction. The most familiar catalysts for oxygen reduction are the noble and coinage metals, especially Pt and gold (Au).

1.2 Literature Review: Development of DMFC Anode

Oxidation of methanol at Pt-based electrodes has been extensively studied. Although the methanol oxidation is still a subject of interest, the applicability of Pt-based electrodes has unavoidably been restricted due to the accumulation of surface-poisoning intermediates (*e.g.*, CO), leading to the loss of electroactivity with time.

T. Iwasita [3] investigated the oxidation of methanol at Pt electrodes by means of voltammetric and spectroscopic techniques. Parallel reaction pathways for the formation of CO₂ and either formic acid or formaldehyde were proposed, depending upon several parameters such as methanol concentration, electrode roughness, and electrolysis time.

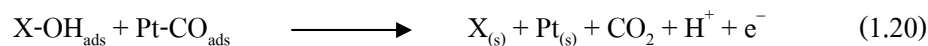
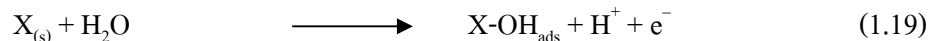
H. Nonaka *et al.* [4] used a pressure cell equipped with silver/silver chloride/0.10 M potassium chloride external pressure-balanced reference electrode (EPBRE) to electrochemically probe the oxidation of methanol on the Pt electrode under high temperatures (92-252°C) at the sweep rate of 1 or 10 mVs⁻¹. The measured potential (*vs.* EPBRE) was corrected to the reversible hydrogen electrode (RHE) scale based on the experimental or theoretically calculated pH of the solution at high temperature. Results showed that, in comparison with the methanol oxidation at the ambient temperature, the strongly adsorbed CO intermediate was presumably formed, but it was oxidized at a lower potential at higher temperature.

A. Kucernak *et al.* [5] employed a mesoporous Pt catalyst containing the pore diameter of 34 Å as a catalytic material for the electrooxidation of methanol. Using the mesoporous Pt catalyst, the oxidation of 1.00 M methanol in 0.50 M sulfuric acid gave rise to the peak potential at 0.55 V (*vs.* RHE) with the current of 42 mAcm⁻² (20 Ag⁻¹) at 65°C. Compared to the normal dispersed Pt catalysts, the activity of methanol oxidation by the mesoporous catalyst seems to be significantly improved.

Since Pt can be poisoned by adsorbed CO and other intermediates during the methanol oxidation, its catalytic performance was improved by addition of an oxophilic metal [6]. In the bimetallic systems, the Pt accomplishes the dissociative chemisorption of methanol while the

added metal forms oxygenated species which will oxidize the carbonaceous residues to CO₂ (equations (1.19)-(1.20)).

When X represents any oxophilic metal such as ruthenium (Ru) and tin (Sn),



W. Chrzanowski *et al.* [7] studied the effects of controlled amounts of electrodeposited Ru on the catalytic activity of low-index single-crystal Pts (Pt (111), Pt (100), and Pt (110)) and polycrystalline Pt. They found that the Pt (111) surface covered with 0.20 monolayer of Ru was the best laboratory-scale anode material for DMFC.

W.F. Lin *et al.* [8] investigated the electrochemical deposition of Ru on Pt (111) surface in a closed ultra high vacuum (UHV) transfer system by means of electron diffraction and Auger spectroscopy. Ru formed a monoatomic commensurate layer at small coverage whereas mostly islands with a bilayer height at higher coverage were detected. Using cyclic voltammetry and *in situ* FTIR spectroscopy, adsorption and electrooxidation of CO at such Ru modified Pt (111) electrodes were examined. Compared to the pure Pt, the Ru-CO bond is weakened and the Pt-CO bond is strengthened on the modified electrodes. It was concluded that the electrooxidation of CO would take place preferably at the Ru layer to which the adsorbed CO on the Pt surface tended to migrate.

S.G. Lemos *et al.* [9] observed the oxidation of methanol using a metallic bilayer electrodeposited on a Pt substrate. In the blank solution, it was shown that the electrochemical behavior of both the Pt/Ru/Pt and the bulk Pt were similar, except in the oxygen-evolution potential region. The electroactive areas and the roughness mean square (RMS) factors measured by atomic force microscopy (AFM) for both materials are the same. Linear voltammetric results of CO confirmed that the systems have same real surface area and also showed a 54-mV shift in the negative direction for the CO peak potential at the bilayer electrode.

In addition, new catalyst supporters which are nanoporous carbon materials, carbon nanofibers (CNFs), highly ordered pyrolytic graphite (HOPG), and carbon nanotubes (CNTs)

have been investigated. Results suggested that these materials would promote the electrocatalytic activity of the Pt catalyst.

A.J. Dickinson *et al.* [10] presented Pt–Ru catalysts deposited on carbon substrate for the oxidation of methanol. The catalysts were produced by the deposition of metal carbonyl precursors on carbon substrate in a high boiling-point solvent. Pt–Ru catalysts with high dispersion and narrow size distribution were obtained. These catalysts showed comparable activity with the catalysts produced by the conventional procedure, but offered much easier route to generate ternary and quaternary anode catalysts.

O.V. Cherstiouk *et al.* [11] demonstrated a possible approach to design electrodes for studying the effects of particle size on electrocatalytic activity. Simple chemical deposition was introduced to reproducibly prepare 1.5–3.0 nm Pt nanoparticles anchored to the surface of glassy carbon (GC) or HOPG. The prepared electrodes were used to probe the electrooxidation of adsorbed CO and methanol. Results illustrated that the reactivity of Pt nanoparticles for these reactions was considerably low in comparison with the polycrystalline Pt.

F.J. Rodríguez-Nieto *et al.* [12] compared the catalytic activity for methanol oxidation of the Pt–Ru electrodes produced by either sequential or simultaneous linear-potential electrodeposition on HOPG substrate. After the methanol oxidation, the Ru content in both electrodes decreased. However, the reactivation of simultaneously formed Pt–Ru electrode was observed in the negative potential scan and this reactivation increased when the Ru content on the Pt surface decreased. Morphological and microscopic surface characterization was carried out by scanning electron microscopy (SEM) and AFM.

T. Kim *et al.* [13] prepared highly dispersed Pt and Pt–Ru alloy particles on carbon support by the alcohol reduction method using polyvinylpyrrolidone as a stabilizer. In order to develop these materials as catalysts for polymer electrolyte fuel cell, they were characterized by means of ultraviolet–visible spectroscopy, electron microscopy, X-ray diffraction, and X-ray photoelectron spectroscopy (XPS). Cyclic voltammetric results showed that, compared to the commercial materials, the catalysts had promising activity for oxygen reduction and methanol oxidation.

Z. He *et al.* [14] investigated the oxidation of methanol by Pt–Ru nanoparticles deposited on CNT electrode. Using the potentiostatic method, the Pt–Ru nanoparticles were synthesized from 0.50 M sulfuric acid solution containing ruthenium chloride and chloroplatinic acid. The particle sizes of the prepared Pt–Ru catalyst are approximately 60–80 nm. To study the electrocatalytic properties of the Pt–Ru/CNT/graphite electrodes for methanol oxidation, cyclic voltammograms recorded with these electrodes for the solutions containing 0.10 M methanol and 0.50 M sulfuric acid were obtained. Results showed that the anodic peak potential for methanol oxidation shifted positively, leading to the conclusion that the existing Ru might improve the stability and activity of the electrodes towards methanol oxidation.

Z. Liu *et al.* [15] prepared nano-size Pt and Pt–Ru colloids by microwave-assisted polyol process. Then, the colloids were transferred to the toluene solution of decanthiol with the addition of Vulcan XC-72 as an adsorbant. The metal particle sizes are 4.70 nm and 4.50 nm for the Pt and Pt–Ru catalysts, respectively. At the room temperature, the electrooxidation of liquid ethanol by these catalysts was investigated by cyclic voltammetric method, demonstrating that the Pt–Ru alloy is more catalytically active than the pure Pt. Preliminary tests on a single cell of direct ethanol fuel cell (DEFC) indicated that a Pt₅₂–Ru₄₈/C anode catalyst gave the best electrocatalytic performance among all the carbon-supported Pt and Pt–Ru catalysts.

J.W. Guo *et al.* [16] used Pt–Ru/carbon (PtRu/C) nanocatalysts for direct methanol oxidation. Using sodium borohydride as a reducing agent, the nanocatalysts were prepared by varying the molar ratio of citric acid (reagent) to PtRu salts from 1:1, 2:1, 3:1, and 4:1. It was clear that the electrode with 1:1 citric acid-to-PtRu gave relatively higher current for methanol oxidation and displayed greater tolerance to intermediate species. The fact that the nanocatalysts had well-dispersed PtRu particle sizes around 2.6 nm might possibly enhance the methanol oxidation at lower potential region. Testing PtRu/C catalysts as the anode of DMFC indicated that the in-house PtRu/C nanocatalysts gave slightly higher performance than the commercial PtRu/C (E-TEK) catalysts did.

However, these supports present serious problems such as low stability and the formation of oxide intermediates at the high anodic potentials. Recent achievements in the preparation of highly boron-doped diamond (BDD) on silicon substrate can be an interesting approach. The advantages of BDD as the catalyst support are the following:

- (i) A macroscopic oxide layer does not form on the surface of BDD while putting in contact with an aqueous solution.
- (ii) BDD shows high chemical and electrochemical stability.
- (iii) BDD has very low background current and large electrochemical window.
- (iv) BDD can be heated in air up to 500°C without undergoing significant surface oxidation.

All these properties make BDD a very attractive material to be used as a support in electrocatalysis.

K. Honda *et al.* [17] studied electrocatalytic behavior of boron-doped nanoporous honeycomb diamond film modified with Pt nanoparticles (10-150 nm) in acidic solution by means of cyclic voltammetry and electrochemical impedance spectroscopy. These electrodes exhibited high electroactivity towards the oxidation of several alcohols. In comparison with the bulk Pt electrode, the current density for the methanol oxidation at the Pt-modified honeycomb diamond electrode with the pore size of 400 nm was relatively high. This enhancement was attributed to both high surface area of the nano-honeycomb structure and high electrocatalytic activity of the well-dispersed Pt nanoparticles inside the pores.

F. Montilla *et al.* [18] applied two methods to deposit Pt particles on synthesized BDD surfaces: chemical deposition and electrodeposition under potentiostatic condition. The electrodeposition method led higher dispersion of Pt with the particle sizes of 10-50 nm. However, the stability of the deposited particles was terribly low and could be either dissolved or re-deposited by potential cycling. Using the electrodes for the oxidation of methanol in acidic media, it has been found that, compared to the electrode with one-step deposition, the electrode prepared by multi-step deposition resulted in higher surface area and electroactivity.

Y. Zhang *et al.* [19] electrochemically deposited Au nanoparticles on both hydrogen-terminated and oxygen-terminated BDDs. As noted by linear sweep voltammetry, the surface coverage of Au nanoparticles were 0.07 and 0.18, corresponding to their areas of 0.012 and 0.029 cm^2 , respectively. SEM studies indicated various morphologies of the obtained Au nanoparticles, *i.e.*, random distribution of small spherical particles and clusters. Electrochemical behavior for oxygen reduction of the BDDs was probed by differential pulse voltammetry, showing that the Au modified BDDs were more suitable for oxygen reduction than the polycrystalline Au electrode.

J.A. Bennett *et al.* [20] prepared Pt particles on electrically conducting micro-crystalline and nanocrystalline diamond thin-film electrodes by pulsed galvanostatic deposition. The deposition was varied as functions of pulse number (10-50) and current density (0.50-1.50 mAcm^{-2}). For both morphological BDDs, the nominal Pt particle size was 30 nm with RSD of 50% and the particle coverage was 10^7 - 10^{10} cm^{-2} under the optimum conditions. Typical specific surface areas of 10-50 m^2 per g of Pt, which were more favorable values than those of sp^2 electrodes (*e.g.*, carbon and graphite), were calculably obtained.

I. González-González *et al.* [21] examined the electrochemical behavior of BDD films in 0.50 M sulfuric acid using cyclic voltammetry and sequentially electrodeposited Pt and Ru particles by potential cycling the BDDs in the solutions of these metals between 0.00 and 1.50 V *vs.* silver/silver chloride electrode. The particles were observed by SEM and their composition was verified by energy dispersive spectroscopy (EDS) and XPS, demonstrating that the average particle size was approximately 105 ± 57 nm for Pt–Ru with the coverage of 1.4×10^9 cm^{-2} . Catalytic activity of the electrodeposited metals was also tested by cyclic voltammetry, showing that the maximum current densities for the oxidation of 0.10 M methanol were 0.73 and 0.94 mAcm^{-2} , respectively, for Pt and Pt–Ru deposited on BDD.

G. Siné *et al.* [22] synthesized Pt nanoparticles by the water-in-oil microemulsion technique and deposited the particles onto BDD electrodes. Transmission electron microscopy showed that Pt particles had small spherical shape. Additionally, the catalytic activity of the modified BDD electrode was tested with methanol solution.

H.B. Suffredini *et al.* [23] presented a detailed description of the preparation, characterization, and electrochemical performance towards methanol and ethanol oxidation in acidic media of Pt–ruthenium dioxide (RuO_2) carbon powder composite. The composite was prepared by sol-gel technique and then fixed on the surface of BDD electrode. In comparison with the composite/GC electrode, the composite/BDD had superior performance, probably related to its low capacitive current. Cyclic voltammetry, Tafel plot analysis, and chronoamperometry were used to compare the prepared electrodes to the commercial Pt/carbon powder composite one, displaying that the Pt– RuO_2 /carbon composite electrode gave the maximum anodic current density among all the materials.

G.R. Salazar-Banda *et al.* [24] reported the oxidation of methanol and ethanol at the BDD electrode modified with Pt, Pt– RuO_2 , and Pt– RuO_2 –rhodium dioxide (RhO_2) by sol-gel method. X-ray diffraction analyses confirmed the formation of nanoparticles on the BDD surfaces. SEM and AFM also indicated the existence of nano-clusters whereas the EDX maps showed that the metals were homogeneously distributed on the BDD surface. The CO poisoning effect on methanol and ethanol oxidation was studied by cyclic voltammetric and chronoamperometric techniques. Results illustrated that the catalyst containing Pt, Pt– RuO_2 , and Pt– RuO_2 – RhO_2 deposited on BDD by this method might be one promising alternative for DMFC anode.

1.3 Objective and Scopes of This Thesis

The objective of this research is to develop metal nano-catalysts for the oxidation of methanol deposited on BDD electrode. The thesis is divided into four parts. For the first part, the oxidation of methanol was studied by means of cyclic voltammetry with pure and metal modified Pt as working electrodes to gain necessitated electrochemical information of the metal catalysts. The second part, which is the main part of the thesis, involves optimizing potentiostatic conditions for the modification of BDD electrodes by metal electrocatalysts. Deposition parameters including deposition methodology, deposition time, and potentiostatic step width were determined. Cyclic voltammetric measurement was utilized to investigate not only the effects of the parameters, but also the electrocatalytic activities of the metal catalysts towards methanol oxidation. For the third part, characterization and morphology the modified BDD electrodes were examined by SEM. Finally, the stability of the metal modified BDD electrodes in methanol solution have been tested.



สถาบันวิทยบริการ
จุฬาลงกรณ์มหาวิทยาลัย

CHAPTER II

THEORY

2.1 Electrochemical Techniques

Electroanalytical techniques are concerned with the interplay between electricity and chemistry. They deal with the measurements of electrical quantities, such as current, potential, and charge related to chemical parameters.

Electroanalytical methods have some general advantages over other types of analyses. First, electrochemical measurements are often specific for a particular oxidation state of an element. Second, the instrumentation of electrochemical methods is relatively inexpensive. Third, the features of electrochemical methods provide information about activities rather than concentrations of species.

In this research, cyclic voltammetry and chronoamperometry were used. Details of these methods are described in the following section.

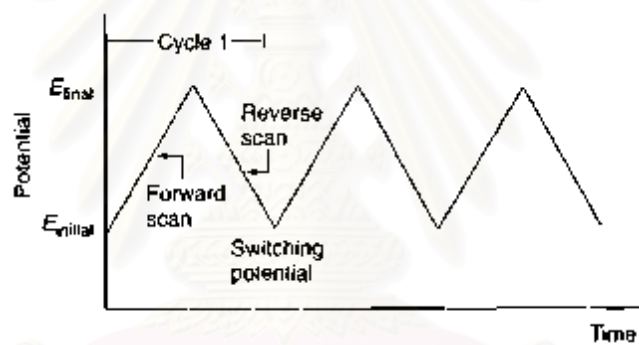
2.1.1 Cyclic Voltammetry

Cyclic voltammetry is the most widely used electrochemical technique for acquiring qualitative information about electron transfer reactions. The significance of cyclic voltammetry results from its ability to rapidly provide considerable information on the thermodynamics of redox processes and the kinetics of heterogeneous electron transfer reactions as well as their coupled chemical reactions or adsorption processes. In electroanalytical investigation, cyclic voltammetry is usually the first experiment performed since it offers a rapid location of redox potentials of the electroactive species and convenient evaluation of the effect of media on the redox process.

Cyclic voltammetry consists of the linearity of scanning potential with a triangular waveform that produces forward and reverse scans (Figure 2.1a). The resulting plot of the

observed current vs. the applied potential is called cyclic voltammogram. The potential is measured between the reference electrode and the working electrode whereas the current is measured between the working electrode and the counter electrode. For this waveform, the forward scan produces a cathodic current for any analyte that can be reduced through the range of the scanned potential. On the contrary, the reverse scan yields an anodic current for the product of the forward scan to be reoxidized. Thus, there are reduction and oxidation peaks observed for a reversible reaction (Figure 2.1b). Significant parameters in a cyclic voltammogram are cathodic peak potential (E_{pc}), anodic peak potential (E_{pa}), cathodic peak current (i_{pc}), and anodic peak current (i_{pa}).

(a)



(b)

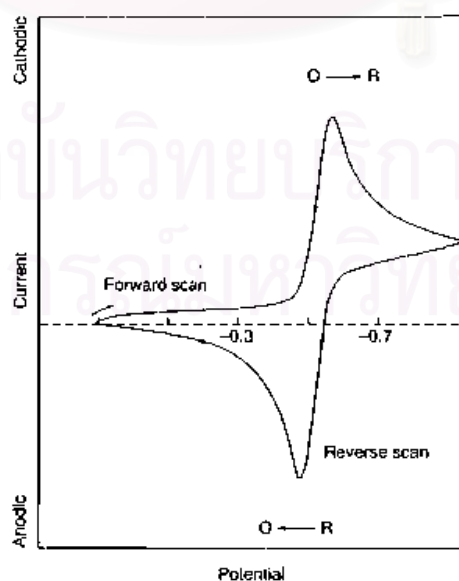


Figure 2.1 Schematic of (a) cyclic voltammetric waveform and (b) cyclic voltammogram

2.1.2 Chronoamperometry

Chronoamperometry involves stepping the potential of the working electrode from a value at which no faradaic reaction occurs to a potential at which faradaic reaction occurs dramatically until the surface concentration of the electroactive species is effectively zero. Figure 2.2 displayed the applied potential-time waveform of this technique. Chronoamperometry is used to study the current-time behavior with no influence of potential change because the potential of the working electrode was changed instantaneously before the current-time response or chrono-amperogram is recorded. Furthermore, chronoamperometry can be applied for the deposition of electroactive species onto the working electrode.

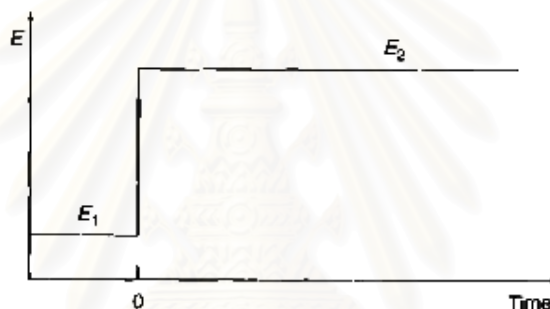


Figure 2.2 Potential-time waveform of chronoamperometry

2.2 Scanning Electron Microscopy

Scanning electron microscope (SEM) is a type of electron microscope that creates various images by focusing the high energy beam of electrons onto the surface of a sample and detecting signals from the interaction of the incident electrons with the sample's surface. Figure 2.3 represents the schematic of a general SEM. Three types of signals gathered from a SEM are secondary electrons, characteristic X-rays, and back-scattered electrons. In SEM, these signals come not only from the primary beam impinging on the sample, but also from other interactions within the sample near its surface. SEM is capable of producing high resolution images of the sample surface in its primary mode, secondary electron imaging. Due to the manner in which the images are created, SEM images have great depth of field that yields a three-dimensional

appearance used for understanding the surface structure of a sample. This great depth of field and the wide range of magnifications are the most familiar imaging mode for specimens in SEM. Characteristic X-rays are emitted when the primary beam causes the ejection of inner shell electrons from the sample and they are used to tell the elemental composition of the sample. Emitted from the sample, the back-scattered electrons may be either separately used to form an image or applied in conjunction with the characteristic X-rays as atomic number contrast clues to the elemental composition of the sample.

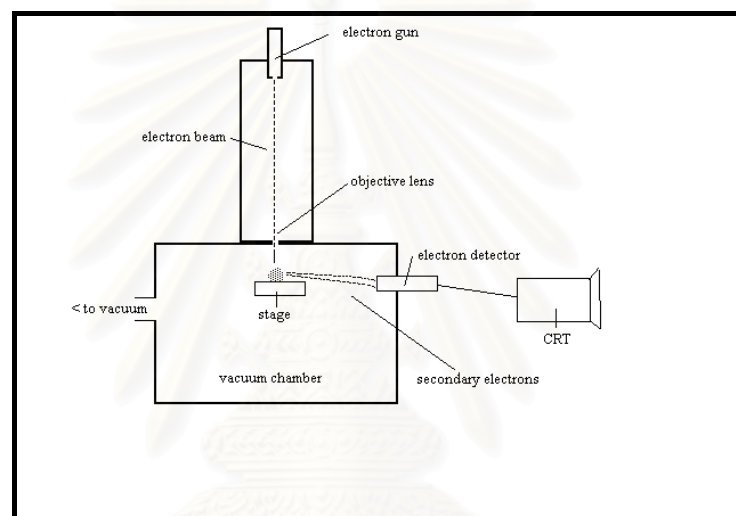


Figure 2.3 Schematic of general SEM

2.3 Energy Dispersive X-ray Spectroscopy

Energy dispersive X-ray spectroscopy (EDS or EDX) is an analytical technique used predominantly for elemental analysis or chemical characterization of a specimen. Being a type of spectroscopy that relies on sample investigation through interaction between electromagnetic radiation and matter, EDX analyzes the X-rays emitted from the matter in the particular fashion. Its characterization capabilities are largely due to the fundamental principle that each element of the periodic table has unique atomic structure giving distinguishable characteristic X-rays. To stimulate the emission of the characteristic X-rays, either the high energy beam of charged particles (*e.g.*, electrons and protons) or the beam of X-rays is focused into a sample. The

incident beam may excite an electron in an inner shell of a atom within the sample, prompting its ejection that results in the formation of an electron hole within the atom's electronic structure. An electron from an outer, higher energy shell then fills the hole, causing the release of X-ray energy which corresponds to the energy difference between the higher energy shell and the lower energy shell. The released X-rays are then detected and analyzed by energy dispersive spectrometer and can be used as the characteristics of the atomic structure of each element.



สถาบันวิทยบริการ
จุฬาลงกรณ์มหาวิทยาลัย

CHAPTER III

EXPERIMENTAL

3.1 Instruments and Apparatus

3.1.1 Electrochemical Instruments

The employed electrochemical instruments and apparatus are summarized in Table 3.1.

Table 3.1 Electrochemical instruments

Instrument	Model	Company (Country)
1. potentiostat	PG-30	Methrom (Switzerland)
2. working electrode		
2.1 boron-doped diamond (BDD)		CSEM (Switzerland)
2.2 platinum (Pt)	MW-2030	BAS (Japan)
3. reference electrode	Ag/AgCl electrode	BAS (Japan)
4. auxiliary electrode	homemade Pt wire	
5. other apparatus		
5.1 homemade cap cell		
5.2 homemade glass cell		
5.3 o-ring	silicone	Japan
5.4 homemade brass holder		
5.5 0.30 μm -alumina powder polishing set	AM 0782	Alpha (USA)
5.6 1.00 μm -alumina powder polishing set	AM 0786	Alpha (USA)
5.7 homemade salt-bridge		

3.1.2 Electron Microscope Instruments

The instruments of electron microscope are given in Table 3.2.

Table 3.2 Electron microscope instruments

Instrument	Model	Company (Country)
1. scanning electron microscope	JSM-6480LV	JEOL (Japan)
2. energy dispersive X-ray	7573	Oxford (England)

3.2 Chemicals

All chemicals used in this research were AR grade. Obtained from Milli-Q-system, deionized-distilled water was used for preparing all chemical solutions. Chemicals and their suppliers are summarized in Table 3.3.

Table 3.3 Chemicals

Chemicals	Manufacturer (Country)
1. sulfuric acid, H_2SO_4	Merck (Germany)
2. methanol, CH_3OH	Merck (Germany)
3. hydrogen hexachloroplatinate (IV) hydrate, $H_2PtCl_6 \cdot xH_2O$	Fluka (Germany)
4. ruthenium (III) chloride hydrate, $RuCl_3 \cdot xH_2O$	Sigma Aldrich (Germany)
5. hydrogen tetrachloroaurate (III) trihydrate, $HAuCl_4 \cdot 3H_2O$	Sigma Aldrich (Germany)
6. rhodium (III) chloride trihydrate, $RhCl_3 \cdot 3H_2O$	Wako (Japan)
7. chromium (III) chloride hexahydrate, $CrCl_3 \cdot 6H_2O$	Fluka (Germany)
8. iron (II) sulfate heptahydrate, $FeSO_4 \cdot 7H_2O$	Fluka (Germany)
9. cobalt (II) sulfate heptahydrate, $CoSO_4 \cdot 7H_2O$	Sigma Aldrich (Germany)
10. palladium (II) acetate, $Pd(C_2H_3O_2)_2$	Wako (Japan)
11. silver (I) nitrate, $AgNO_3$	Sigma Aldrich (Germany)

3.3 Preparation of Reagents

The following section explained procedures for the preparation of metal solutions in this work.

3.3.1 Electrolyte Solutions

3.3.1.1 Sulfuric Acid Solution (0.10 M)

An aliquot of 5.34 mL of concentrated sulfuric acid was diluted with deionized-distilled water and was made to the final volume of 1.00 L.

3.3.1.2 Sulfuric Acid Solution (0.50 M)

The procedure described in section 3.3.1.1 was applied to prepare the solution, except that 26.74 mL of concentrated sulfuric acid was used.

3.3.2 Stock Solutions

3.3.2.1 Platinum (IV) Solution (2.00 mM)

Accurate weight (4.1 mg) of hydrogen hexachloroplatinate (IV) hydrate was dissolved in 5.00 mL of 0.50 M sulfuric acid solution.

3.3.2.2 Ruthenium (III) Solution (2.00 mM)

Accurate weight (2.1 mg) of ruthenium (III) chloride hydrate was dissolved in 5.00 mL of 0.50 M sulfuric acid solution.

3.3.2.3 Gold (III) Solution (2.00 mM)

Accurate weight (3.9 mg) of hydrogen tetrachloroaurate (III) trihydrate was dissolved in 5.00 mL of 0.50 M sulfuric acid solution.

3.3.2.4 Rhodium (III) Solution (2.00 mM)

Accurate weight (2.6 mg) of rhodium (III) chloride trihydrate was dissolved in 5.00 mL of 0.50 M sulfuric acid solution.

3.3.2.5 Chromium (III) Solution (2.00 mM)

Accurate weight (2.7 mg) of chromium (III) chloride hexahydrate was dissolved in 5.00 mL of 0.50 M sulfuric acid solution.

3.3.2.6 Iron (II) Solution (2.00 mM)

Accurate weight (2.8 mg) of iron (II) sulfate was dissolved in 5.00 mL of 0.50 M sulfuric acid solution.

3.3.2.7 Palladium (II) Solution (2.00 mM)

Accurate weight (2.3 mg) of palladium (II) acetate was dissolved in 5.00 mL of 0.50 M sulfuric acid solution.

3.3.2.8 Cobalt (II) Solution (2.00 mM)

Accurate weight (2.8 mg) of cobalt (II) sulfate heptahydrate was dissolved in 5.00 mL of 0.50 M sulfuric acid solution.

3.3.2.9 Silver (I) Solution (2.00 mM)

Accurate weight (1.7 mg) of silver (I) nitrate was dissolved in 5.00 mL of 0.50 M sulfuric acid solution.

3.3.3 Metal Composite Solutions

3.3.3.1 Platinum–Ruthenium Solutions

Platinum–ruthenium (Pt–Ru) composite solutions were prepared by mixing stock solutions of Pt and Ru (sections 3.3.2.1 and 3.3.2.2). Three composite solutions are listed in Table 3.4.

Table 3.4 Pt–Ru composite solutions

Pt:Ru Ratio	Pt (mL)	Ru (mL)	Total Volume (mL)
80:20	2.40	0.60	3.00
90:10	2.70	0.30	3.00
95:5	2.85	0.15	3.00

3.3.3.2 Platinum–Gold Solutions

Platinum–gold (Pt–Au) composite solutions were prepared by mixing stock solutions of Pt and Au (sections 3.3.2.1 and 3.3.2.3). Three composite solutions are listed in Table 3.5.

Table 3.5 Pt–Au composite solutions

Pt:Au Ratio	Pt (mL)	Au (mL)	Total Volume (mL)
80:20	2.40	0.60	3.00
90:10	2.70	0.30	3.00
95:5	2.85	0.15	3.00

3.3.3.3 Platinum–Rhodium Solutions

Platinum–rhodium (Pt–Rh) composite solutions were prepared by mixing stock solutions of Pt and Rh (sections 3.3.2.1 and 3.3.2.4). Three composite solutions are listed in Table 3.6.

Table 3.6 Pt–Rh composite solutions

Pt:Rh Ratio	Pt (mL)	Rh (mL)	Total Volume (mL)
80:20	2.40	0.60	3.00
90:10	2.70	0.30	3.00
95:5	2.85	0.15	3.00

3.3.3.4 Platinum–Ruthenium–Gold Solutions

Platinum–ruthenium–gold (Pt–Ru–Au) composite solutions were prepared by mixing stock solutions of Pt, Ru, and Au (sections 3.3.2.1, 3.3.2.2, and 3.3.2.3). The prepared composite solutions are shown in Table 3.7.

Table 3.7 Pt–Ru–Au composite solutions

Pt:Ru:Au Ratio	Pt (mL)	Ru (mL)	Au (mL)	Total Volume (mL)
95:5:0	2.85	0.15	-	3.00
95:4:1	2.85	0.12	0.03	3.00
95:3:2	2.85	0.09	0.06	3.00
95:2:3	2.85	0.06	0.09	3.00
95:1:4	2.85	0.03	0.12	3.00
95:0:5	2.85	-	0.15	3.00

3.4 Experimental Procedures

In this section, it mainly consists of procedures for electrode modification, studying deposition parameters, examining properties of the modified electrodes, probing the electrode towards methanol oxidation, and studying the stability of the modified electrode.

3.4.1 Electrode Modification

3.4.1.1 Platinum Electrode

In this experiment, metal solutions were firstly studied by means of cyclic voltammetry to gain information about deposition potentials. Metals were deposited at platinum (Pt) electrode by chronoamperometric method with potentiostatic conditions. Electrochemical measurements were performed in a compartment glass cell using a potentiostat. Figure 3.1 shows an electrochemical cell for the experiment. The Pt electrode (0.075 cm^2 -area) was used as a working electrode. Silver/silver chloride (Ag/AgCl) electrode and Pt wire electrode were used as reference and auxiliary electrodes, respectively.



Figure 3.1 Electrochemical cell with Pt working electrode

3.4.1.2 Boron-Doped Diamond Electrode

In this experiment, metal solutions were firstly studied by means of cyclic voltammetry to gain information about deposition potentials. Metals were deposited at boron-doped diamond (BDD) by chronoamperometric method with potentiostatic conditions. Electrochemical measurements were performed in a compartment cap cell using a potentiostat. Figure 3.2 shows an electrochemical cell for the experiment. BDD electrode (0.017 cm^2 -area) was used as a working electrode. Ag/AgCl electrode and Pt wire electrode were used as reference and auxiliary electrodes, respectively. The diamond electrode was pressed at the bottom of the cell by a smooth ground joint sealed with o-ring. Ohmic contact was made by placing the backside of the gold (Au) substrate of the diamond electrode on a brass plate. Activation of BDD electrode was performed with the use of anodic pretreatment in 0.10 M sulfuric acid solution by cyclic voltammetry.



Figure 3.2 Electrochemical cell with BDD working electrode

3.4.2 Effects of Deposition Conditions

3.4.2.1 Deposition Methodology

- Sequential Deposition

In this experiment, Pt was firstly deposited onto BDD electrode. Then, the Pt/BDD was used as a working electrode for coating the second metal as a co-catalyst. Deposition method was earlier mentioned in section 3.4.1.2.

- Simultaneous Deposition

In this experiment, activated BDD electrode was used as a working electrode. Metal composite solutions in section 3.3 were used as metal precursors for the deposition. Deposition method was earlier mentioned in section 3.4.1.2.

3.4.2.2 Effect of Deposition Time

Effect of deposition time was studied by varying the total time of metal deposition during electrode modification. These studies were carried out in order to find the optimized deposition time that gave the modified electrode with the highest electrocatalytic activity for the oxidation of methanol.

3.4.2.3 Effect of Potentiostatic Step

Since the metal was deposited onto the electrode by chopping the applied potential signal into multiple potentiostatic deposition steps, the duration of the potentiostatic step was varied to find the optimized potentiostatic step that caused the modified electrode with the highest electrocatalytic activity for methanol oxidation.

3.4.3 Characterization of The Modified Electrodes

3.4.3.1 Background Current

The modified electrodes were used as working electrodes. Ag/AgCl electrode and Pt wire electrode were used as reference and auxiliary electrodes, respectively. Cyclic voltammograms were obtained in the solution of 0.50 M sulfuric acid which served as a supporting electrolyte.

3.4.3.2 Morphology of The Modified Electrodes

The morphology of the modified electrodes were examined by means of scanning electron microscopy.

3.4.4 Catalytic Activity of The Modified Electrodes

Electrocatalytic activity of the modified electrodes for methanol oxidation was investigated by obtaining their cyclic voltammograms in 0.10-10.00 M methanol solution containing 0.50 M sulfuric acid at the room temperature.

3.4.5 Stability of The Modified Electrodes

The stability of the modified electrodes was probed by collecting current vs. time curve for the oxidation of 1.00 M methanol in 0.50 M sulfuric acid. Using chronoamperometric technique, the potential of the modified electrode was constantly hold at 0.64 V to allow the existence of the methanol oxidation.

CHAPTER IV

RESULTS AND DISCUSSION

This chapter described results related to the electrodes modified by the potentiostatic method. All the modified electrodes were discussed in terms of their current densities for methanol oxidation. In addition, the morphology of the optimum modified electrodes were carried out.

4.1 Platinum Electrode

4.1.1 Background Current

The background current of the platinum (Pt) electrode was studied by cyclic voltammetry. Figure 4.1 shows the background voltammogram of the bare Pt electrode in 0.50 M sulfuric acid solution. For the Pt electrode, the voltammogram reveals well characterized Pt oxide formation–reduction processes [25]. The anodic peak in the potential range of 0.70-1.10 V represents the formation process whereas the cathodic peak at 0.70-0.20 V is the reduction process. Note that all the potentials in the thesis correspond to the silver/silver chloride (Ag/AgCl) reference electrode.

4.1.2 Methanol Oxidation by Platinum Electrode

Methanol oxidation process in acidic medium on the Pt electrode was initially studied with 0.10 M methanol using cyclic voltammetry at the scan rate of 50 mVs^{-1} from 0.00 V to 1.10 V. Figure 4.2 displays the anodic peak at 0.55 V in the positive potential sweep. Furthermore, during the negative sweep from 1.10 V to 0.00 V, another anodic peak related to methanol re-oxidation process was observed.

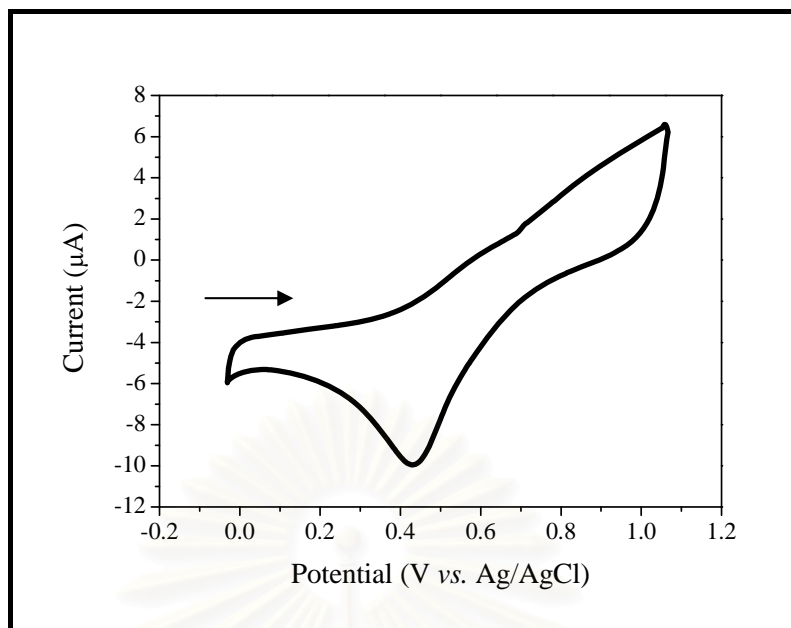


Figure 4.1 Cyclic voltammogram for the electrolyte solution of 0.50 M sulfuric acid recorded with Pt electrode at the scan rate of 50 mVs^{-1}

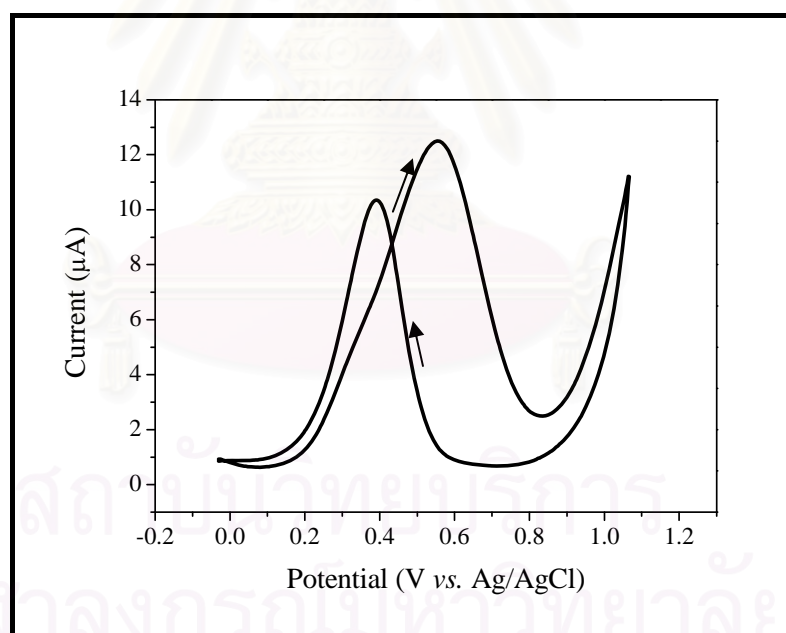
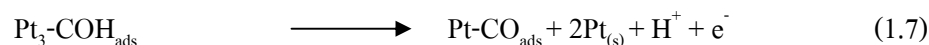
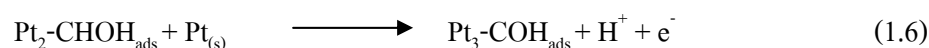
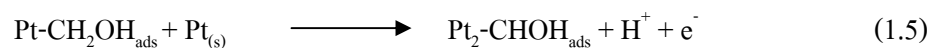
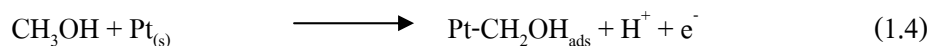
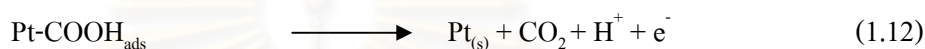
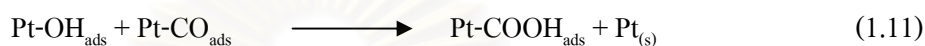


Figure 4.2 Cyclic voltammogram for 1.00 M methanol in 0.50 M sulfuric acid solution recorded with the Pt electrode at the scan rate of 50 mVs^{-1}

The first anodic peak in the cyclic voltammogram for methanol oxidation on Pt can be explained as the dehydrogenation of methanol followed by the oxidation of adsorbed intermediates. As mentioned in Chapter 1 (p. 4), the possible reactions are [2]:



The second anodic peak for the methanol re-oxidation was observed in the reverse scan. The main products of the re-oxidation process are adsorbed carbon monoxide (CO) and carbon dioxide (CO₂). Possible reactions for the process are:



4.1.3 Effect of Oxygen

Cyclic voltammetric experiment with a Pt electrode was used to study the influence of oxygen gas (O₂) on the oxidation of methanol. In this experiment, nitrogen gas (N₂) was purged into the studied solution for 15 min to confirm the absence of O₂. Table 4.1 shows the anodic peak potential and current for the oxidation of 1.00 M methanol in 0.50 M sulfuric acid at the scan rate of 50 mVs⁻¹. Shown in Table 4.1, obtained from repetitive scans, the anodic peak currents for methanol oxidation in the presence of atmospheric O₂ (air) had inconsistent values. However, the fact that current sizes for the methanol oxidation in air are significantly higher than those obtained in N₂ implies that O₂ might possibly promote the methanol oxidation process. From this point of view, it should be advantageous to perform all the experiments in air.

Table 4.1 Anodic peak potentials and currents for the oxidation of 1.00 M methanol in 0.50 M sulfuric acid using Pt electrode at the scan rate of 50 mVs⁻¹ (number of repetitive scans = 5)

Atmosphere	E _p ^{ox} (V vs. Ag/AgCl)	i _p ^{ox} (mAcm ⁻²)
air	0.5596±0.0071	0.2363±0.0657
N ₂	0.6653±0.0130	0.0362±0.0047

4.2 Modification of Platinum Electrode with Co-metal Catalysts

Seriously, methanol oxidation at the Pt electrode has the problem about the accumulation of surface poisoning intermediates. Poisoning phenomena can be avoided by alloying Pt with oxophilic metals such as ruthenium (Ru), rhodium (Rh), *etc.*

4.2.1 Electrochemical Reactions of Metal Solutions and Metal Deposition on Platinum Electrode

Firstly, cyclic voltammogram experiment at the Pt electrode was used to examine the electrochemical reaction of each metal solution. Figure 4.3 shows cyclic voltammograms sweeping towards negative direction obtained from 2.00 mM metal precursor solutions which are: (a) Ru (III); (b) Rh (III); (c) chromium (III) or Cr (III); (d) cobalt (II) or Co (II); (e) iron (II) or Fe (II); (f) palladium (II) or Pd (II); and (g) silver (I) or Ag (I) solutions, respectively. The cathodic peaks of Ru (III) ion at 0.28 V (Figure 4.3a) and Rh (III) ion at 0.27 V (Figure 4.3b) represented the deposition of Ru and Rh on the Pt electrode. Shown in Figures 4.3c and 4.3d, there was no cathodic peak observed, meaning that neither Cr or Co was deposited on the Pt electrode at this potential region. Figure 4.3e shows reversible couple of Fe (III)/Fe (II) ions. Thus, it is unlikely to deposit Fe on the Pt electrode. The cathodic peak of Pd (II) ion at 0.18 V and that of Ag (I) ion at 0.28 V were shown in Figures 4.3f and 4.3g, respectively, displaying that both metals might be deposited on the Pt electrode.

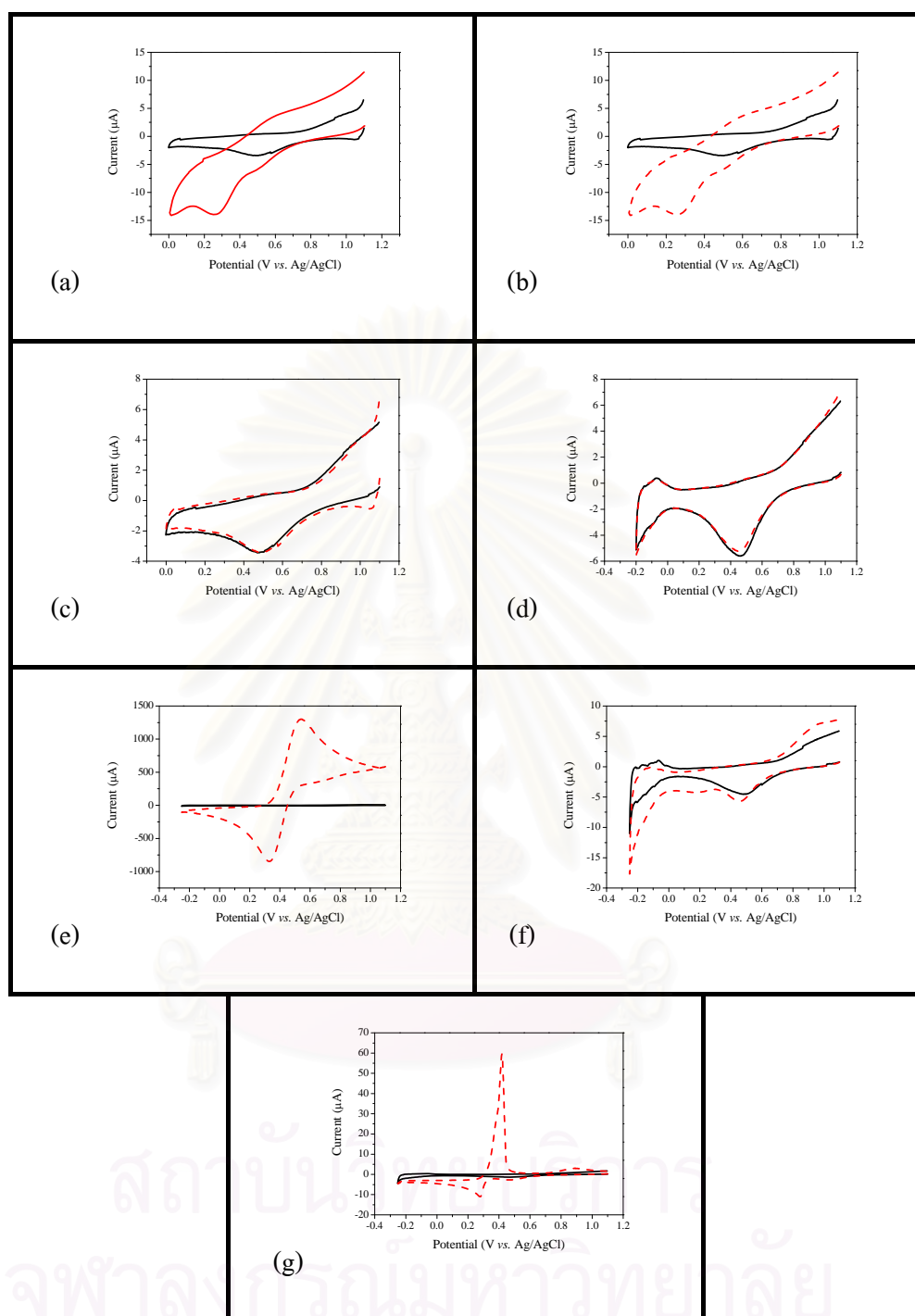


Figure 4.3 Cyclic voltammograms recorded with Pt electrode at the scan rate of 50 mVs^{-1} for 0.50 M sulfuric acid (solid lines) and 0.50 M sulfuric acid containing 2.00 mM of (a) Ru (III), (b) Rh (III), (c) Cr (III), (d) Co (II), (e) Fe (II), (f) Pd (II), and (g) Ag (I) solutions (dash lines)

After gaining electrochemical information in Figure 4.3, the deposition potential for each possible metal was chosen to be slightly more negative than its reduction potential. Table 4.2 lists electrochemical data from cyclic voltammograms in Figure 4.3 and the potentiostatic conditions for metal deposition via chronoamperometry. These data are deposition potential (E_{dep}) and deposition time (Time_{dep}).

Table 4.2 Cathodic peak potentials of 2.00 mM metal solutions and their potentiostatic conditions for the deposition at the Pt electrode

Metal	$E_{\text{p}}^{\text{red}}$ (V vs. Ag/AgCl)	E_{dep} (V vs. Ag/AgCl)	Time_{dep} (s)
Ru	0.28	0.15	90
Rh	0.25	0.15	90
Cr	-	-	-
Co	-	-	-
Fe	0.33	-	-
Pd	0.17	0.03	90
Ag	0.28	0.00	90

4.2.2 Electrochemical Characterization of Metal Modified Platinum Electrodes

Obtained via chronoamperometric technique, the electrochemical properties of the modified Pt electrodes were investigated by means of cyclic voltammetry. Cyclic voltammograms were recorded at the scan rate of 50 mVs^{-1} from 0.00 V to 1.10 V (vs. Ag/AgCl) in a glass cell using 0.50 M sulfuric acid as an electrolyte. Figure 4.4 shows characteristic voltammograms of the Pt electrode modified with metals via potentiostatic conditions. Figure 4.4a presents cyclic voltammograms of the Pt electrode and the Pt modified with Ru (PtRu) electrode. It was found that the PtRu electrode provided higher current for metal oxide reduction at 0.50 V than the Pt electrode. Cyclic voltammogram of the Rh-modified Pt (PtRh) electrode is shown in Figure 4.4b. Similar to the PtRu electrode, the PtRh electrode provided higher current for metal oxide reduction than the Pt electrode. Note that the characteristic peaks of Ru and Rh in

Figures 4.4a and 4.4b were mentioned in the literature [26]. These metal oxide reduction peaks became broad due to the potential overlapping between the reduction of Pt oxide and the reduction of Ru oxide or Rh oxide. Figure 4.4c compares cyclic voltammograms of the Pt and the Pd-modified Pt (PtPd) electrodes. The cathodic peak of Pd oxide reduction at 0.30 V was previously seen in voltammetric curves published elsewhere for PtPd/carbon electrode [27]. Cyclic voltammograms recorded with the Pt electrode and the Ag-modified Pt (PtAg) electrode are shown in Figure 4.4d. Characteristic oxidation at 0.20 V and reduction at 0.10 V of Ag were observed [28]. As illustrated in Figure 4.4, we have successfully deposited Ru, Rh, Pd, and Ag on the Pt electrode.

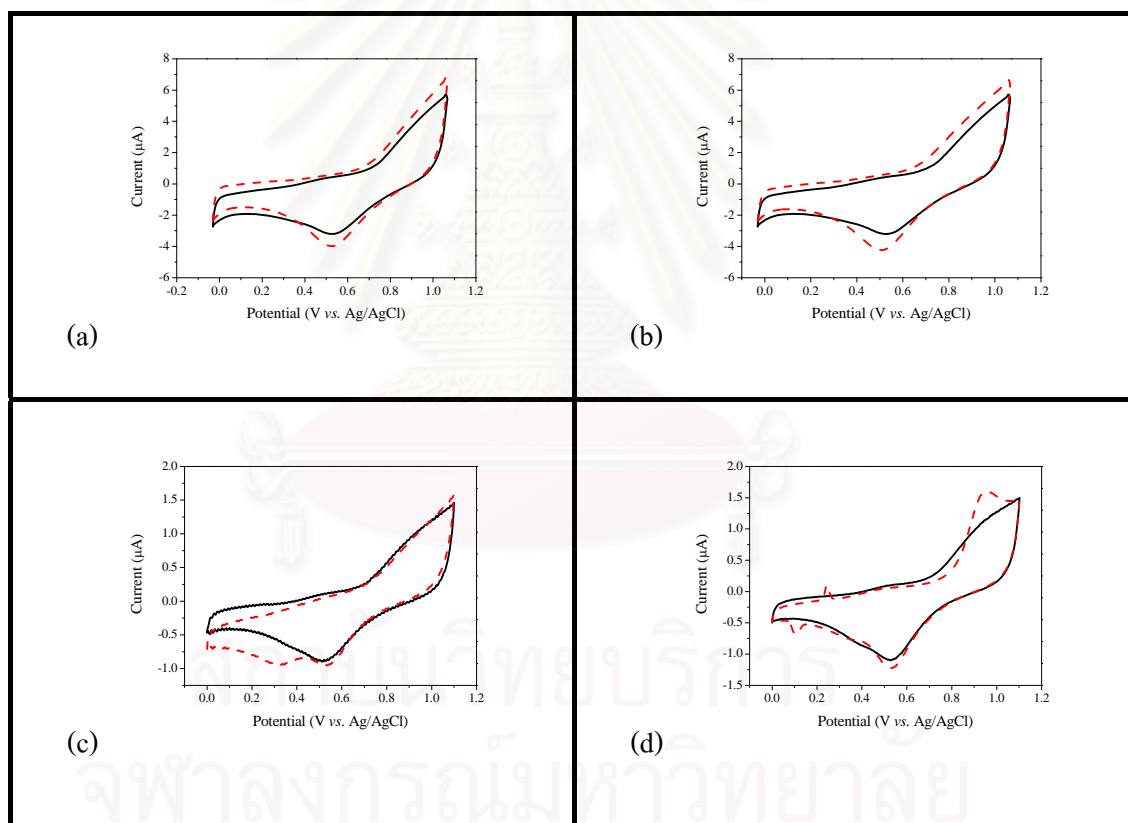


Figure 4.4 Cyclic voltammograms for 0.50 M sulfuric acid recorded with the Pt electrode (solid lines) and the modified electrodes: (a) PtRu, (b) PtRh, (c) PtPd, and (d) PtAg (dash lines) at the scan rate of 50 mVs^{-1}

4.2.3 Catalytic Activity of Metal Modified Electrodes

Activity of the metal modified electrodes towards methanol oxidation was investigated by using cyclic voltammetry. Cyclic voltammograms recorded with the modified electrodes were obtained at the room temperature in a glass cell containing 0.10 M, 0.25 M, 0.50 M, 1.00 M, 2.00 M, and 4.00 M methanol in 0.50 M sulfuric acid solutions. At the scan rate of 50 mVs^{-1} , the activity of the electrodes was estimated from the anodic peak current obtained from the tenth cycle of the forward voltammetric scan (0.00-1.10 V) where the anodic current was at the constant value. The concept of using data from the tenth cycle was applied throughout this research. It should be pointed out that these experimental conditions were used to probe activity for methanol oxidation of all electrodes in the thesis. Figure 4.5 presents the relationships between anodic current density and methanol concentration. In all methanol concentrations, the PtRu was the most sensitive electrode towards methanol. Both PtRu and PtRh electrodes gave higher current density for methanol oxidation than the Pt electrode. As shown in equations 1.8-1.12 (p. 4), it has been well known that poisoning CO at the pure Pt surface can react with oxygenated species to yield CO_2 . The formation of oxygenated species at the pure Pt electrode requires severe condition (*i.e.*, Pt-OH is only formed in substantial quantities at the potential above 0.70 V *vs.* reversible hydrogen electrode) whereas the oxophilic metals that are easily oxidized than Pt could oxidize surface-adsorbed species at a lower potential [6], as shown in equations 1.19-1.20 (p. 7). Figure 4.5 also displays that Pd was the poorest co-catalyst for methanol oxidation among Ru, Rh, and Pd. For the case of the PtAg electrode, it was not suitable for methanol oxidation because there was no anodic peak observed during the experiment with methanol.

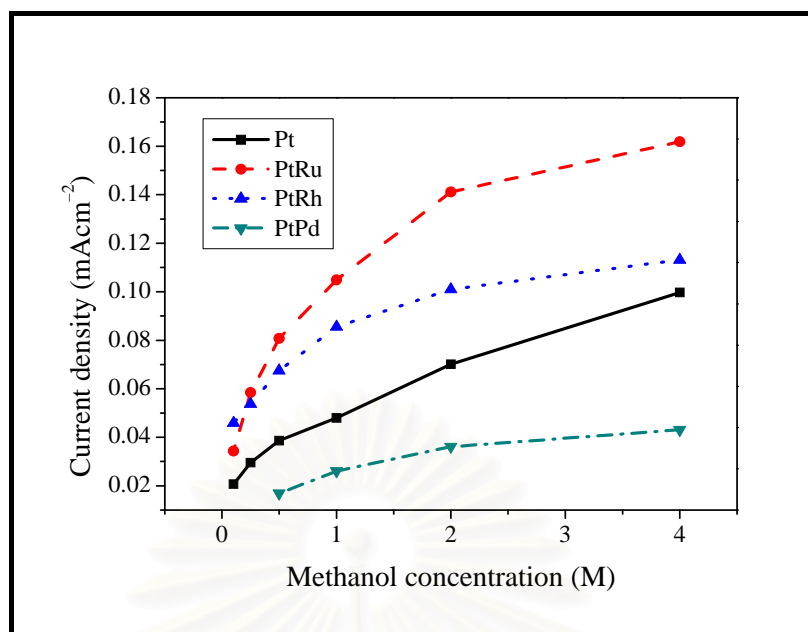


Figure 4.5 Relationships between current density for methanol oxidation in 0.50 M sulfuric acid and methanol concentration of Pt, PtRu, PtRh, and PtPd electrodes at the scan rate of 50 mVs^{-1}

4.3 Boron-Doped Diamond Electrode

From the results with the Pt working electrode, we had found that the addition of proper co-catalyst accelerated methanol oxidation process. Therefore, boron-doped diamond (BDD) electrode was used as a supporting material for the metal catalysts with the intention of improving overall catalytic performance for methanol oxidation.

4.3.1 Background Current

The background current of BDD electrode was studied by obtaining cyclic voltammogram of 0.50 M sulfuric acid scanned from 0.00 V to 1.10 V in the homemade cap cell. Shown in the solid line of Figure 4.6, BDD electrode gave low background current after the anodic pretreatment step. It has been known that anodic pretreatment causes BDD electrode to become hydrophilic [29], improving its ability for attaching with another species.

4.3.2 Methanol Oxidation by Boron-Doped Diamond Electrode

Without the deposition of any metal catalyst, BDD electrode was used to probe methanol oxidation process in acidic medium. Cyclic voltammogram for 0.10 M methanol solution recorded with BDD electrode at the scan rate of 50 mVs^{-1} (Figure 4.6, dash line) shows no peak for methanol oxidation, revealing that BDD electrode has low activity towards the oxidation of methanol [17].

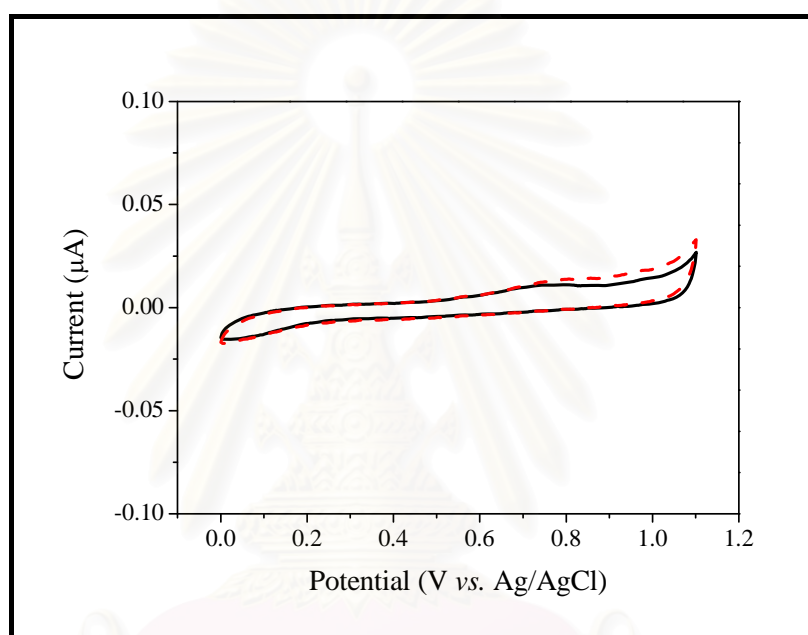


Figure 4.6 Cyclic voltammograms for 0.50 M sulfuric acid containing 0.00 M (solid line) and 1.00 M (dash line) methanol recorded with BDD electrode at the scan rate of 50 mVs^{-1}

4.4 Modification of Boron-Doped Diamond Electrode with Platinum

Electrochemical Reaction of Platinum Solution and Platinum Deposition on Boron-Doped Diamond Electrode

Since it was well known that Pt served as a catalyst for methanol oxidation, we firstly tested whether Pt could be deposited on BDD electrode as a base catalyst. In this experiment, cyclic voltammetry at BDD electrode was brought to study electrochemical reaction of Pt (IV) solution in the potential range between 1.10 V and -0.30 V . Figure 4.7 shows the first-cycle cyclic voltammogram for 2.00 mM Pt (IV) solution recorded at BDD electrode. The

voltammogram had similar shape with voltammetric results of Pt published elsewhere [20]. At the forward scan heading towards negative potential, the cathodic peak for the reduction of Pt (IV) ion to metallic Pt at approximately -0.19 V was observed. Thus, the Pt deposition potential was selected to be slightly more negative than -0.19 V in order to guarantee the completion of the deposition. For comparison, the background voltammogram is displayed in the solid line.

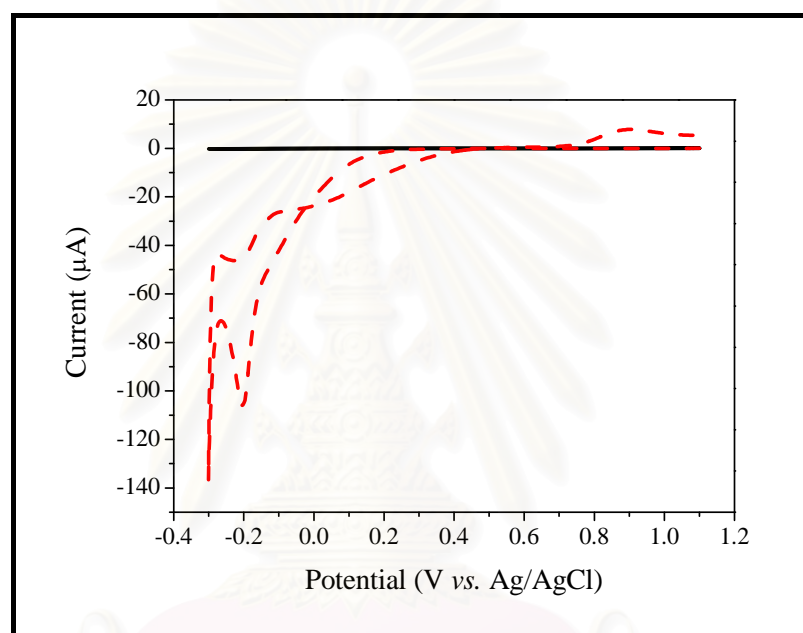


Figure 4.7 Cyclic voltammograms for 0.50 M sulfuric acid containing 0.00 mM (solid line) and 2.00 mM (dash line) Pt (IV) solution recorded with BDD electrode at the scan rate of 50 mVs^{-1}

Electrochemical deposition of Pt on BDD electrode was carried out by chronoamperometry with potentiostatic conditions. The conditions were the deposition potential of -0.24 V, the potentiostatic step of 90 s, and the total deposition time of 450 s. Previous studies about the mechanism for electrochemical deposition of Pt on BDD electrode [11] found that multi-step deposition led to Pt particles with nano-sizes. Figure 4.8 plots the observed current during the course of potentiostatic deposition. Between the adjacent 90 s-potentiostatic steps, there was equilibration period for 10 s.

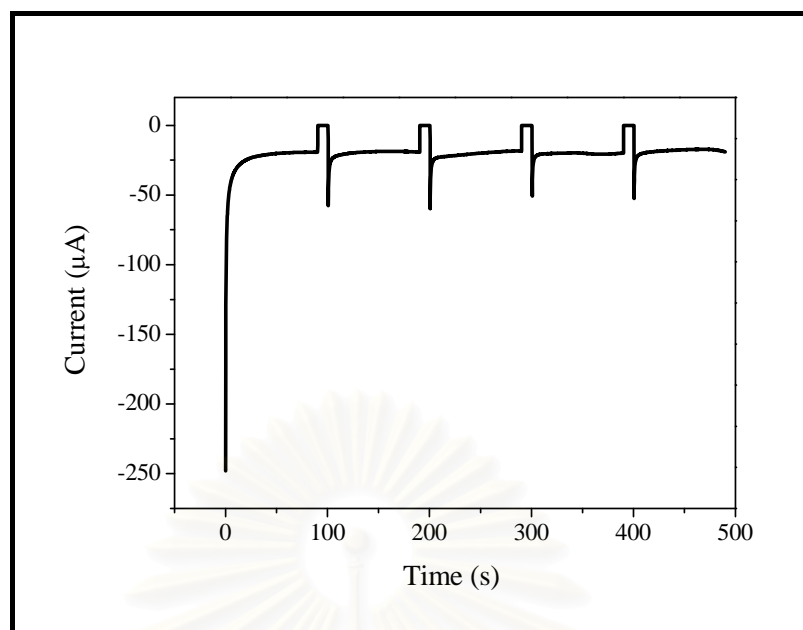


Figure 4.8 Current vs. time plot obtained during the deposition of 2.00 mM Pt (IV) solution on BDD electrode with potentiostatic conditions (initial potential = 1.10 V; deposition potential = -0.24 V; potentiostatic step = 90 s; and total deposition time = 450 s)

Electrochemical Characterization of Platinum Modified Boron-Doped Diamond

Electrode

Electrochemical characterization of Pt modified BDD (Pt/BDD) electrode was revealed by its cyclic voltammogram for 0.50 M sulfuric acid solution that was swept from -0.30 V to 1.10 V at the scan rate of 50 mVs^{-1} (Figure 4.9). The voltammogram presents typical electrochemical processes of polycrystalline Pt surface [30] such as hydrogen adsorption/ desorption (-0.30 V to 0.00 V), the oxide formation (0.80 V to 1.10 V), and the oxide reduction (0.70 V to 0.30 V), demonstrating that Pt particles were successfully deposited onto BDD surface with a good electrical contact.

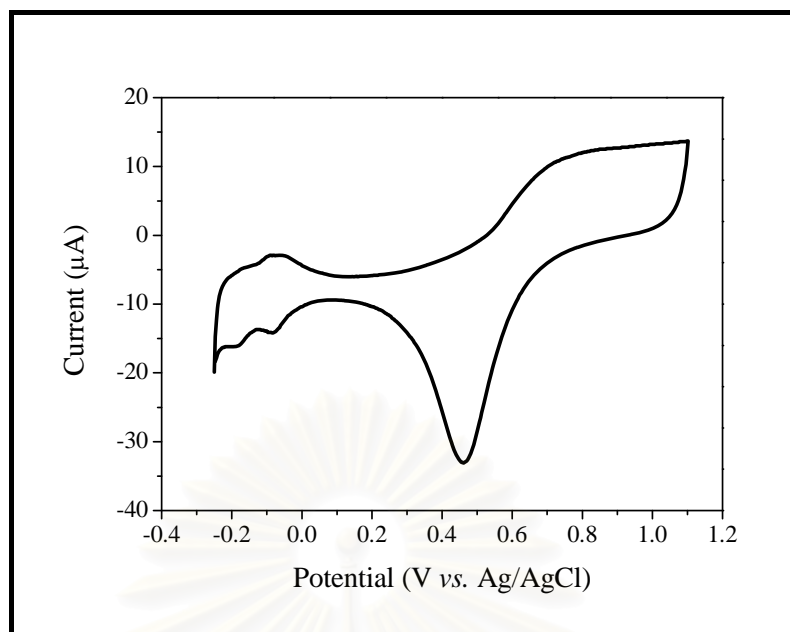


Figure 4.9 Cyclic voltammogram for 0.50 M sulfuric acid recorded with Pt/BDD electrode at the scan rate of 50 mVs^{-1}

Catalytic Activity of Platinum Modified Boron-Doped Diamond Electrode

Cyclic voltammetry was used to investigate the activity of Pt/BDD electrode in methanol solution at the potential range from 0.00 V to 1.10 V. The electrode activity was estimated from the anodic peak current obtained from the forward scan of the tenth voltammetric cycle where the anodic current became constant. Shown in Figure 4.10, the methanol oxidation reaction by Pt/BDD electrode was similar to the reaction by Pt electrode. Figure 4.11 directly compares current density–methanol concentration relationships of the two electrodes, illustrating that the Pt/BDD electrode gave 10 times higher current density than the Pt electrode. It was clear that the BDD supporter enhanced the catalytic activity of the deposited Pt for methanol oxidation in acidic solution.

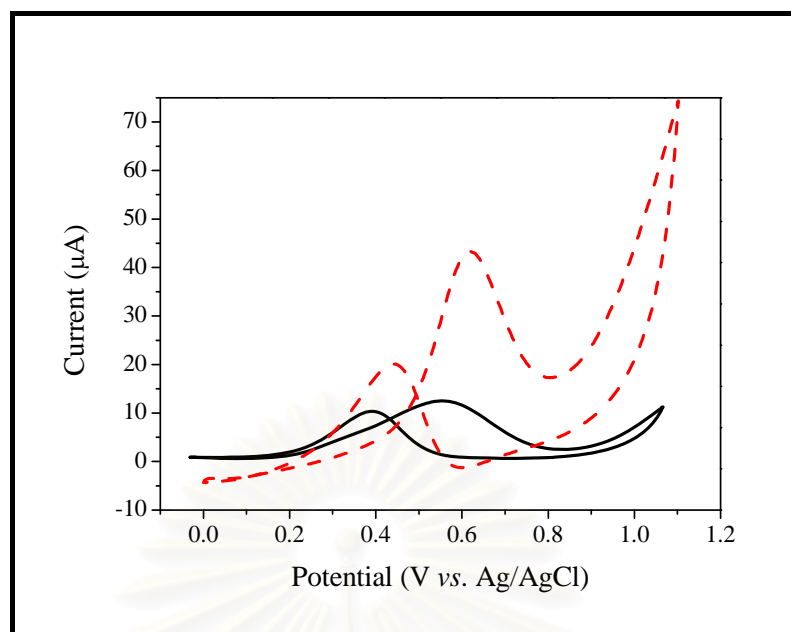


Figure 4.10 Cyclic voltammogram for 1.00 M methanol in 0.50 M sulfuric acid solution recorded with Pt (solid line) and Pt/BDD (dash line) electrodes at the scan rate of 50 mVs^{-1}

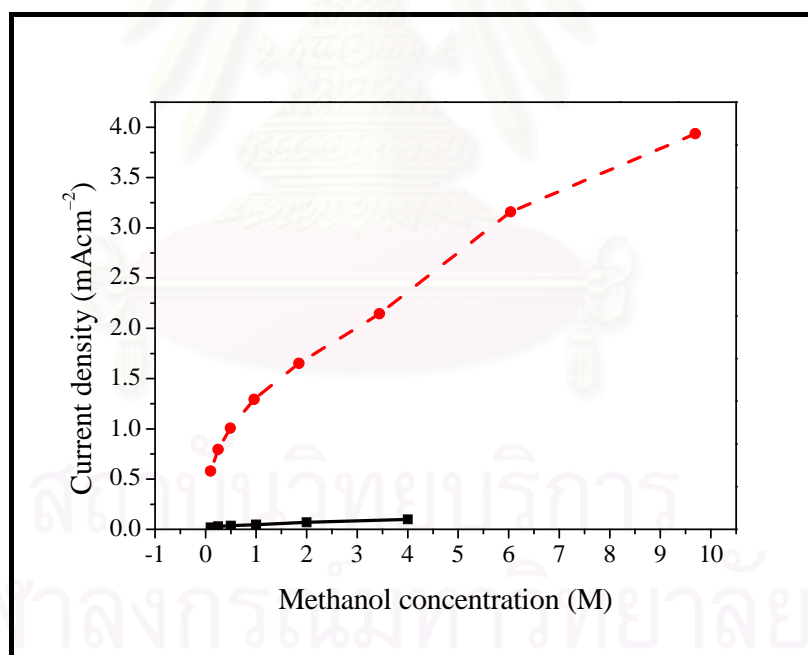


Figure 4.11 Current density vs. methanol concentration curves of Pt (solid line) and Pt/BDD (dash line) electrodes obtained in 0.50 M sulfuric acid at the scan rate of 50 mVs^{-1}

4.4.1 Effect of Potentiostatic Step

With the same total deposition time, we compared catalytic performance of Pt/BDD electrodes prepared by one-step and multi-step deposition. Table 4.3 exhibits potentiostatic conditions in this comparison using 2.00 mM Pt (IV) precursor solution containing 0.50 M sulfuric acid. Expectedly, characteristic features of one-step Pt/BDD and multi-step Pt/BDD (Figure 4.9, p. 41) were the same.

Table 4.3 Potentiostatic conditions for preparing Pt/BDD electrodes (deposition potential = -0.24 V and total deposition time = 450 s)

Condition	Potentiostatic Step	
	Time (s)	Number
one-step	450	1
multi-step	90	5

Using the anodic peak current density for methanol oxidation at the tenth cycle of cyclic voltammogram, Figure 4.12 displays relationships between methanol concentration and the current density of the Pt/BDD electrodes. The electrode with multi-step deposition provided higher current density than the one-step electrode (*i.e.*, 25% higher at 1.00 M methanol). This result agrees with previous literature saying that multi-step deposition is suitable for preparing Pt/BDD electrode [11].

4.4.2 Effect of Total Deposition Time

With multi-step deposition using 90 s-potentiostatic step, this section studied the effect of total deposition time by varying the total deposition time among 270 s, 450 s, and 630 s. Figure 4.13 exhibits characteristic voltammograms of Pt/BDD electrodes prepared with various total deposition times. The longer the total deposition time was, the higher current for Pt oxide reduction at 0.47 V was obtained, implying more Pt deposition.

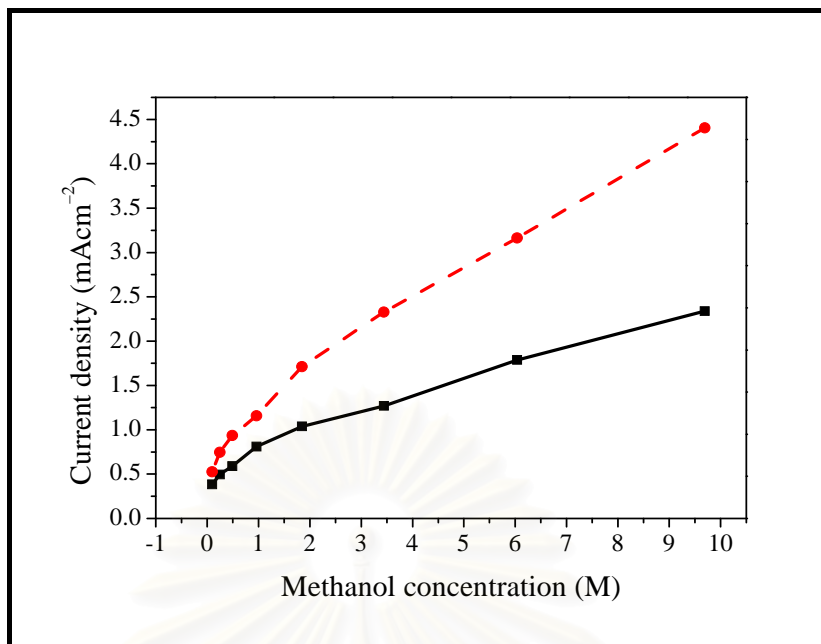


Figure 4.12 Current density vs. methanol concentration curves of Pt/BDD electrodes prepared with one-step deposition (solid line) and multi-step deposition (dash line) obtained in 0.50 M sulfuric acid at the scan rate of 50 mVs^{-1}

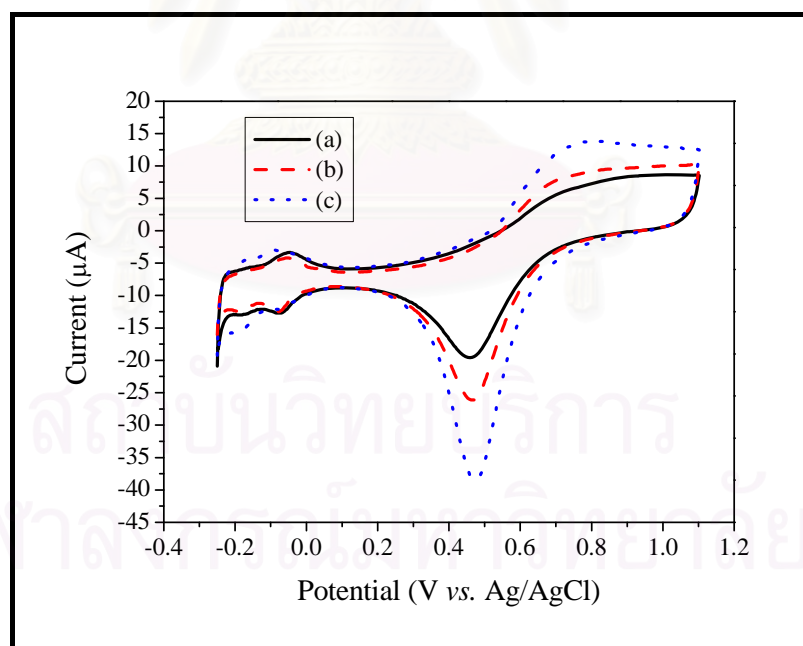


Figure 4.13 Cyclic voltammograms for 0.50 M sulfuric acid recorded at the scan rate of 50 mVs^{-1} by Pt/BDD electrodes prepared with the total deposition times of (a) 270 s, (b) 450 s, and (c) 630 s (electrode preparation: deposition potential = -0.24 V and potentiostatic step = 90 s)

In order to find the optimized total deposition time, the activity of each Pt/BDD for methanol oxidation was examined by cyclic voltammetry. Figure 4.14 reveals that the Pt/BDD electrode with 450 s-total deposition time showed the best performance towards methanol oxidation. Thus, for the preparation Pt/BDD electrode, the total deposition time of 450 s is the optimum condition.

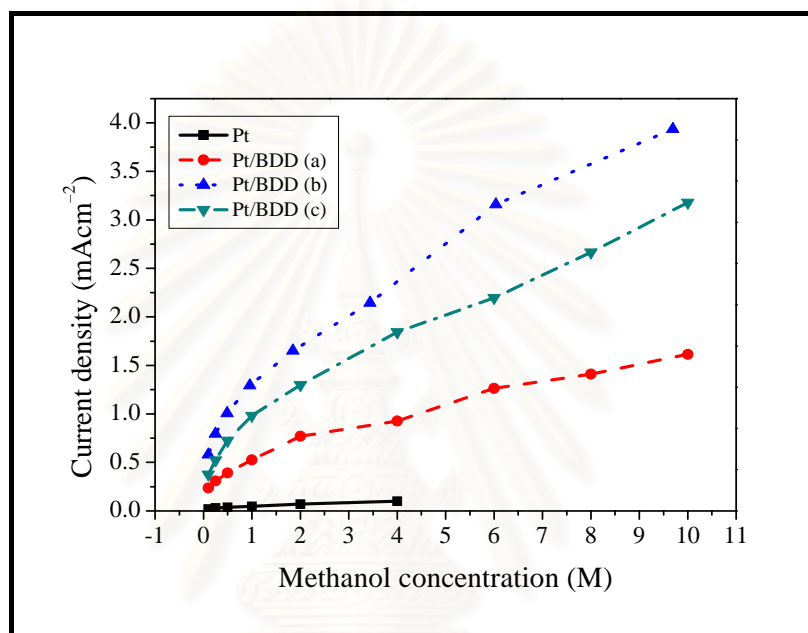


Figure 4.14 Current density vs. methanol concentration curves of Pt electrode and Pt/BDD electrodes prepared with the total deposition times of (a) 270 s, (b) 450 s, and (c) 630 s for methanol oxidation in 0.50 M sulfuric acid at the scan rate of 50 mVs^{-1}

4.5 Modification of Boron-Doped Diamond Electrode with Bi-metallic Catalysts

The choice of pure Pt as a catalyst for methanol oxidation is not favorable since Pt can be readily poisoned by strongly adsorbed intermediates [31]. Combination of Pt with the second or third component might be a convenient way to enhance the electrocatalytic property of Pt for methanol oxidation. According to the results of the modified Pt electrodes (section 4.2.3, p. 36), and data in the literature [32], three oxophilic metals, Ru, Rh, and Au were selected as the co-catalyst.

4.5.1 Platinum–Ruthenium Modified Boron-Doped Diamond Electrode

4.5.1.1 Effect of Deposition Methodology

In this section, two deposition methodologies, sequential deposition and simultaneous deposition, were compared.

Sequential Deposition

In order to select the potential for Ru deposition, Pt/BDD was used as a working electrode to study the electrochemical reaction of Ru (III) solution by means of cyclic voltammetry. Scanned from 1.10 V to 0.00 V at the scan rate of 50 mVs^{-1} , cyclic voltammogram of Ru (III) solution is shown in Figure 4.15. The cathodic peak for the reduction of Ru (III) ion to metallic Ru at 0.30 V was observed [12]. Therefore, the deposition potential of 0.20 V was chosen for depositing Ru on the Pt/BDD electrode under potentiostatic conditions. The total deposition times of 10 s, 90 s, and 450 s were investigated by using 2.00 mM Ru (III) precursor solution.

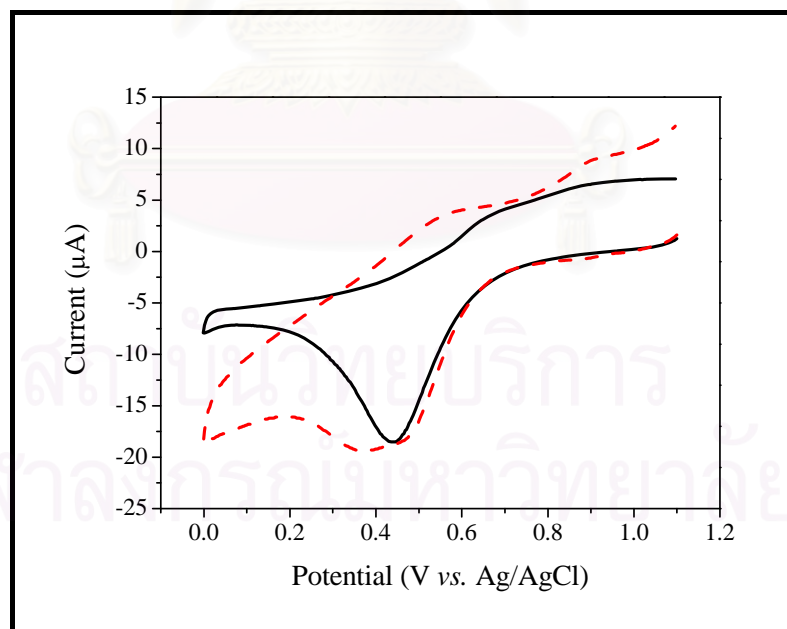


Figure 4.15 Cyclic voltammograms for 0.50 M sulfuric acid containing 0.00 mM (solid line) and 2.00 mM (dash line) Ru (III) solution recorded with the Pt/BDD electrode at the scan rate of 50 mVs^{-1}

After preparing the Pt–Ru modified BDD (PtRu/BDD) electrodes with the sequential deposition strategy, their characteristic voltammograms (Figure 4.16) in the potential range of -0.25 V to 1.10 V were obtained at the scan rate of 50 mVs^{-1} . Characteristic peak of Ru oxide reduction was observed at the potential of 0.20 V during the negative scan. The cathodic peak current for the reduction of Ru oxide increased with the time of Ru deposition (*i.e.*, the PtRu/BDD with 450 s-Ru deposition showed the highest current at the potential of 0.20 V). Since the cathodic peak for Pt oxide reduction decreased its size with the addition of Ru, it was likely that Ru partially covered Pt surface.

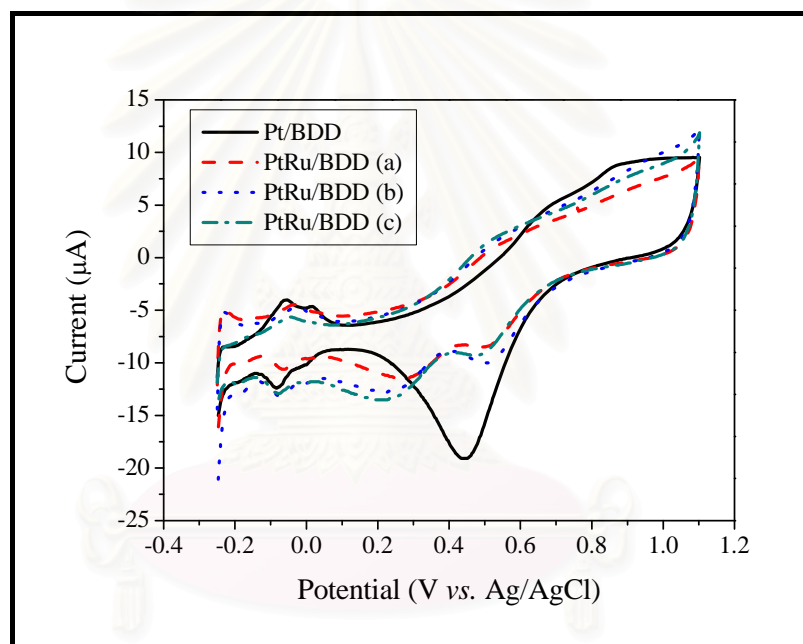


Figure 4.16 Cyclic voltammograms for 0.50 M sulfuric acid recorded at the scan rate of 50 mVs^{-1} by Pt/BDD electrode (solid line) and PtRu/BDD electrodes using the Ru deposition times of (a) 10 s, (b) 90 s, and (c) 450 s

Figure 4.17 compares electroactivity of the Pt and PtRu modified electrodes for the oxidation of methanol. Unfortunately, the activity of the PtRu/BDD electrodes was poorer than that of the Pt/BDD electrode. Pt surface might possibly be covered by Ru particles, lowering Pt active sites for methanol oxidation.

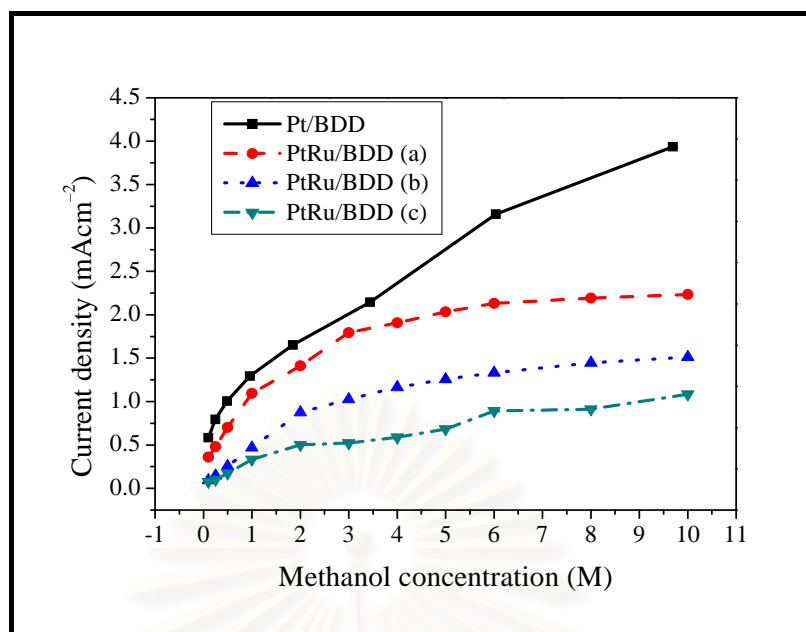


Figure 4.17 Current density vs. methanol concentration curves of Pt/BDD electrode and PtRu/BDD electrodes using the Ru deposition times of (a) 10 s, (b) 90 s, and (c) 450 s for methanol oxidation in 0.50 M sulfuric acid at the scan rate of 50 mVs^{-1}

Simultaneous Deposition

Using BDD electrode as a working electrode, both Pt and Ru were simultaneously deposited onto BDD in this experiment. The Pt–Ru composite solutions in Table 3.4 (p. 23) were used as metals precursors. Cyclic voltammograms of Pt–Ru composite solutions at BDD electrode are shown in Appendix A (p. 77). Since the reduction peaks of Pt (IV) and Ru (III) ions in the composite solutions were related to the value obtained from separated Pt (IV) or Ru (III) solution, the deposition potential of -0.24 V , the total deposition time of 450 s, and the potentiostatic step of 90 s were applied during the deposition. Figure 4.18 shows cyclic voltammograms of PtRu/BDD electrodes prepared with simultaneous deposition in 0.50 M sulfuric acid. Characteristic peaks of Pt (at 0.45 V) and Ru (at 0.20 V) were observed as one overlapping peak. The overlapping peak at 0.45 V (curve a) shifted negatively when more Ru involved in the composite solution, as seen in curves b and c.

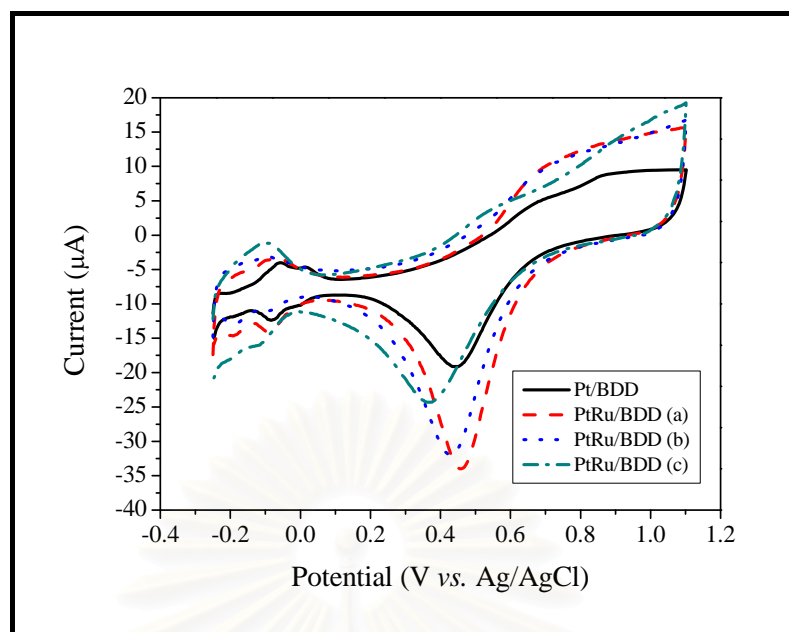


Figure 4.18 Cyclic voltammograms for 0.50 M sulfuric acid recorded at the scan rate of 50 mVs^{-1} by Pt/BDD electrode (solid line) and PtRu/BDD electrodes prepared with Pt:Ru composite precursors of (a) 95:5, (b) 90:10, and (c) 80:20

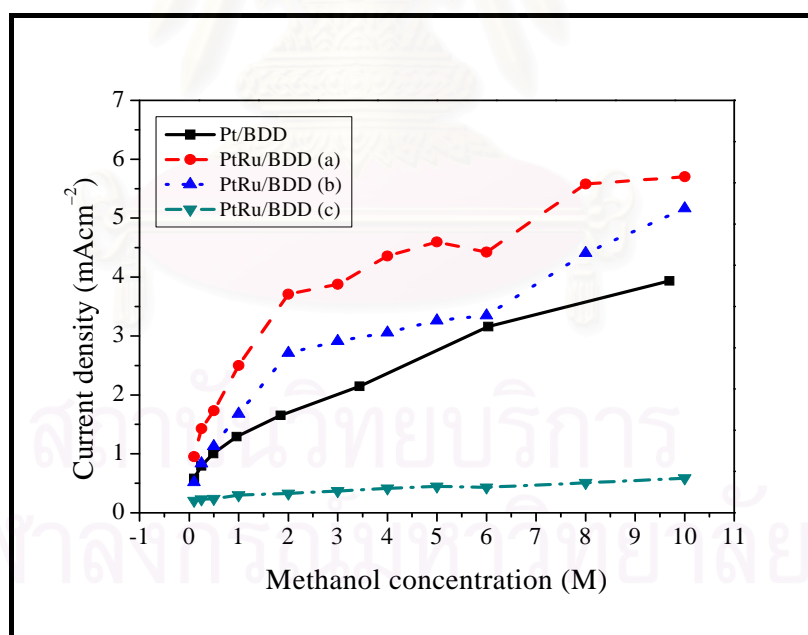


Figure 4.19 Current density vs. methanol concentration curves of Pt/BDD, (a) $\text{Pt}_{0.95}\text{Ru}_{0.05}/\text{BDD}$, (b) $\text{Pt}_{0.90}\text{Ru}_{0.10}/\text{BDD}$, and (c) $\text{Pt}_{0.80}\text{Ru}_{0.20}/\text{BDD}$ electrodes for methanol oxidation in 0.50 M sulfuric acid at the scan rate of 50 mVs^{-1}

Activity of the PtRu modified BDD electrodes were shown in Figure 4.19. The best Pt:Ru ratio in the composite solution for preparing PtRu/BDD electrode was 95:5. The $\text{Pt}_{0.95}\text{Ru}_{0.05}/\text{BDD}$ electrode gave the anodic current density of 2.50 mAcm^{-2} for 1.00 M methanol in 0.50 M sulfuric acid solution (curve a). The value is 2.5 times higher than the current density of the Pt/BDD. Hence, this composition was selected as the Pt–Ru precursor solution for the preparation of PtRu/BDD. In addition, curves b and c revealed that high percentage of Ru in the composite solutions dramatically decreased the activity of the PtRu/BDD electrodes towards methanol oxidation.

4.5.1.2 Effect of Total Deposition Time

In this experiment, we studied the effect of total deposition time on the activity of $\text{Pt}_{0.95}\text{Ru}_{0.05}/\text{BDD}$ electrodes by varying the total deposition times of 270 s, 450 s, 630 s, 720 s, 810 s, and 900 s. Other potentiostatic conditions used were the deposition potential of -0.24 V and the potentiostatic step of 90 s. Figure 4.20 presents characteristic peak of the modified electrodes in 0.50 M sulfuric acid obtained at the scan rate of 50 mVs^{-1} in the potential range of -0.30 - 1.10 V . The characteristic overlapping peak prominently showed Pt oxide reduction. There was progressive enhancement of the peak current for metal oxide reduction at 0.50 V as the total deposition time was increased from 270 s to 900 s, indicating higher area of the electrochemically active metals.

Figure 4.21 shows catalytic activity of the modified electrodes for methanol oxidation in this experiment. The activity of the modified electrode increased with the total deposition time (curves a-d) until the optimum point was reached (curve f). Possibly, the excess amount of Ru on the BDD surface might inhibit the Pt active site for methanol reaction. Prepared by using the total deposition time of 810 s, the $\text{Pt}_{0.95}\text{Ru}_{0.05}/\text{BDD}$ electrode showed highest current density for methanol oxidation, giving the anodic current of 4.28 mAcm^{-2} for 1.00 M methanol.

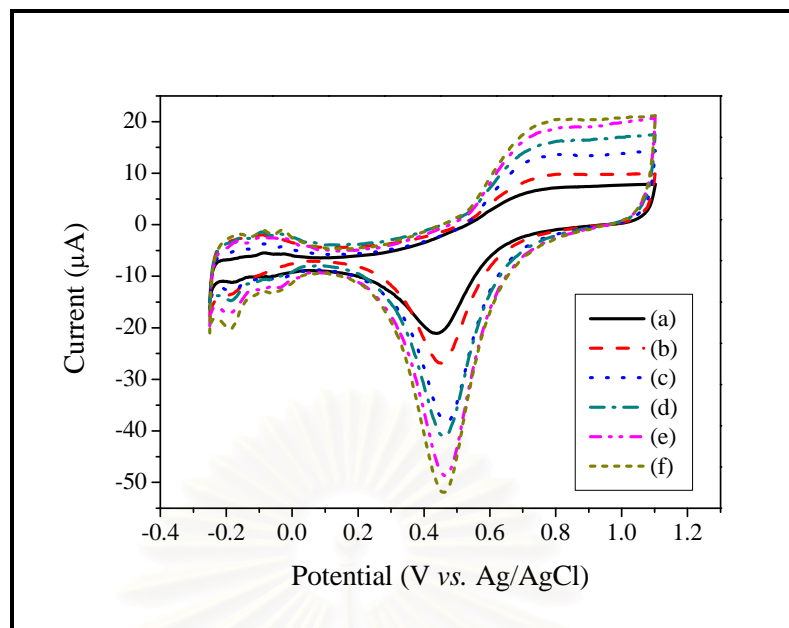


Figure 4.20 Cyclic voltammograms for 0.50 M sulfuric acid recorded at the scan rate of 50 mVs^{-1} by $\text{Pt}_{0.95}\text{Ru}_{0.05}/\text{BDD}$ electrodes prepared with the total deposition times of (a) 270 s, (b) 450 s, (c) 630 s, (d) 720 s, (e) 810 s, and (f) 900 s

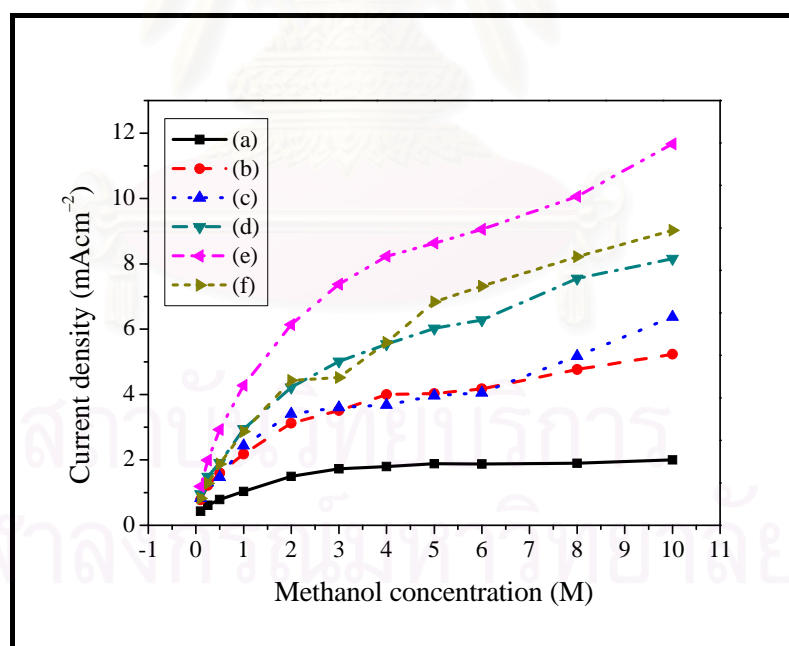


Figure 4.21 Current density vs. methanol concentration curves of $\text{Pt}_{0.95}\text{Ru}_{0.05}/\text{BDD}$ electrodes prepared with the total deposition times of (a) 270 s, (b) 450 s, (c) 630 s, (d) 720 s, (e) 810 s, and (f) 900 s for methanol oxidation in 0.50 M sulfuric acid at the scan rate of 50 mVs^{-1}

4.5.1.3 Effect of Potentiostatic Step

In this section, we studied the effect of the width of each potentiostatic step during BDD surface modification. Table 4.4 presents all potentiostatic conditions for the preparation of Pt_{0.95}Ru_{0.05}/BDD electrodes with the total deposition time of 810 s.

Table 4.4 Potentiostatic conditions for preparing Pt_{0.95}Ru_{0.05}/BDD electrodes with various potentiostatic step widths (deposition potential = -0.24 V and total deposition time = 810 s)

Sample Label	Width of Potentiostatic Step (s)	Number of Potentiostatic Step
(a)	10.0	81
(b)	22.5	36
(c)	45.0	18
(d)	90.0	9
(e)	135.0	6
(f)	202.5	4

Figure 4.22 presents cyclic voltammograms of the modified electrodes in 0.50 M sulfuric acid, illustrating that the characteristic peak of metal oxide reduction was seen and increased in size with the numbers of potentiostatic steps when same total deposition time was applied. Displayed in Figure 4.23, the activity of Pt_{0.95}Ru_{0.05}/BDD electrodes for methanol oxidation corresponded with the size of metal oxide reduction peak (Figure 4.22). Pt_{0.95}Ru_{0.05}/BDD electrode prepared by using shortest potentiostatic step (10 s, curve a) showed highest electrocatalytic activity with the anodic current of 12.97 mAcm⁻² for 1.00 M methanol. These results might be related with the issue regarding metal particle sizes that will be discussed later in this thesis. Moreover, the optimized Pt_{0.95}Ru_{0.05}/BDD electrode (curve a) provides 4 times higher electrocatalytic activity than the PtRu/BDD electrode previously prepared by the electrodeposition with cyclic voltammetry [21].

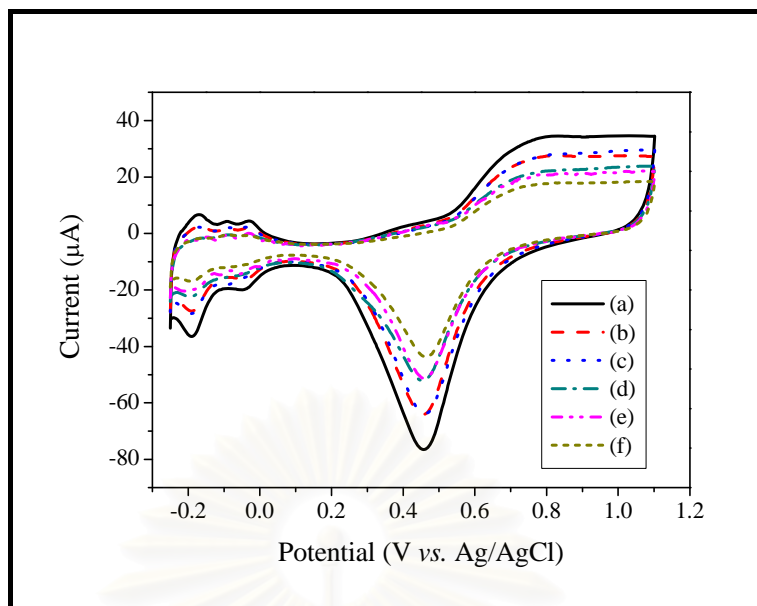


Figure 4.22 Cyclic voltammograms for 0.50 M sulfuric acid recorded at the scan rate of 50 mVs^{-1} by $\text{Pt}_{0.95}\text{Ru}_{0.05}/\text{BDD}$ electrodes prepared with the potentiostatic step widths of (a) 10.0 s, (b) 22.5 s, (c) 45.0 s, (d) 90.0 s, (e) 135.0 s, and (f) 202.5 s

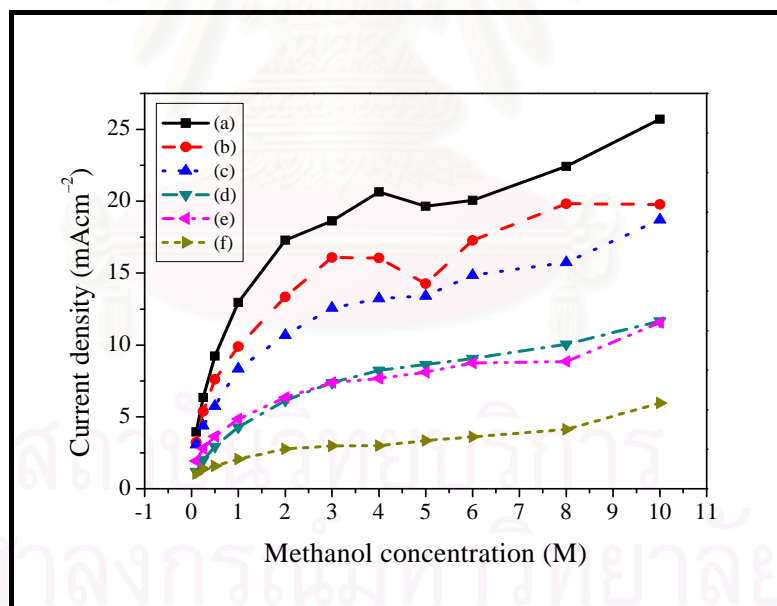


Figure 4.23 Current density vs. methanol concentration curves of $\text{Pt}_{0.95}\text{Ru}_{0.05}/\text{BDD}$ electrodes prepared with the potentiostatic step widths of (a) 10.0 s, (b) 22.5 s, (c) 45.0 s, (d) 90.0 s, (e) 135.0 s, and (f) 202.5 s for methanol oxidation in 0.50 M sulfuric acid solution at the scan rate of 50 mVs^{-1} (electrode preparation: deposition potential = -0.24 V and total deposition time = 810 s)

4.5.2 Platinum–Gold Modified Boron-Doped Diamond Electrode

4.5.2.1 Effect of Deposition Methodology

Similar to the case of PtRu/BDD, we examined two methodologies, sequential deposition and simultaneous deposition, for the preparation of Pt–Au modified BDD (PtAu/BDD) electrode.

Sequential Deposition

In this experiment, Pt/BDD was used as a working electrode to probe the electrochemical process of Au (III) solution by cyclic voltammetry. Shown in Figure 4.24 the standard potential for the reduction of AuCl_4^- to metallic Au was observed at 0.70 V [32]. Chronoamperometric technique with potentiostatic conditions were then utilized to deposit Au onto Pt/BDD electrode at the potential of 0.60 V. The PtAu/BDD electrodes with three values of total deposition times (10.0 s, 45.0 s, and 90.0 s) were prepared.

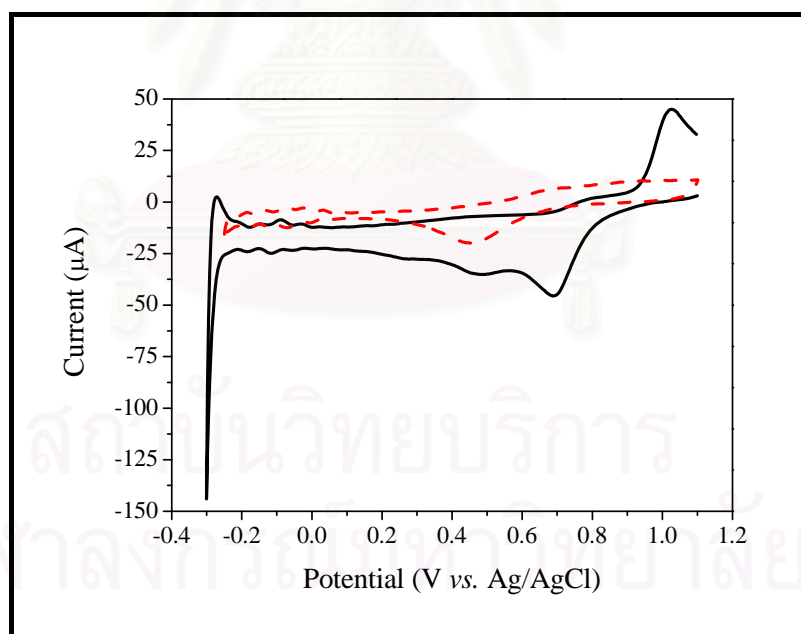


Figure 4.24 Cyclic voltammograms recorded with Pt/BDD at the scan rate of 50 mVs^{-1} for 0.50 M sulfuric acid containing 0.00 mM (dash line) and 2.00 mM (solid line) Au (III) solution

Figure 4.25 shows cyclic voltammograms for 0.50 M sulfuric acid recorded with PtAu/BDD electrodes in the potential range of 0.00-1.10 V at the scan rate of 50 mVs^{-1} . No cathodic peak for Pt oxide reduction at 0.70-0.30 V was observed, implying that Au particles might totally cover the deposited Pt on the BDD surface.

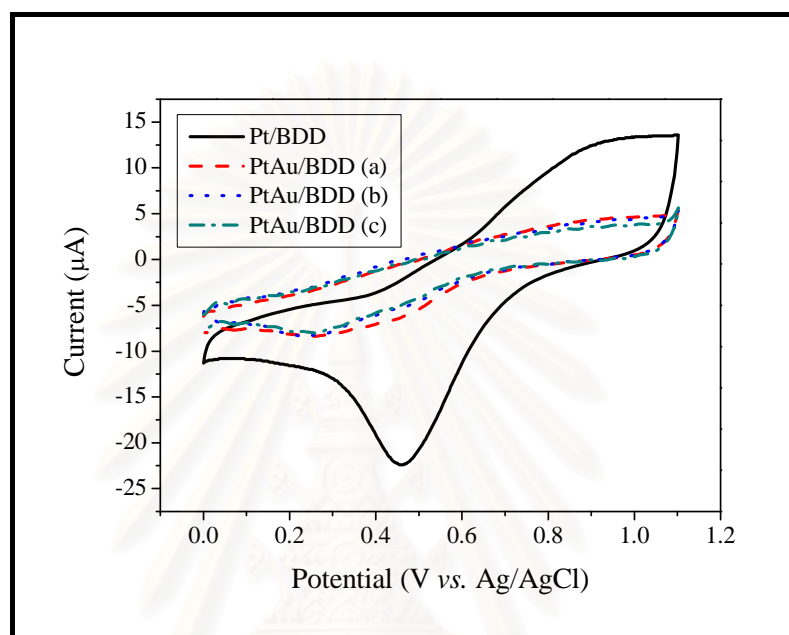


Figure 4.25 Cyclic voltammograms for 0.50 M sulfuric acid recorded at the scan rate of 50 mVs^{-1} by Pt/BDD electrode (solid line) and PtAu/BDD electrodes with the Au deposition times of (a) 10 s, (b) 45 s, and (c) 90 s

Activity of the PtAu/BDD electrodes towards methanol oxidation was studied by cyclic voltammetry (Figure 4.26), revealing that the activity of PtAu/BDD electrodes was lower than that of Pt/BDD electrode. It is likely that Pt surface on BDD might be covered with Au particles, causing less Pt active sites for methanol oxidation.

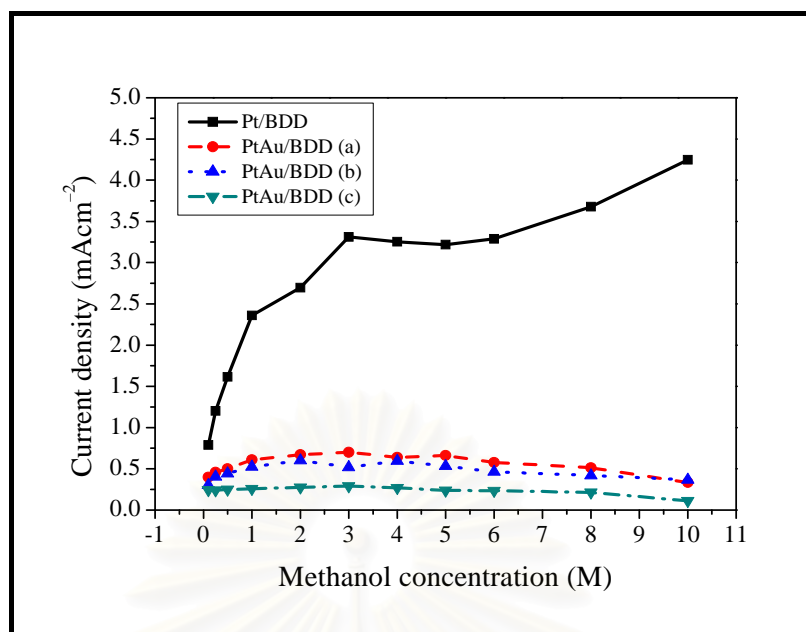


Figure 4.26 Current density vs. methanol concentration curves of Pt/BDD electrode and PtAu/BDD electrodes prepared with the Au deposition times of (a) 10 s, (b) 45 s, and (c) 90 s for methanol oxidation in 0.50 M sulfuric acid at the scan rate of 50 mVs^{-1}

Simultaneous Deposition

For simultaneous deposition, BDD electrode was used as a working electrode and Pt–Au composite solutions in Table 3.5 (p. 23) were used as metals precursors. Cyclic voltammograms of BDD for Pt–Au solutions are shown in Appendix B (p. 78), illustrating the oxidation–reduction of metallic Au–Au (III) ion couple [32]. Then, the potential of -0.24 V was applied to BDD during 450 s–Pt–Au deposition time with the potentiostatic step of 90 s to ensure the successful preparation of PtAu/BDD. Figure 4.27 displays cyclic voltammograms of PtAu/BDD electrodes scanned positively in 0.50 M sulfuric acid from -0.30 V to 1.10 V at the scan rate of 50 mVs^{-1} . Characteristic peak of PtAu/BDD at 0.90 V revealed the reduction of Au oxide which was also observed at the Au/BDD electrode [32]. Additionally, the reduction peak at 0.40 V in curves a–c of this figure corresponds to Pt oxide reduction. Furthermore, activity of the PtAu/BDD electrodes towards methanol oxidation is shown in Figure 4.28. Unfortunately, the activity of PtAu/BDD electrodes were worse than that of Pt/BDD electrode, implying that Au might not improve the performance of Pt/BDD electrode.

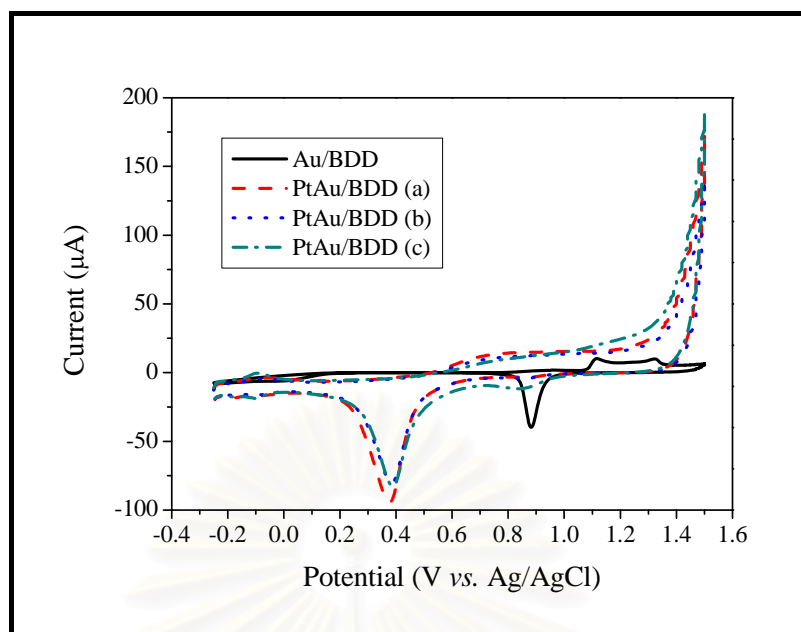


Figure 4.27 Cyclic voltammograms for 0.50 M sulfuric acid recorded at the scan rate of 50 mVs^{-1} by Au/BDD electrode (solid line) and PtAu/BDD electrodes with the Pt:Au precursors of (a) 95:5, (b) 90:10, and (c) 80:20

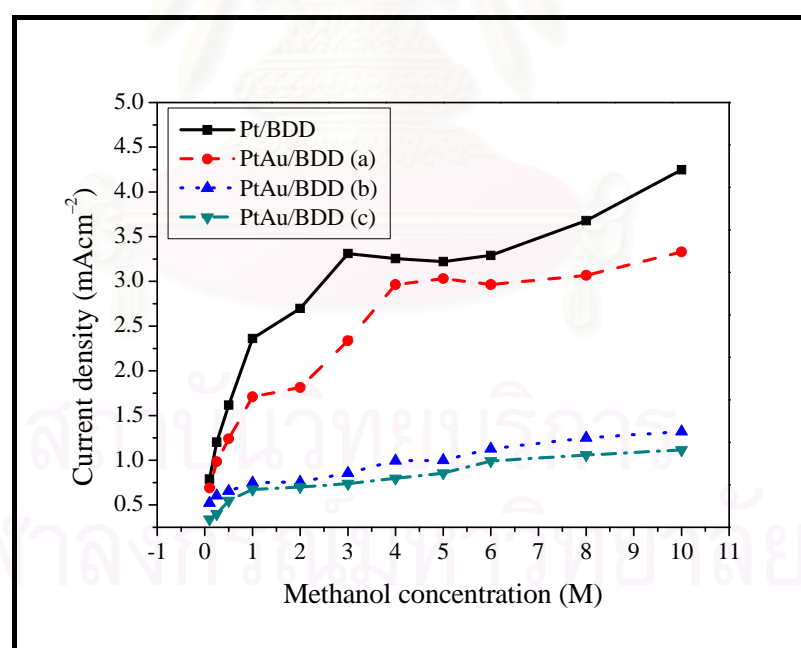


Figure 4.28 Current density vs. methanol concentration curves of Pt/BDD, (a) $\text{Pt}_{0.95}\text{Au}_{0.05}$ /BDD, (b) $\text{Pt}_{0.90}\text{Au}_{0.10}$ /BDD, and (c) $\text{Pt}_{0.80}\text{Au}_{0.20}$ /BDD electrodes for methanol oxidation in 0.50 M sulfuric acid at the scan rate of 50 mVs^{-1}

4.5.3 Platinum–Rhodium Modified Boron-Doped Diamond Electrode

4.5.3.1 Effect of Deposition Methodology

Sequential deposition and simultaneous deposition were employed to prepare Pt–Rh modified BDD (PtRh/BDD) electrodes.

Sequential Deposition

In this experiment, Pt had been deposited onto BDD and Rh was sequentially deposited onto the Pt/BDD electrode. To get the deposition potential for Rh, cyclic voltammogram for Rh (III) solution recorded with the Pt/BDD electrode from 1.10 V to -0.30 V at the scan rate of 50 mVs^{-1} (Figure 4.29) was obtained. Since the cathodic peak for the reduction of Rh (III) to Rh (0) was observed at -0.17 V, the potential of -0.20 V was used to deposit Rh on Pt/BDD electrode. The PtRh/BDD electrodes with three values of total deposition times (10.0 s, 45.0 s, and 90.0 s) were prepared.

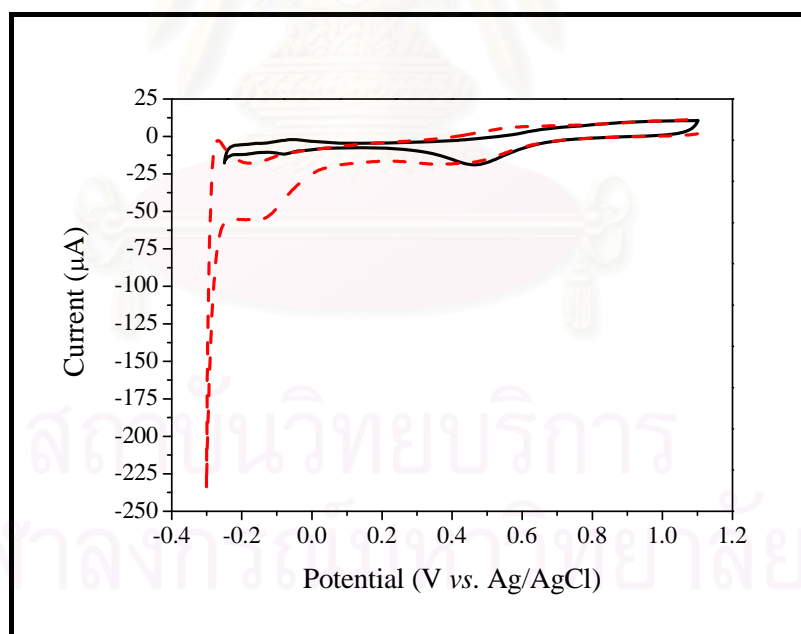


Figure 4.29 Cyclic voltammograms of Pt/BDD electrode for 0.50 M sulfuric acid containing 0.00 mM (solid line) and 2.00 mM (dash line) Rh (III) solution at the scan rate of 50 mVs^{-1}

Prepared with the sequential deposition strategy, the PtRh/BDD electrodes were characterized by obtaining their cyclic voltammograms (Figure 4.30) in the potential range of -0.25 V to 1.10 V at the scan rate of 50 mVs^{-1} . Characteristic peak of Rh oxide reduction was observed at 0.12 V during the negative scan [33]. The cathodic peak current for the reduction of Rh oxide increased with the Rh deposition time (*i.e.*, the PtRh/BDD with 90 s-Rh deposition showed highest current at the potential of 0.20 V). Since the cathodic peak for Pt oxide reduction decreased its size with the addition of Rh, it is likely that Rh might partially cover Pt surface.

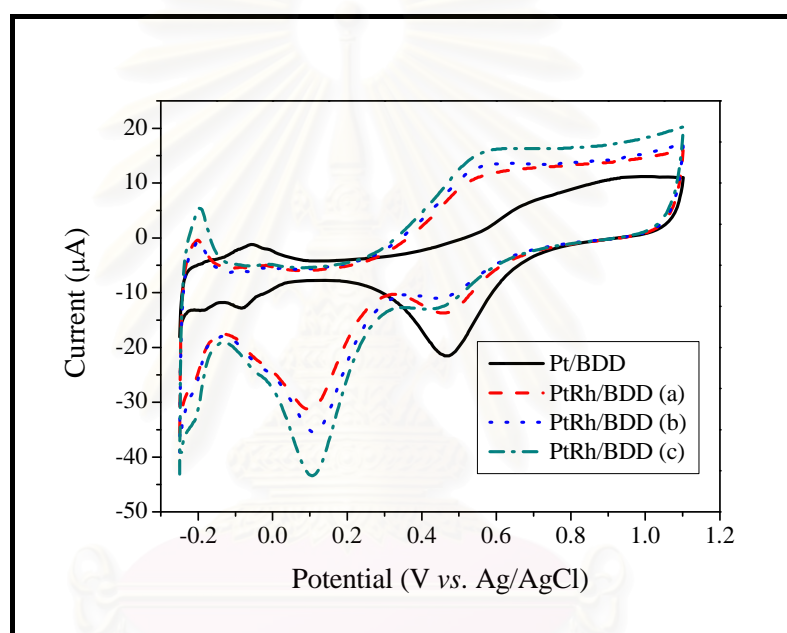


Figure 4.30 Cyclic voltammograms for 0.50 M sulfuric acid recorded with Pt/BDD electrode (solid line) and PtRh/BDD electrodes prepared with the Rh deposition times of (a) 10 s, (b) 45 s, and (c) 90 s at the scan rate of 50 mVs^{-1}

Figure 4.31 compares electroactivity of the Pt and PtRh modified electrodes for the oxidation of methanol. Prepared by using the Rh deposition time of 10 s, the PtRh/BDD electrode showed the highest current density for methanol oxidation, giving the anodic current density of 2.31 mAcm^{-2} for 1.00 M methanol.

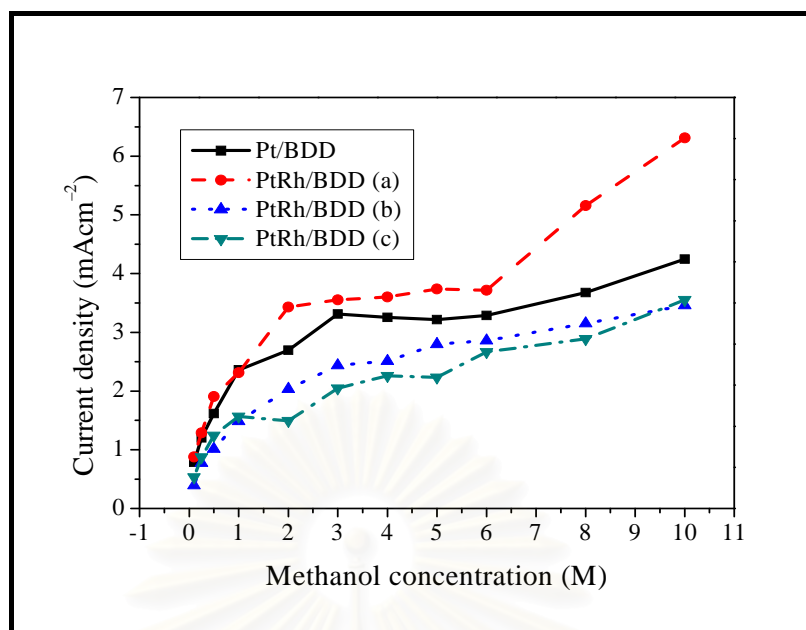


Figure 4.31 Current density vs. methanol concentration curves of Pt/BDD electrode and PtRh/BDD electrodes prepared with the Rh deposition times of (a) 10 s, (b) 45 s, and (c) 90 s for methanol oxidation in 0.50 M sulfuric acid at the scan rate of 50 mVs^{-1}

Simultaneous Deposition

Both Pt and Rh were simultaneously deposited onto BDD in this section. The Pt–Rh composite solutions in Table 3.6 (p. 24) were applied as metals precursors. Cyclic voltammograms of Pt–Rh composite solutions by BDD electrode are shown in Appendix C (p. 79). Similar to the case of the PtRu/BDD electrode, the deposition potential of -0.24 V was used for the potentiostatic deposition. Figure 4.32 shows cyclic voltammograms of the PtRh/BDD electrodes in 0.50 M sulfuric acid. Characteristic peaks of Pt and Rh overlapped into one peak. When more Rh involved in the composite solutions, the overlapping peak shifted towards negative direction. In addition, activity of the PtRh/BDD electrodes for methanol oxidation was investigated by cyclic voltammetry (Figure 4.33), showing that the activity of PtRh/BDD electrodes was lower than that of Pt/BDD electrode.

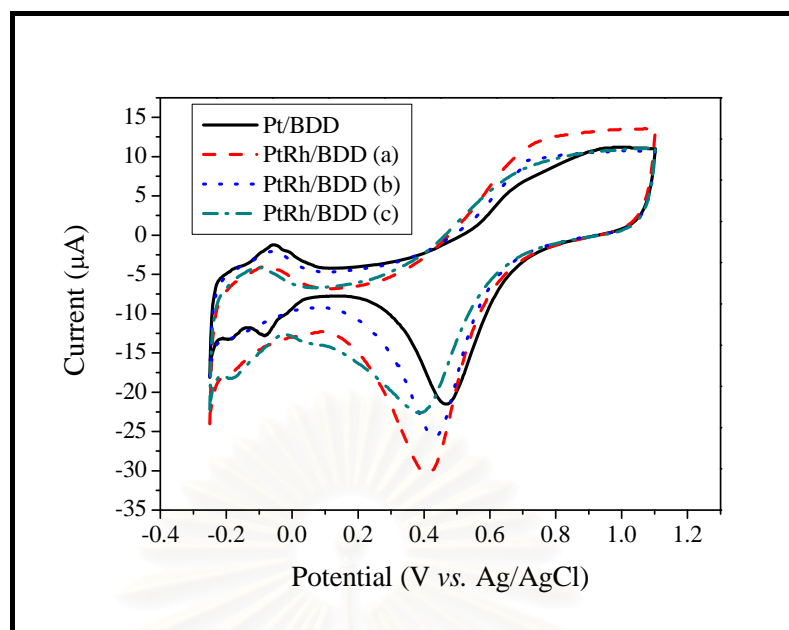


Figure 4.32 Cyclic voltammograms for 0.50 M sulfuric acid recorded at the scan rate of 50 mVs^{-1} by Pt/BDD, (a) $\text{Pt}_{0.95}\text{Rh}_{0.05}/\text{BDD}$, (b) $\text{Pt}_{0.90}\text{Rh}_{0.10}/\text{BDD}$, and (c) $\text{Pt}_{0.80}\text{Rh}_{0.20}/\text{BDD}$ electrodes

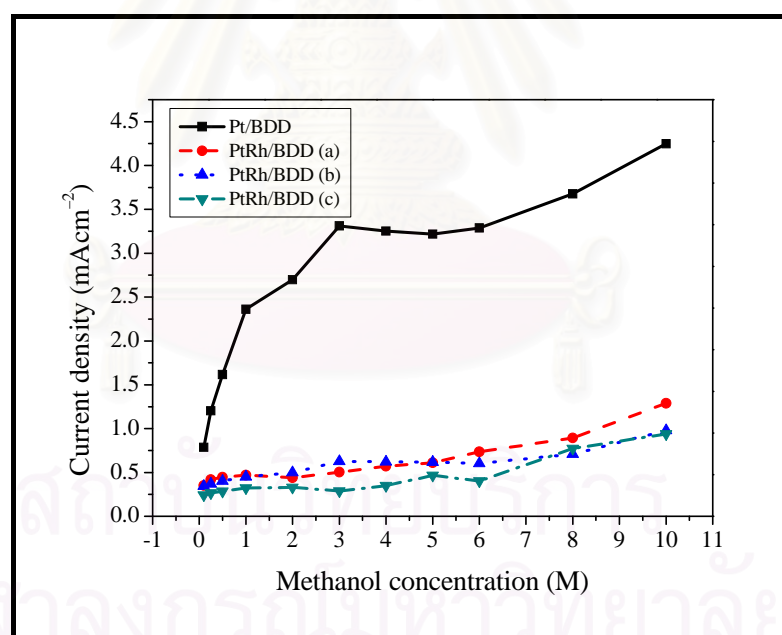


Figure 4.33 Current density vs. methanol concentration curves of Pt/BDD, (a) $\text{Pt}_{0.95}\text{Rh}_{0.05}/\text{BDD}$, (b) $\text{Pt}_{0.90}\text{Rh}_{0.10}/\text{BDD}$, and (c) $\text{Pt}_{0.80}\text{Rh}_{0.20}/\text{BDD}$ electrodes for methanol oxidation in 0.50 M sulfuric acid at the scan rate of 50 mVs^{-1}

4.6 Modification of Boron-Doped Diamond Electrode with Tri-metallic Catalysts

Results from the previous section have shown that the bi-metallic catalysts are able to catalyze the oxidation of methanol. To improve the electrocatalytic activity of the bi-metallic catalysts, the third component was added.

4.6.1 Platinum–Ruthenium–Gold Modified Boron-Doped Diamond Electrode

According to earlier results, suitable method for depositing Ru or Au with Pt onto BDD electrode was simultaneous deposition. Thus, Pt, Ru, and Au were simultaneously deposited onto BDD with the use of the Pt–Ru–Au composite solutions in Table 3.7 (p. 24) as metal precursor solutions. Cyclic voltammograms of Pt–Ru–Au composite solutions at BDD are shown in Appendix D (p. 80). The -0.24 V-deposition potential, the 810 s-total deposition time, and the 90 s-potentiostatic step were conditions for the potentiostatic deposition. Displayed in Figure 4.34, cyclic voltammograms of PtRuAu/BDD electrodes in 0.50 M sulfuric acid reveal the overlapping peak of Pt and Ru. The overlapping peak at 0.45 V (curve d of Figure 4.34i) shifted negatively when more Ru was present in the composited solutions (curves a-c of Figure 4.34i). At the potential of 0.85 V (Figure 4.34ii), the peak of PtRuAu/BDD represented the reduction of Au oxide which was also observed at the Au/BDD electrode (Figure 4.27, p. 57).

Figure 4.35 shows the activity of the PtRuAu/BDD electrodes for the oxidation of methanol. Unfortunately, the activity of most of PtRuAu/BDDs electrodes (curves d-f) were worse than that of PtRu/BDD electrode, suggesting that Au might not improve the performance of PtRu/BDD. Only the $\text{Pt}_{0.95}\text{Ru}_{0.04}\text{Au}_{0.01}$ /BDD electrode (curve c) showed comparable catalytic performance with the PtRu/BDD electrode whereas it gave the anodic current density at 1.00 M methanol 2.5 times higher than that of PtAu/BDD electrode (curve b). Therefore, unlike Ru, Au was not suitable to serve as a metal co-catalyst for methanol oxidation.

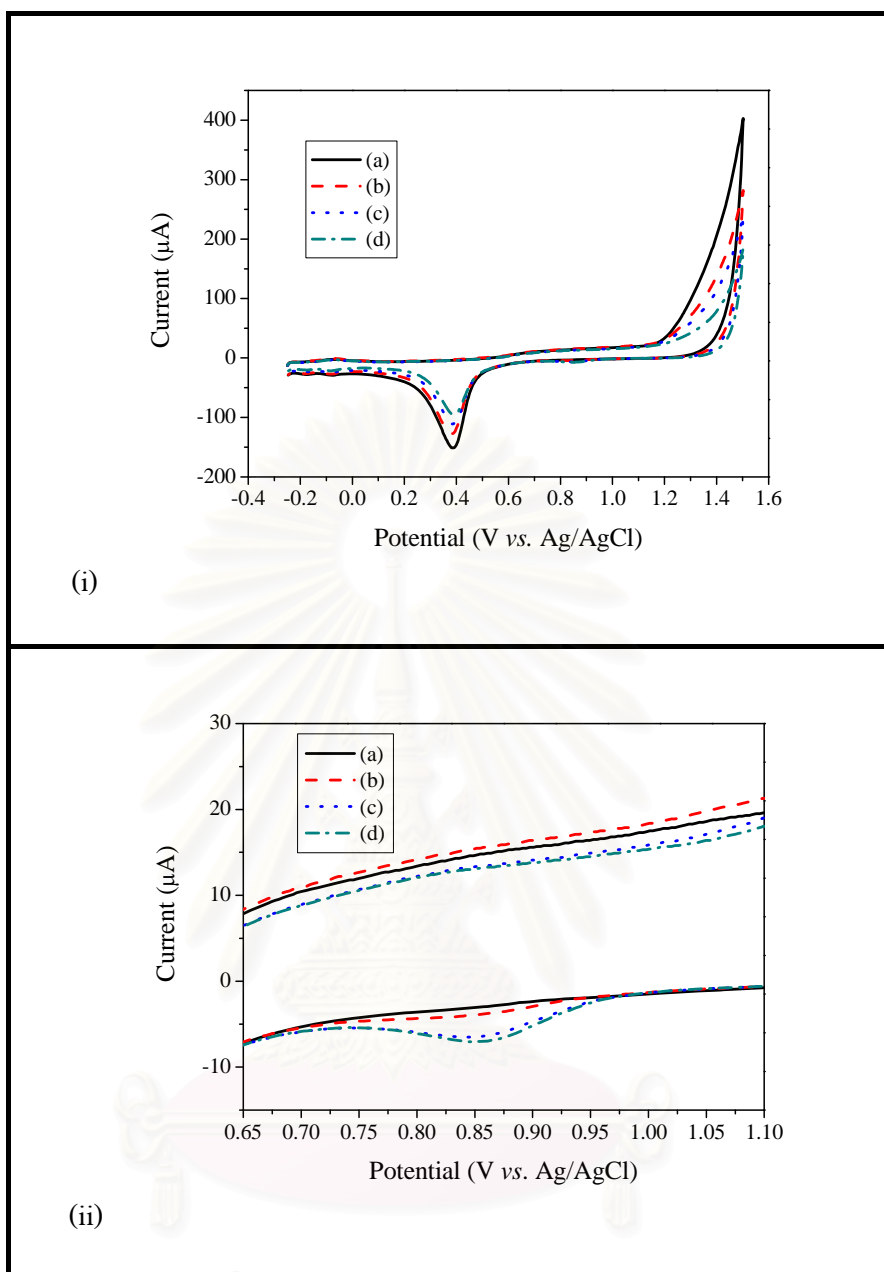


Figure 4.34 Cyclic voltammograms for 0.50 M sulfuric acid recorded with (a) $\text{Pt}_{0.95}\text{Ru}_{0.04}\text{Au}_{0.01}/\text{BDD}$, (b) $\text{Pt}_{0.95}\text{Ru}_{0.03}\text{Au}_{0.02}/\text{BDD}$, (c) $\text{Pt}_{0.95}\text{Ru}_{0.02}\text{Au}_{0.03}/\text{BDD}$, and (d) $\text{Pt}_{0.95}\text{Ru}_{0.01}\text{Au}_{0.04}/\text{BDD}$ at the scan rate of 50 mVs^{-1} ((i) Pt–Ru oxide reduction region and (ii) Au oxide reduction region)

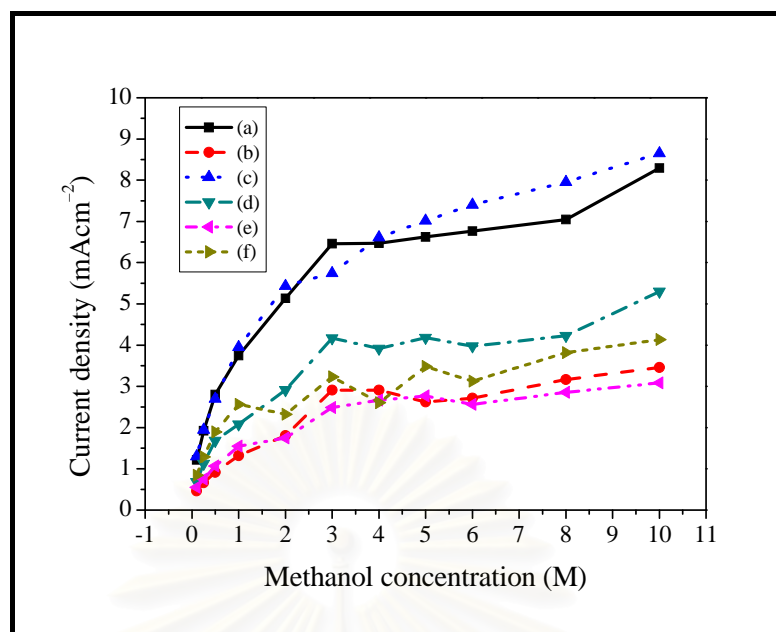


Figure 4.35 Current density vs. methanol concentration curves of (a) Pt_{0.95}Ru_{0.05}/BDD, (b) Pt_{0.95}Au_{0.05}/BDD, (c) Pt_{0.95}Ru_{0.04}Au_{0.01}/BDD, (d) Pt_{0.95}Ru_{0.03}Au_{0.02}/BDD, (e) Pt_{0.95}Ru_{0.02}Au_{0.03}/BDD, and (f) Pt_{0.95}Ru_{0.01}Au_{0.04}/BDD electrodes for methanol oxidation in 0.50 M sulfuric acid at the scan rate of 50 mVs⁻¹

4.6.2 Platinum–Ruthenium–Rhodium Modified Boron-Doped Diamond Electrode

Since proper method for the modification of Pt or Ru on BDD was simultaneous deposition and that of Rh was sequential deposition, we prepared PtRuRh/BDD by sequential deposition of Rh onto simultaneously deposited PtRu/BDD. In order to select the potential for Rh deposition, Pt_{0.95}Ru_{0.05}/BDD was used as a working electrode to study the electrochemical reaction of Rh (III) solution by cyclic voltammetry in the potential range from 1.10 V to -0.30 V at the scan rate of 50 mVs⁻¹ (Figure 4.36). Since the cathodic peak for the reduction of Rh (III) to Rh (0) was observed at -0.17 V, the potential of -0.20 V was selected for depositing Rh on PtRu/BDD electrode. Three total deposition times (10.0 s, 45.0 s, and 90.0 s) were applied.

Shown in Figure 4.37, characteristic voltammograms of the PtRuRh/BDD electrodes were obtained in the potential range of -0.25 V to 1.10 V at the scan rate of 50 mVs⁻¹. During the negative scan, the overlapping peak for Pt oxide reduction–Ru oxide reduction at 0.45 V and the peak for Rh oxide reduction at 0.12 V were observed. The cathodic peak current for the reduction

for Rh oxide increased with the time of Rh deposition (*i.e.*, the PtRuRh/BDD with 90 s-Rh deposition gave the highest current density at 0.12 V). Due to the fact that the cathodic peak for Pt oxide reduction decreased its size with the addition of Rh, it is likely that Rh might partly cover Pt surface.

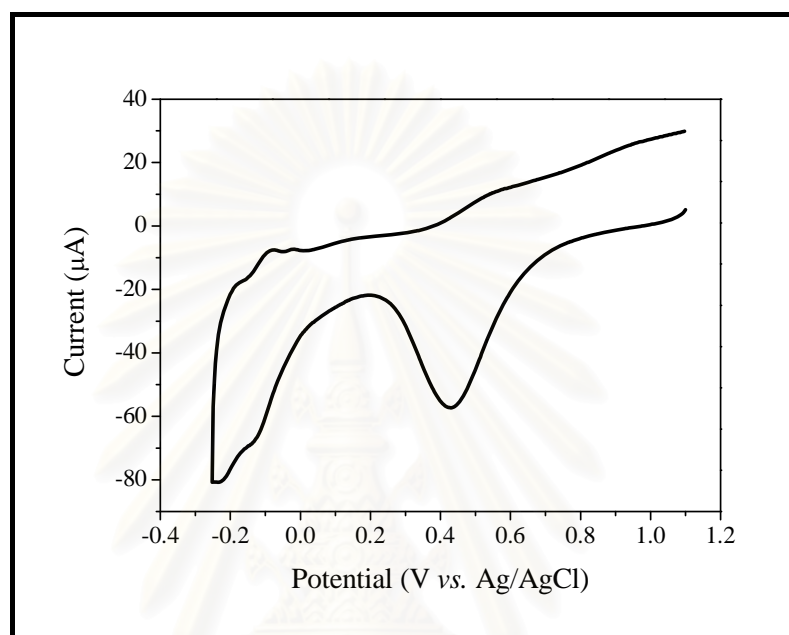


Figure 4.36 Cyclic voltammogram for Rh (III) solution recorded with Pt_{0.95}Ru_{0.05}/BDD electrode at the scan rate of 50 mVs⁻¹

Figure 4.38 displays catalytic activity of PtRuRh/BDD electrodes towards methanol oxidation. All PtRuRh/BDD electrodes gave higher current for methanol oxidation than the optimized PtRu/BDD electrode. The PtRuRh/BDD electrode prepared by 10 s-Rh deposition showed the best catalytic performance with the anodic current density of 17.58 mAcm⁻² for 1.00 M methanol in 0.50 M sulfuric acid. The activity of PtRuRh/BDD was 1.3 and 17 times higher than PtRu/BDD and Pt/BDD, respectively. This could be interpreted as highly efficient direct oxidation with the ternary catalyst that leads to the elimination of unwanted intermediates on the BDD surface. Moreover, it has been found that the PtRuRh/BDD electrode prepared by our method provided 1.8 times higher current density for methanol oxidation than the Pt–RuO₂–RhO₂/BDD electrode prepared by the sol-gel method [24].

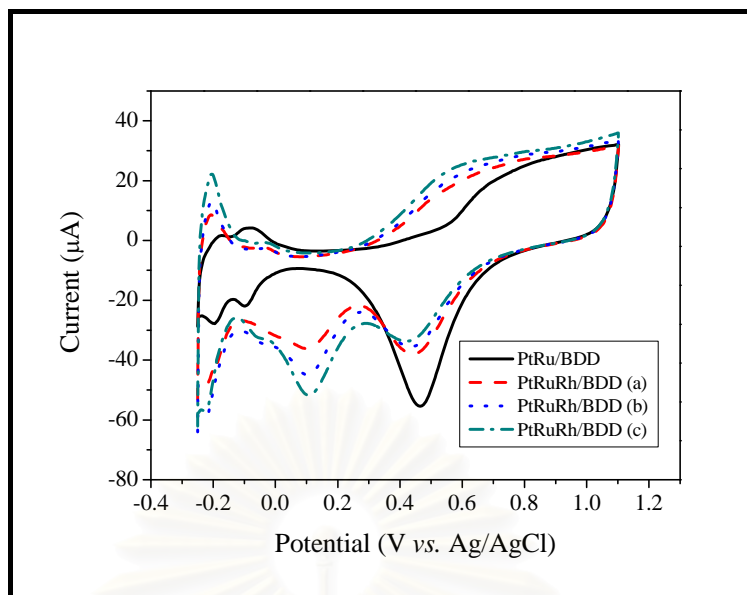


Figure 4.37 Cyclic voltammograms for 0.50 M sulfuric acid recorded at the scan rate of 50 mVs^{-1} by $\text{Pt}_{0.95}\text{Ru}_{0.05}/\text{BDD}$ electrode (solid line) and PtRuRh/BDD electrodes with the Rh deposition times of (a) 10 s, (b) 45 s, and (c) 90 s

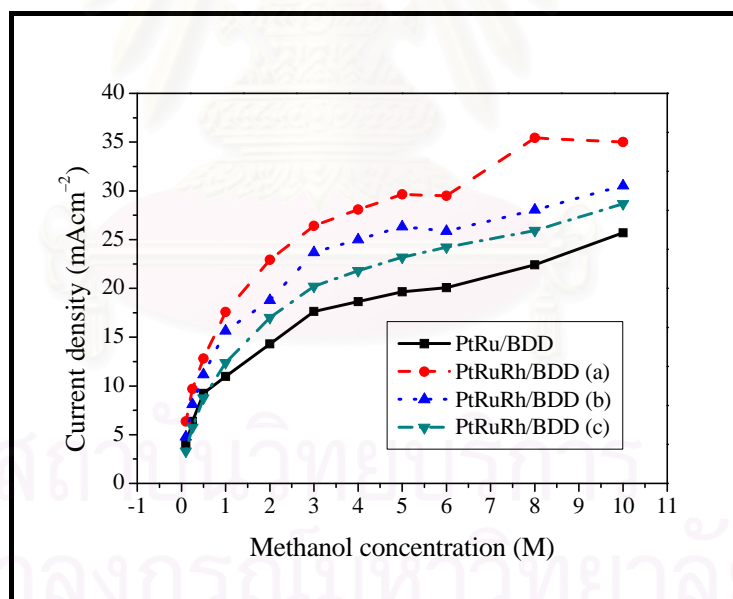


Figure 4.38 Current density vs. methanol concentration curves of $\text{Pt}_{0.95}\text{Ru}_{0.05}/\text{BDD}$ electrode and PtRuRh/BDD electrodes with the Rh deposition times of (a) 10 s, (b) 45 s, and (c) 90 s for methanol oxidation in 0.50 M sulfuric acid at the scan rate of 50 mVs^{-1}

4.7 Characterization of The Modified Electrodes

After cyclic voltammetry was used to confirm the presence of each deposited metal onto BDD surfaces, scanning electron microscopy (SEM) was introduced to characterize the morphology of the modified electrodes. Note that we had selected some modified BDD electrodes as examples for this study.

4.7.1 Platinum/Boron-Doped Diamond Electrode

Figure 4.39 shows SEM images of the surfaces of Pt/BDD electrodes with multi-step (5×90 s, Figures 4.39a and b) and one-step (450 s, Figure 4.39c and d) electrodeposition. Displayed clearly in Figures 4.39b and 4.39d, the images of both Pt/BDD electrodes revealed the existence of Pt micro-clusters, arising from the agglomeration of several Pt nanoparticles. Table 4.5 exhibits cluster and particle sizes of Pt at Pt/BDD electrodes prepared with multi-step and one-step deposition. Compared with one-step deposition, it can be seen that multi-step deposition caused better Pt dispersion at the BDD surfaces, leading to more active surface areas to react with methanol. SEM results are in agreement with voltammetric results where the Pt/BDD electrode with multi-step deposition provides higher anodic current than that of one-step deposition (Figure 4.12, p. 44). In addition, earlier work had reported the deposition of Pt with the particle size of 150-800 nm on BDD [18, 34].

Table 4.5 Effect of deposition method on the cluster and particle sizes of Pt at BDD surfaces

Multi-step Deposition (450 s)		One-step Deposition (5×90 s)	
Cluster Sizes (nm)	Cluster Sizes (nm)	Cluster Sizes (nm)	Particle Sizes (nm)
299.80 \pm 72.48	299.80 \pm 72.48	390.71 \pm 36.61	92.48 \pm 12.25

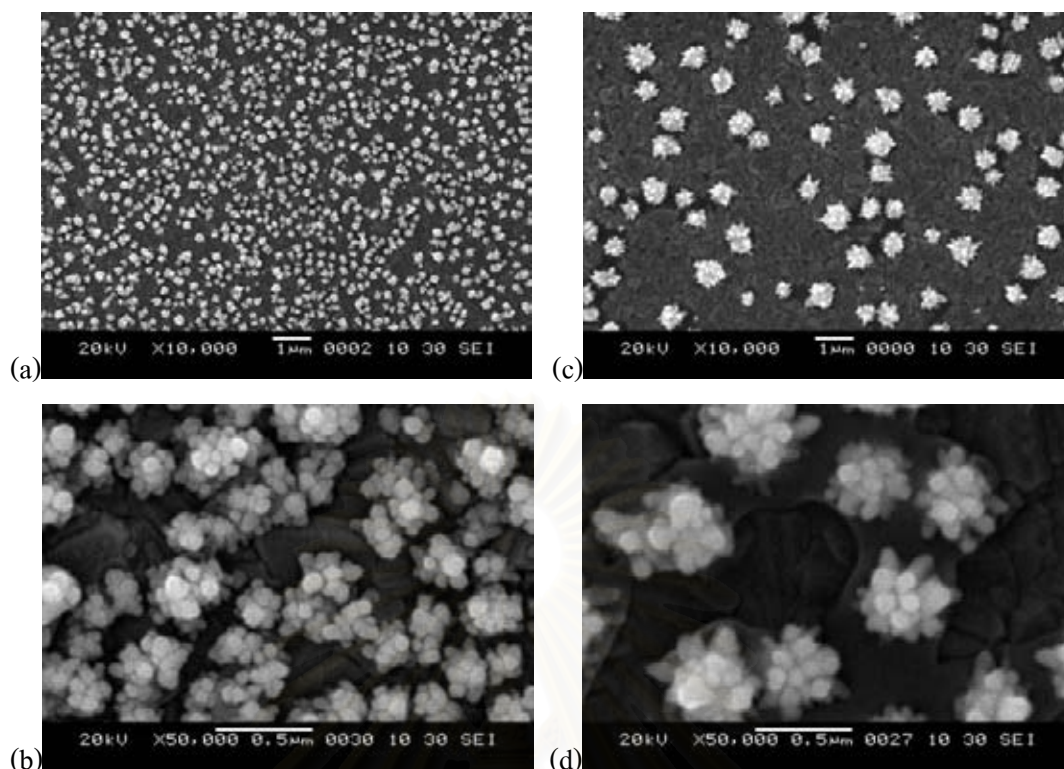


Figure 4.39 SEM images of Pt/BDD electrodes prepared by multi-step deposition (5×90 s, a and b) and one-step deposition (450 s, c and d) at the magnification of 10,000 (a and c) and 50,000 (b and d)

4.7.2 Platinum–Ruthenium/Boron-Doped Diamond Electrode

Figure 4.40 presents SEM images of $\text{Pt}_{0.95}\text{Ru}_{0.05}/\text{BDD}$ electrode prepared by using the optimized conditions obtained from section 4.5.1 (pp. 46-53). These images revealed that the deposited catalysts were arranged as micro-clusters on the BDD surface. These clusters were composed of metal nanoparticles with the sizes of 90-110 nm. In addition, we had compared SEM images of two types of $\text{Pt}_{0.95}\text{Ru}_{0.05}/\text{BDD}$ electrodes prepared by using different potentiostatic step width (10 s and 90 s, section 4.5.1.3, pp. 52-53). Table 4.6 displays the Pt–Ru cluster and Pt–Ru particle sizes on BDD surfaces. The results showed that Pt–Ru particles on BDD deposited by shorter potentiostatic step (10 s) had smaller particle and cluster sizes.

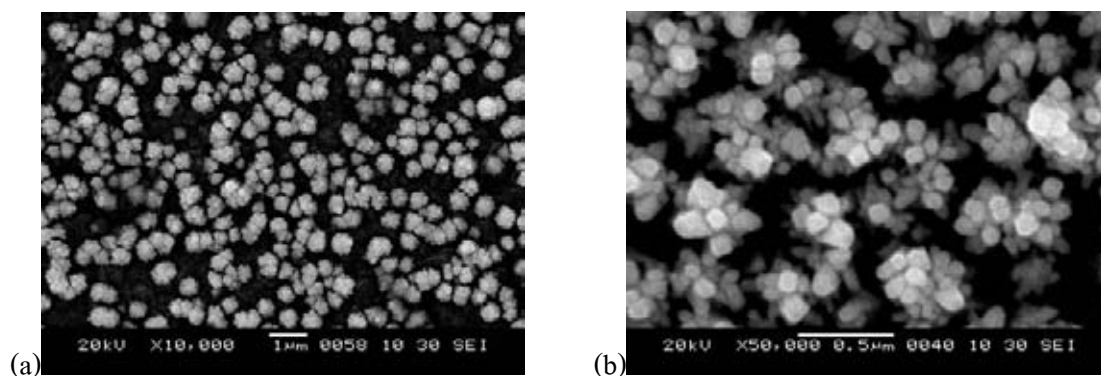


Figure 4.40 SEM images of Pt_{0.95}Ru_{0.05}/BDD electrode prepared by potentiostatic conditions (deposition potential = -0.24 V; total deposition time = 810 s; and potentiostatic step width = 10 s) at the magnification of (a) 10,000 and (b) 50,000

Table 4.6 Effect of potentiostatic step on Pt-Ru cluster and particle sizes at BDD surfaces of Pt_{0.95}Ru_{0.05}/BDD electrodes (preparation: deposition potential = -0.24 V and total deposition time = 810 s)

Potentiostatic Step Width = 10 s		Potentiostatic Step Width = 90 s	
Cluster Sizes (nm)	Particle Sizes (nm)	Cluster Sizes (nm)	Particle Sizes (nm)
393.89±16.58	97.63±8.35	485.40±21.87	110.16±11.85

4.7.3 Platinum–Ruthenium–Rhodium/Boron-Doped Diamond Electrode

Figure 4.41 shows the SEM images of PtRuRh/BDD electrode prepared by the optimum potentiostatic conditions in section 4.6.2 (pp. 64-66). Similar to Pt/BDD and PtRu/BDD electrodes, the metal micro-clusters on the BDD surface can be seen. The cluster sizes are 327.70±91.96 nm and the particle sizes are 91.96±12.95 nm. According to SEM results, the metal modified BDD electrodes prepared by electrodeposition under potentiostatic conditions contained the nano-scale metal particles which significantly enhanced the reaction sites for methanol oxidation on BDD surfaces.

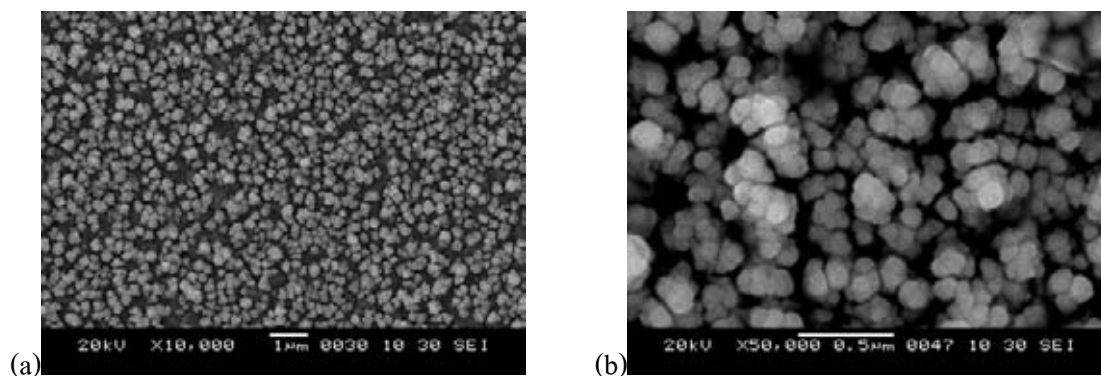


Figure 4.41 SEM images of $\text{Pt}_{0.95}\text{Ru}_{0.05}\text{Rh/BDD}$ electrodes with Rh deposition time of 10 s at the magnification of (a) 10,000 and (b) 50,000

4.8 Stability Studies of The Modified Electrodes

The stability of the modified electrodes has been tested by chronoamperometry. Figure 4.42 shows the current densities obtained from the oxidation of methanol at 0.64 V by the Pt/BDD, PtRu/BDD, and PtRuRh/BDD electrodes. Results illustrated that the addition of Ru and RuRh to Pt catalyst can improve the performance of the Pt catalyst by decreasing the poisoning effect caused by strongly adsorbed CO species on active site of Pt. These co-catalysts probably facilitate the cleavage of the carbon–carbon bond of the adsorbed intermediates. At the methanol oxidation potential of 0.64 V, it was observed that Ru oxide and Rh oxide were inert under reduction condition, causing their contribution as an oxidative catalyst as normally. Compared with earlier work [24] regarding the $\text{Pt-RuO}_2\text{-RhO}_2\text{/BDD}$ prepared by the sol-gel method, our PtRuRh/BDD electrode showed 10 times higher electrocatalytic activity for methanol at the reaction time of 2,000 s.

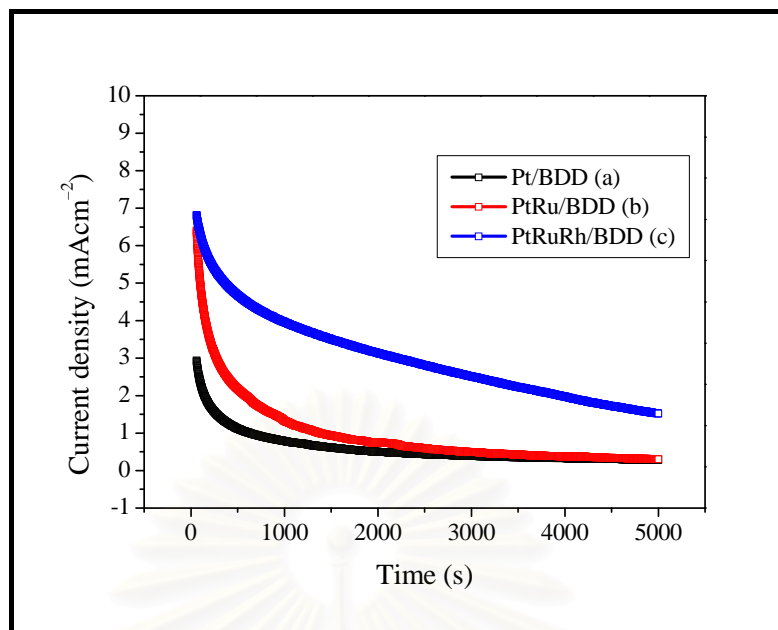


Figure 4.42 Current density measured at the potential of 0.64 V vs. time for the electrooxidation of 1.00 M methanol at (a) Pt/BDD, (b) PtRu/BDD, and (c) PtRuRh/BDD electrodes

CHAPTER V

CONCLUSIONS

In this thesis, the potentiostatic method has been demonstrated to be suitable for preparing nm-sized platinum (Pt)-based bimetallic and trimetallic catalysts supported on boron doped diamond (BDD) thin film electrode. Electrodeposition of Pt with multi-step deposition has been found to provide well-dispersed Pt particles on BDD surface. Addition of the second element to Pt evidently improved the oxidation of methanol. It was found that both ruthenium (Ru) and rhodium (Rh) were good additives, enhancing the electrode activity for methanol oxidation whereas gold (Au) did not have this property. Pt-rich bimetallic surfaces exhibited better electrocatalytic activities and higher tolerance towards carbon monoxide (CO) poisoning, due to the ability to eliminate surface-adsorbed intermediates at the room temperature. In this sense, prepared with potentiostatic method, Pt_{0.95}Ru_{0.05}/BDD electrode was the optimized electrocatalyst for methanol oxidation among the electrodes with various ratios of Pt:Ru.

Addition of Rh to Pt_{0.95}Ru_{0.05}/BDD improved electrocatalytic activity for methanol oxidation. Pt_{0.95}Ru_{0.05}Rh/BDD electrode prepared by depositing Rh electrochemically onto Pt_{0.95}Ru_{0.05}/BDD electrode showed 1.5 times higher electrocatalytic activity than Pt_{0.95}Ru_{0.05}/BDD electrode for the oxidation of 1.00 M methanol in 0.50 M sulfuric acid. In addition, the Pt_{0.95}Ru_{0.05}Rh/BDD electrode exhibited better long-term stability than Pt/BDD and Pt_{0.95}Ru_{0.05}/BDD electrodes. Scanning electron microscopic (SEM) images of the prepared electrodes revealed that the particle size of metals deposited on BDD is approximately 100 nm.

REFERENCES

1. Parson, R.; and Vandernoot, T. The oxidation of small organic molecules: a survey of recent fuel cell related research. J. Electroanal. Chem. 257 (1988): 9-45.
2. Hamnett, A. Mechanism and electrocatalysis in the direct methanol fuel cell. Catal. Today 38 (1997): 445-457.
3. Iwasita, T. Electrocatalysis of methanol oxidation. Electrochim. Acta 47 (2002): 3663-3674.
4. Nonaka, H.; and Matsumura, Y. Electrochemical oxidation of carbon monoxide, methanol, formic acid, ethanol, and acetic acid on a platinum electrode under hot aqueous conditions. J. Electroanal. Chem. 520 (2002): 101-110.
5. Kucernak, A.; and Jiang, J. Mesoporous platinum as a catalyst for oxygen electroreduction and methanol electrooxidation. Chem. Eng. J. 93 (2003): 81-90.
6. Frelink, T.; Visscher, W.; and Veen, J.A.R.V. On the role of Ru and Sn as promoters of methanol electro-oxidation over Pt. Surf. Sci. 335 (1995): 353-360.
7. Chrzanowski, M.; and Wieckowski, A. Surface structure effects in platinum/ruthenium methanol oxidation electrocatalysis. Langmuir 14 (1998): 1967-1970.
8. Lin, W.F.; Zei, M.S.; Eiswirth, M.; and Eril, G. Electrocatalytic activity of Ru-modified Pt (111) electrodes toward CO oxidation. J. Phys. Chem. B 103 (1999): 6968-6977.
9. Lemos, S.G.; Oliveira, R.T.S.; Santos, M.C.; Nascente, P.A.P.; Bulhoes, L.O.S.; and Pereira, E.C. Electrocatalysis of methanol, ethanol, and formic acid using a Ru/Pt metallic bilayer. J. Power Sources 163 (2007): 695-701.
10. Dickinson, A.J.; Carrette, L.P.L.; Collins, J.A.; Friedrich, K.A.; and Stimming, U. Preparation of Pt-Ru/C catalyst from carbonyl complexes for fuel cell applications. Electrochim. Acta 47 (2002): 3773-3739.

11. Cherstiouk, O.V.; Simonov, P.A.; and Savinova, E.R. Model approach to evaluate particle size effects in electrocatalysis: preparation and properties of Pt nanoparticles supported on GC and HOPG. Electrochim. Acta 48 (2003): 3851-3860.
12. Rodríguez-Nieto, F.J.; Morante-Catacora, T.Y.; and Cabrera, C.R. Sequential and simultaneous electrodeposition of Pt–Ru electrocatalysts on a HOPG substrate and the electro-oxidation of methanol in aqueous sulfuric acid. J. Electroanal. Chem. 571 (2004): 15-26.
13. Kim, T.; Takahashi, M.; Nagai, M.; and Koboyashi, K. Preparation and characterization of carbon supported Pt and PtRu alloy catalysts reduced by alcohol for polymer electrolyte fuel cell. Electrochim. Acta 50 (2004): 817-821.
14. He, Z.; Chen, J.; Liu, D.; Zhou, H.; and Kuang, Y. Electrodeposition of Pt–Ru nanoparticles on carbon nanotubes and their electrocatalytic properties for methanol electrooxidation. Diam. Rel. Mat. 13 (2004): 1764-1770.
15. Liu, Z.; Ling, X.Y.; Su, X.; Lee, J.Y.; and Gan, L.M. Preparation and characterization of Pt/C and PtRu/C electrocatalysts for direct ethanol fuel cells. J. Power Sources 149 (2005): 1-7.
16. Guo, J.W.; Zhou, T.S.; Prabhuram, J.; Chen, R.; and Wong, C.W. Preparation and characterization of a PtRu/C nanocatalyst for direct methanol fuel cells. Electrochim. Acta 51 (2005): 754-763.
17. Honda, K.; Yoshimura, M.; Rao, T.N.; Tryk, D.A.; Fujishima, A.; Yasui, K.; Sakamoto, Y.; Nishio, K.; and Masuda, H. Electrochemical properties of Pt-modified nano-honeycomb diamond electrodes. J. Electroanal. Chem. 514 (2001): 35-50.
18. Montilla, F.; Morallon, E.; Duo, I.; Comminellis, C.; and Vazquez, J.L. Platinum particles deposited on synthetic boron-doped diamond surfaces. Application to methanol oxidation. Electrochim. Acta 48 (2003): 3891-3897.
19. Zhang, Y.; Suryanarayanan, V.; Nakazawa, I.; Yoshihara, S.; and Shirakashi, T. Electrochemical behavior of Au nanoparticle deposited on as-grown and O-

- terminated diamond electrodes for oxygen reduction in alkaline solution. Electrochim. Acta 49 (2003): 5235-5240.
20. Bennett, J.A.; Show, Y.; Wang, S.; and Swain, G.M. Pulsed galvanostatic deposition of Pt particles on microcrystalline and nanocrystalline diamond thin-film electrodes. J. Electrochem. Soc. 152 (2005): E184-E185.
 21. Gonzalez-Gonzalez, I.; Tryk, D.A.; and Cabrera, C.R. Polycrystalline boron-doped diamond films as supports for methanol oxidation electrocatalysts. Diam. Rel. Mat. 15 (2006): 275-278.
 22. Sine, G.; and Comninellis, C. Nafion-assisted deposition of microemulsion-synthesized platinum nanoparticles on BDD. Electrochim. Acta 50 (2005): 2249-2254.
 23. Suffredini, H.B.; Tricol, V.; Vastias, N.; and Avaca, L.A. Electro-oxidation of methanol and ethanol using a Pt–RuO₂/C composite prepared by the sol–gel technique and supported on boron-doped diamond. J. Power Sources 158 (2006): 124-128.
 24. Salazar-Banda, G.R.; Suffredini, H.B.; Calegari, M.L.; Tanimoto, S.T.; and Avaca, L.A. Sol-gel-modified boron-doped diamond surfaces for methanol and ethanol electro-oxidation in acid medium. J. Power Sources 162 (2006): 9-20.
 25. Conway, B.E. Electrochemical oxide film formation at noble metals as a surface-chemical process. Progr. Surface Sci. 49 (1995): 331-452.
 26. Correia, A.N.; Mascaro, L.H.; Machado, S.A.S.; and Avaca, L.A. Active surface area determination of Pd-Si alloys by H-adsorption. Electrochim. Acta 42 (1997): 493-495.
 27. Avila-Garcia, I.; Plata-Torres, M.; Dominguez-Crespo, M.A.; Ramirez-Rodriguez, C.; and Arce-Estrada, E.M. Electrochemical study of Pt–Pd, Pt–Ru, Pt–Rh and Pt–Sn/C in acid media for hydrogen adsorption–desorption reaction. J. Alloys Comp. 434-435 (2007): 764-767.
 28. Furukawa, H.; Ajito, K.; Takahashi, M.; and Ito, M. SERS and FT-IR studies of CO adsorbed on underpotential deposited Ag/Pt electrodes. J. Electroanal. Chem. 280 (1990): 415-423.

29. Gao, J.; Arunagiri, T.; Chen, J.; Goodwill, P.; Chyan, O.; Perez, J.; Golden, D. Preparation and characterization of metal nanoparticles on a diamond surface. Chem. Mater. 12 (2000): 3495-3500.
30. Liu, Y.; Mitsushima, S.; Oct, K.; and Kamiya, N. Electro-oxidation of dimethyl ether on Pt/C and PtMe/C catalysts in sulfuric acid. Electrochim. Acta 51 (2006): 6503-6509.
31. Lasch, K.; Jorissen, L.; and Garche, J. The effect of metal oxides as co-catalysts for the electro-oxidation of methanol on platinum–ruthenium. J. Power Sources 84 (1999): 225-230.
32. Finot, M.O.; Braybrook, G.D.; and McDermott, M.T. Characterization of electrochemically deposited gold nanocrystals on glassy carbon electrodes. J. Electroanal. Chem. 446 (1999): 234-241.
33. Oliveira, R.T.S.; Santos, M.C.; Marcussi, B.G.; Nascente, P.A.P.; Bulhoes, L.O.S.; and Pereira, E.C. The use of a metallic bilayer for the oxidation of small organic molecules. J. Electroanal. Chem. 575 (2005): 177-182.
34. Enea, O.; Riedo, B.; and Dietler, G. AFM study of Pt clusters electrochemically deposited onto boron-doped diamond films. Nano Lett. 2 (2002): 241-244.

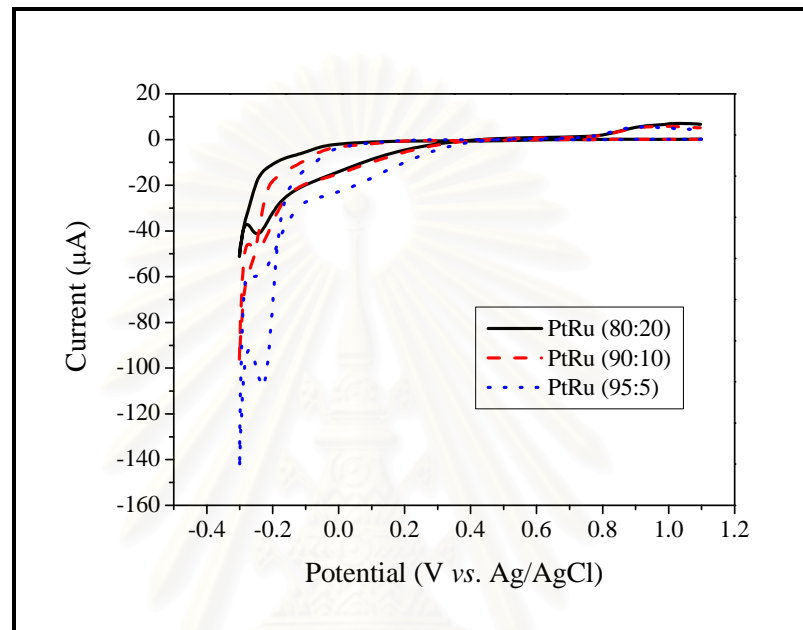


APPENDICES

สถาบันวิทยบริการ
จุฬาลงกรณ์มหาวิทยาลัย

APPENDIXES

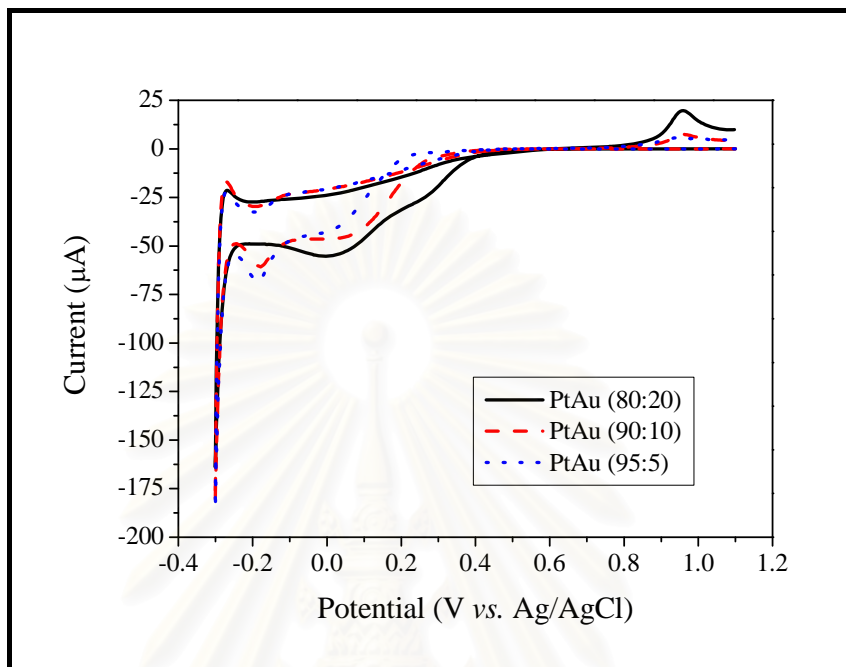
APPENDIX A



Cyclic voltammograms for Pt–Ru composite solutions in 0.50 M sulfuric acid recorded with BDD electrode at the scan rate 50 mVs^{-1}

สถาบันวิทยบริการ
จุฬาลงกรณ์มหาวิทยาลัย

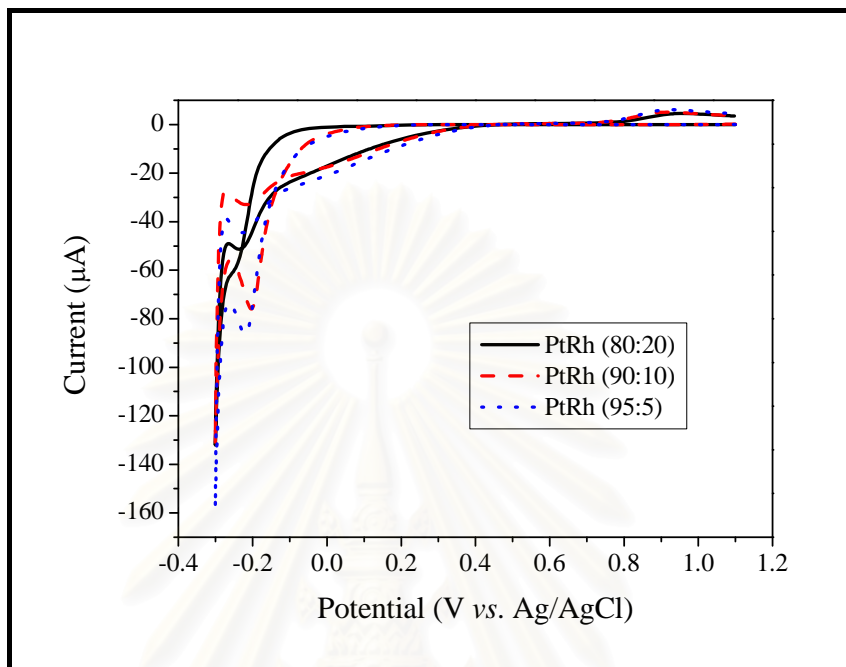
APPENDIX B



Cyclic voltammograms for Pt–Au composite solutions in 0.50 M sulfuric acid recorded with BDD electrode at the scan rate 50 mVs^{-1}

สถาบันวิทยบริการ
จุฬาลงกรณ์มหาวิทยาลัย

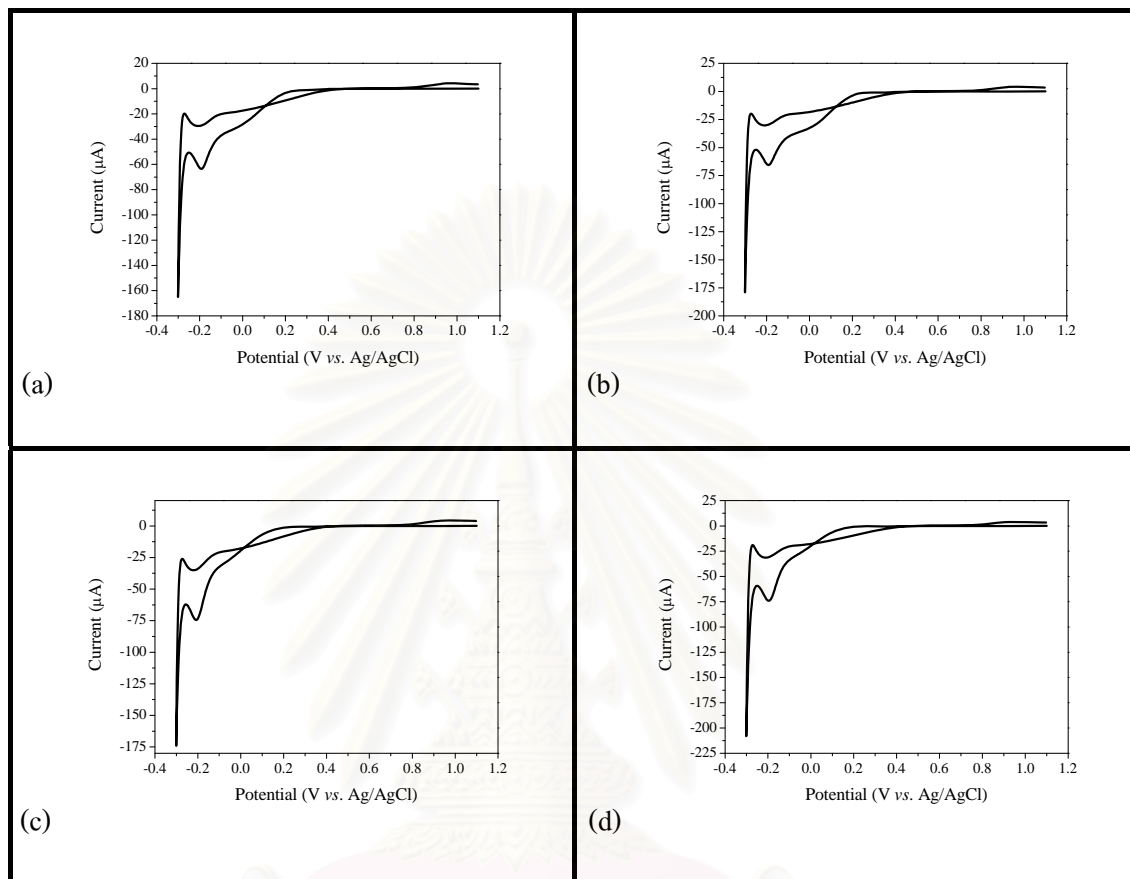
APPENDIX C



Cyclic voltammograms for Pt–Rh composite solutions in 0.50 M sulfuric acid recorded with BDD electrode at the scan rate 50 mVs^{-1}

สถาบันวิทยบริการ
จุฬาลงกรณ์มหาวิทยาลัย

APPENDIX D



Cyclic voltammograms for Pt–Ru–Au composite solutions with the Pt:Ru:Au ratios of (a) 95:4:1, (b) 95:3:2, (c) 95:2:3, and (d) 95:1:4 in 0.50 M sulfuric acid recorded with BDD electrode at the scan rate 50 mVs^{-1}

สถาบันวิทยบริการ
จุฬาลงกรณ์มหาวิทยาลัย

VITA

Name : Mr Worayut Thayavivat

Date of Birth : Sep 25, 1982

Place of Birth : Surat Thani, Thailand

Gender : Male

Education : 2001-2004 Bachelor Degree of Science (Chemistry),
Kasetsart University
2004-2007 Master Degree in the Program
of Petrochemistry and Polymer Science,
Chulalongkorn University

Home Address : 118/41 Aekkachai 64/5, Bangbon, Bangkok 10150

Poster Presentation : 2006 32nd Congress on Science and Technology
of Thailand (STI.32), Bangkok
2006 2nd MPSGC Mathematics and Physical
Sciences Graduate Congress, Singapore
2008 PACCON Pure and Applied Chemistry
International Conference, Bangkok

สถาบันวิทยบริการ
จุฬาลงกรณ์มหาวิทยาลัย